C 51.17/12:987/9
SEP 19 1987
188 #11
C51.17/12:987/9

Tech Notes

SEPTEMBER 1987

PB87-925909

CONTENTS

NTIS

U.S. DEPARTMENT OF COMMERCE
National Technical Information Service
Center for the Utilization of Federal Technology

U. S. DEPARTMENT OF COMMERCE
Secretary of Commerce
Clarence J. Brown, Acting

National Technical Information Service
Joseph F. Caponio, Director

ISSN 0889-8464

COPYRIGHT WARNING
International Copyright © National Technical Information Service, 1987. All portions of this publication are protected against copying or other reproduction outside of the United States under the provisions of Article II of the Universal Copyright Convention. United States copyright is not asserted under the United States Copyright Law, Title 17, United States Code.

The Secretary of Commerce has determined that the publication of this periodical is necessary in the transaction of the public business required by law of this department. Use of funds for printing this periodical has been approved by the Director of the Office of Management and Budget through 1987.

Tech Notes

Highlighting Selected U.S. Government Technology & Resources

SEPTEMBER 1987

Contents

Agriculture & Food 826

Computers 827

Electrotechnology 831

Energy 844

Engineering 850

Environmental Science & Technology 863

Manufacturing, Machinery, & Tools 871

Materials 890

Medicine & Biology 906

Natural Resources Technology & Engineering 911

Physical Sciences 914

Transportation 929

Published monthly by the National Technical Information Service (NTIS), Tech Notes bring togeather individual one to two page fact sheets prepared by Federal agencies, their laboratories, or contractors. These fact sheets highlight current Federal technology determined to have commercial or practical application. Topics cover new processes, materials, techniques, software, instrumentation, and resources.

Some of the current sources are the Department of the Navy, Department of the Army, NASA, Department of Energy , Environmental Protection Agency, Department of the Interior, and the Department of Agriculture.

Special assistance is provided by the Federal Laboratory Consortium.

Change of address or questions concerning subscriptions should be sent to:
Subscriptions Department
National Technical Information Service
Springfield, VA 22161
(703) 487-4630

Suggestions, comments, or questions concerning Tech Notes should be directed to:
Tech Notes Editor
Room 11R
National Technical Information Service
Springfield, VA 22161
(703) 487-4838

How to Use Tech Notes

Every Tech Notes fact sheet lists a source for additional information. The source of this information may be a special support package from the originating agency, a personal contact, a licensing opportunity, or a backup report available from NTIS.

Each fact sheet also is perforated to allow for easy removal for those subscribers who may wish to keep a special fact sheet file or route to others in their organization

Sources of Further Backup Information

Below are two representative examples of how each Tech Note fact sheet provides you with a source of further information. In most cases, this information is provided directly by the agency or its laboratory.

However, there are cases where NTIS is the source for backup documentation. In these cases, use the order form at the end.

Examples:

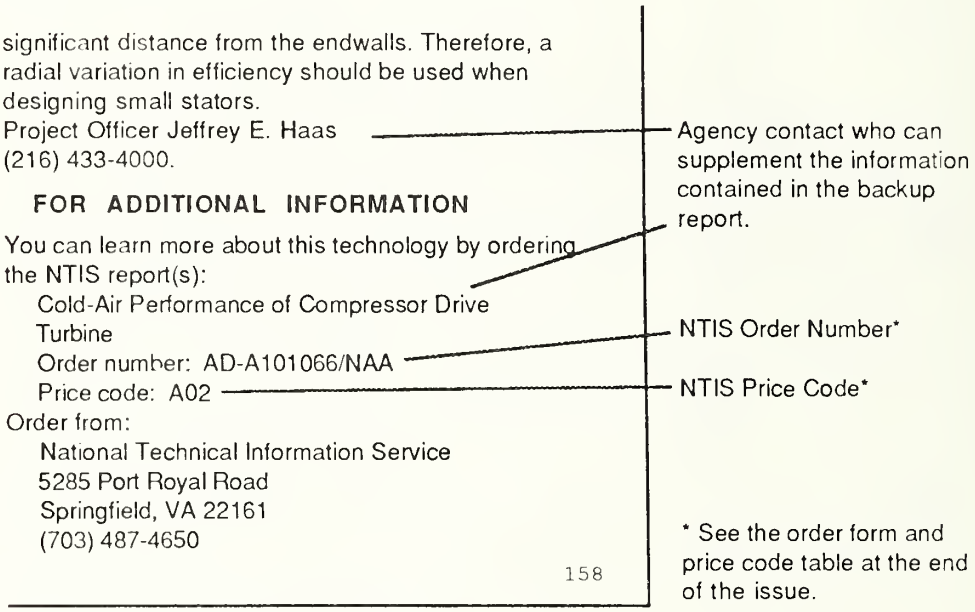

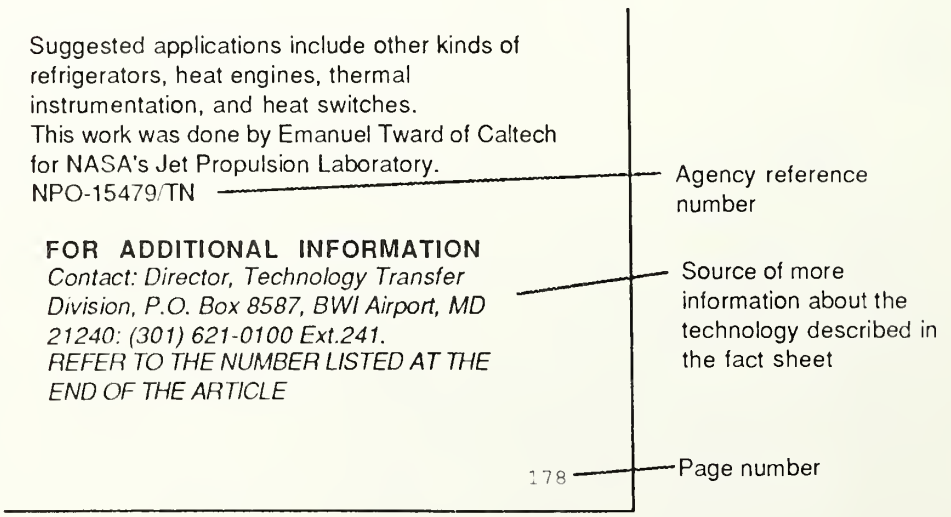

Tech Notes Title List for September 1987

Agriculture & Food

Software

826 Computer-Assisted Placement of Shade Trees

Computers

827 Measuring Computer-Operator Workload — Subjective and objective measurements are found to correlate and complement each other.

828 Design Considerations for High-Speed Control Systems — Existing hardware can be integrated into a versatile, high-speed control systems. (Licensing Opportunity)

Software

829 Ada Language System (ALS), Version 3.0

830 The Intergrated Reliability and Risk Analysis System (IRRAS-PC)

Electrotechnology

831 VHSIC/VHSIC-Like Reliability Modeling

832 Out-of-Band Response of Antenna Arrays

833 Optoelectronic Docking System — Sensors and computers control approach and coupling.

834 Theoretical Efficiencies of Microwave Diode Triplers — Simulations are conducted for 300- to 900-GHz units.

835 MOSFET's for Cryogenic Amplifiers — A study seeks ways to build transistors that function effectively at liquid-helium temperatures.

836 Radar Time-Base and Pseudonoise Generator — Long pulses are effectively compressed by a pseudonoise techique.

837 VLBI System for Satellite Navigation — A system is described, and its anticipated performance is analyzed.

838 Three-Axis Attitude Control With a Single Wheel — Internally gimbaled wheel plus reaction torquing combine to yield three-axis control. (Licensing Opportunity)

839 Switching Circuit for Shop Vacuum System — No internal connections to machine tools are required.

840 Overriding Faulty Circuit Breakers — A retainer keeps power on in an emergency.

Testing & Instrumentation

841 Microelectronic Parts Field Failures — A new project will help engineers avoid predominant failure mechanisms.

842 Effectiveness of Microcircuit Device Screening

843 Infrared Systems Developed to Test Gallium Arsenide Wafers

Other items of Interest

849 Improving Solar Cells with Polycrystalline Silicon — Thin layers arranged strategically would make cells more efficient.

Energy

844 Ceramic Two-Cycle Engine Development

845 CACS Conservation Actions in Small Commerical Building

846 Cooling Season Performance of an Earth-Sheltered Office/Dormitory Building

847 Residential Photovoltaic/Thermal Energy System — A proposed system would supply a house with both heat and electricity.

848 A Surface-Controlled Solar Cell — The open-circuit voltage and the cell efficiency may be increased. (Licensing Opportunity)

849 Improving Solar Cells with Polycrystalline Silicon — Thin layers arranged strategically would make cells more efficient.

Other items of Interest

854 Elastic Hinge for Solar-Cell Array — A lightweight, compact hinge provides part of its own closing torque. (Licensing Opportunity)

911 More Oil and Gas May Be Recovered by Using New Fracture Mapping Tool

Engineering

850 New Standard for Safety Colors

851 Water Purification Production Doubles in Desert

852 Locating Sonic Lines in Transonic Nozzles — New formulas predict accurately the line location in advanced convergent/divergent nozzles.

853 Design Improvement for Airplane-Engine Nacelles — Better streaming reduces drag. (Licensing Opportunity)

854 Elastic Hinge for Solar-Cell Array — A lightweight, compact hinge provides part of its own closing torque. (Licensing Opportunity)

858 Increasing Maintainability of a Wastewater-Recovery Unit — A modified system leaks less and is easier to disassemble for maintenance.

Software

855 Interactive Computer Model for Calculating V-I Curves in Electrostatic Precipitators

856 Analysis of Scramjet Inlets — Viscous flow can be accounted for in the computations.

857 Buckling Analysis of Rectangular Plates With Holes — Loads and deflections are predicted for a variety of cutouts.

Testing & Instrumentation

859 Large-Area Radiation Portal/Personnel Monitor — A faster, more sensitive personnel monitoring system

860 Side-Looking Viewer for Crevices — Gaps only 1 mm wide are inspected with a thin metal mirror.

861 Measuring Thicknesses of Wastewater Films — A sensor resists excessive film buildup.

862 Large Wire Strain Gauges — Wires yield data on average strains over distances ranging from inches to many feet.

Environmental Science & Technology

863 GETS, A Simulation Model for Dynamic Bioaccumulation of Nonpolar Organics by Gill Exchange — A User's Guide

864 Removing Welding Fumes — A duct can be placed quickly where it is needed.

Software

866 Water Quality Models Used By the Corps of Engineers

867 Geotechnical Analysis for Dike Stability (GARDS)

868 Software Evaluates Liquid Waste Soil Liners

869 Integrated Air Pollution Control System Cost Model Version 2 (IAPCS2) — Program estimates costs and performance for coal-fired utility boilers

Testing & Instrumentation

870 Groundwater-Level Monitoring System

Manufacturing, Machinery, & Tools

871 Die-Target for Dynamic Consolidation of Powers

872 Robot to Transfer Wafers in New Integrated Circuit Facility

873 Corrosion and Load Transfer Effects on Fatigue of Mechanically Fastened Joints

874 Wet Winding Improves Coil Encapsulation — Voids are eliminated without special vacuum processing. (Licensing Opportunity)

875 Making Fillets by Electrical-Discharge Machining — A shaped graphite electrode eliminates many hours of hand work.

876 Quick-Release Panel Fastener — The twist of a handle activates and deactivates a clamp.

877 High-Pressure Valve With Controlled Seating Force — The poppet and seat are less likely to be damaged by faulty operation.

878 Magnetic Bearing With Radial and Angular Control — The rotor is stabilized magnetically with a feedback control system. (Licensing Opportunity)

879 Duplex Wrench — A special tool enables one worker to do a two-worker job.

880 Position Control for Nonlinear, Multiple-Link Robots — Several approaches to a complicated control problem are examined.

881 Optical Welding Torch — Arc welds can be viewed along the torch axis. (Licensing Opportunity)

882 Pultrusion Fabrication of Long Boom Models — Composite materials of quasi-isotropic strength are obtained.

883 Making Ceramic Parts by Laminating and Sintering Thin Sheets — The chemical composition can be varied as a function of depth.

884 Deep, Precise Etching in Semiconductors — Semiconductors can be made to accept precise etching after pretreatment.

885 Advanced Data Collection for Inventory Management — Bar-coding, radio-frequency, and voice-operated systems are selected.

886 Microprocessor-Based Valve Controller — A commanded mass-flow rate is maintained.

887 Inflatable Perimeter Seal — Inflatable tubing replaces gaskets or O-rings for sealing flat surfaces.

889 Low-Turbulence Valve — A valve promotes diffusion mixing of liquids rather than turbulence mixing. (Licensing Opportunity)

Testing & Instrumentation

888 Protecting a Ball-Bearing-Deflection Monitor — A thin barrier isolates a probe from liquid oxygen.

Other items of Interest

839 Switching Circuit for Shop Vacuum System — No internal connections to machine tools are required.

Materials

890 Urethane Structural Adhesives

891 NDS Steel in High-Temperature Recuperators — The alloy is far stronger than ordinary Inconel* alloys at temperatures above 1,650 F (899 C).

892 Age Hardening in Binary Iron/Nickel Martensites — Increasing the nickel content and cooling the alloy to a low temperature improves its hardenability.

893 Strengthening Procedure for Magnesium-Base Sheet Alloys

894 Correlating Abrasive Wear to Alloy Additions in Low-Alloy Steel

895 New Foam Traps Moisture and Provides Structural Support

896 New Polymeric Precursors of Silicon Carbide — Silicon carbide is made by pyrolizing the polymers. (Licensing Opportunity)

897 Electrically Conductive, Heat-Resistant Paint — A graphite/silicate paint for titanium substrates withstands vibration and thermal shock.

898 Long-Term Tests of 38 Ball-Bearing Greases — Perfluoroalkylpolyether lubricants performed best.

899 Amorphous-Metal-Film Diffusion Barriers — Incorporation of N into Ni/W films reduces their reactivity with Si substrate.

900 Evaluation of Fiber-Reinforced Composites — The mechanical properties of a graphite/epoxy material are determined.

901 Polyenamines for Films, Coatings, and Adhesives — A relatively easy process makes polymers with good mechanical properties. (Licensing Opportunity)

902 Oxygen-Barrier Coating for Titanium — Submicron Al/SiO2 coating significantly reduces titanium embrittlement. (Licensing Opportunity)

Testing & Instrumentation

903 Detection and Charactization of Damage in Thick Composities

904 Specimen and Holder for Sliding-Mode Fatigue Tests — A single-ended notch design facilitates accurate measurements of crack progression. (Licensing Opportunity)

905 Measuring Poisson Ratios at Low Temperatures — A simple extensometer ring measures the bulges of specimens in compression. (Licensing Opportunity)

Other items of Interest

871 Die-Target for Dynamic Consolidation of Powers

Medicine & Biology

906 NIGMS Human Genetic Mutant Cell Repository
907 Promising New Immunological Adjuvant

Testing & Instrumentation

908 Boosting Cholesterol Test Accuracy is Aim of New Materials
909 New Transducer Could Detect Brain Aneurysms
910 Hand-Strength Meter — A grip meter measures hand strength accurately and reproducibly.

Other items of Interest

859 Large-Area Radiation Portal/Personnel Monitor — A faster, more sensitive personnel monitoring system

Natural Resources Technology & Engineering

911 More Oil and Gas May Be Recovered by Using New Fracture Mapping Tool
912 Microwave Properties of Quiet Seas — Measurements from a satellite provide information for comparisons and analyses.

Software

913 Ionospheric Communications Analysis and Prediction Program (IONCAP) — Predicts high-frequency skywave system performance

Physical Sciences

914 Electrodeposition and Characterization of Niobium from Fused Salt Electrolytes
915 X-Ray Source is an Important Resource for X-Ray Spectroscopy
916 Tiny Device Allows Explosives to Be Ignited Much Faster
917 Reciprocal Taylor Series
918 Field-Reversal Source for Negative Halogen Ions — Large zero-energy electron-attachment cross sections would result in intense ion beams. (Licensing Opportunity)
919 High-Temperature Thermoelectric Energy Conversion — Semiconductor materials are the best choice.

Software

920 Thermal-Analysis Program — Temperature changes with time are modeled with the traditional electrical analog.
921 Designing Echelle Spectrographs — Performance numbers and output maps are computed from inputs supplied by the user.

Testing & Instrumentation

922 Pulse Injection Rate Synchronizer (PIRS) for Gamma Spectrometry
923 Pressure Regulation in a Reduced Pressure Chamber Using a Cryogenic Temperature Controller — An inexpensive, percise, and small regulator developed
924 Automated Laboratory System for Data Acquisition and Control — Programs and techniques detailed for a PDP-11 Computer
925 Sampling and Analysis for High-Molecular-Weight Polar Organic Compounds
926 Calibration of Germanium Resistance Thermometers — Six thermometers can be calibrated at once in the range below 2.17 K.
927 Measuring Shapes of Acoustically Levitated Drops — An instrument records shadows of drops in an acoustic field.
928 Containerless Atomic-Fluorescence Property Measurements — Laser-induced fluorescence can be used to measure high-temperature processes.

Transportation

929 Helicopter Icing Spray System — A spray boom assembly is deployed 19 feet (5.7m) beneath the aircraft from a torque tube through the cargo compartment.
930 Service-Life Extension of Explosive Escape Devices — Chemical and functional tests yield conservative service-life estimates.
931 Translating Canard — Longitudinal trim control is augmented when landing flaps are deployed. (Licensing Opportunity)

Agriculture & Food

Software

826 Computer-Assisted Placement of Shade Trees

Computer-Assisted Placement of Shade Trees

Trees can provide significant savings in energy use by controlling sunlight and shade. A 3% reduction in home heating and cooling costs would save over 153 trillion btus at a cost of over $1 billion per year in the United States. Unless properly placed, the same trees can raise heating costs by shading windows or other solar collectors during winter. Placing trees to provide ample shade in summer but full sun during winter has always defied simple rules of thumb. The sun's angle changes with latitude and with the seasons, as well as throughout each day; and relationships worked out for one window or solar collector may not fit windows or collectors having different dimensions or facing different directions. The SOLPLOT computer program, however, performs the necessary calculations, freeing users to concentrate on desired effects. SOLPLOT was developed specifically to guide the placement of trees to control sunlight and shade.

FOR ADDITIONAL INFORMATION: This "user friendly" program in Microsoft BASIC for microcomputers and FORTRAN 77 for larger computers is available from J. Alan Wagar, USDA Forest Service, P. O. Box 245, Berkeley, CA 94701.

Computers

827 Measuring Computer-Operator Workload — Subjective and objective measurements are found to correlate and complement each other.

828 Design Considerations for High-Speed Control Systems — Existing hardware can be integrated into a versatile, high-speed control systems. (Licensing Opportunity)

Software

829 Ada Language System (ALS), Version 3.0

830 The Intergrated Reliability and Risk Analysis System (IRRAS-PC)

NASA Tech Brief
National Aeronautics and Space Administration
NASA's Jet Propulsion Laboratory, Pasadena, California

Measuring Computer-Operator Workload

Subjective and objective measurements are found to correlate and complement each other.

Two ways of measuring the workload of an operator in a large interactive computer system have been shown to be meaningful and easy to use. One method is based on operators' ratings of stress after subtasks in a continuous task. The other method is based on the workload ratio, W, which is the ratio of the time required for an operator to do a subtask to the time allowed for it.

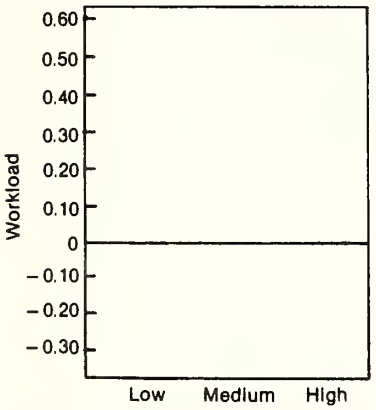

Figure 1. One **Measure of Operator Workload** is the mean normal operator "time stress" rating under low, medium, and high workload conditions.

Both methods are sensitive to the workload level and to individual subtasks in a continuing interactive computer task. They can pinpoint subtasks that press the operator and use up too much of the available time, perhaps leading to operator errors and even failure of the system.

The methods were tried in the NASA Deep Space Network, a computer system that acquires scientific, engineering, and tracking data from spacecraft. Nine experienced operators used the system under low, medium, and high workloads. They used standard equipment in a normal operating environment. A simulated task, composed of five subtasks and requiring a single operator, was designed for the study. It was typical of tracking-station tasks and involved initializing seven different computers so that they would be ready to track a designated spacecraft.

In the low-workload condition, the task was a simple setup with no complications; 12 minutes were allowed. In the medium-workload condition, the setup was extended and required an additional pair of processors for another function; 20 minutes were allowed. In the high-workload condition, the extended task was used, and two computer failures were added. The allowed time remained at 20 minutes. In all three conditions, the allowed times were just enough to enable the completion of the tasks in the absence of malfunctions and errors.

The operators rated the subtasks according to two criteria: mental effort and pressure of time. They gave their ratings on a scale of 1 to 7 by pressing keys on their keyboards at the end of each subtask.

The operators' ratings were obtained directly from a computer printout. The time at which a rating was given was used to calculate the period of time the operator actually needed to do a subtask. This period was used to calculate the workload ratio from the standard allowable time established for the subtask. The pressure-of-time ratings correlated closely with the workload-ratio measurement (see figures).

The correlation indicates that they are measuring essentially the same thing, and one therefore can serve as a check on the other. However, they are not necessarily redundant in an uncontrolled situation in which one might be more readily usable. The pressure-of-time rating is especially easy to use and interpret. It is well-suited to on-the-spot diagnoses of operator problems. The workload ratio yields quantitative data on the time needed to perform subtasks and on the portion of task time spent on each subtask. It gives a clear indication when the operator approaches the allowed time and thus shows when the risk of trouble becomes high.

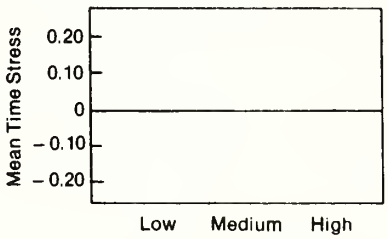

Figure 2. The **Mean Normalized Workload** ratio (W = Tr/Ta) under low, medium, and high workload correlates with the other measure of operator workload. (W = workload, Tr = time required by the operator to perform a specific subtask, and Ta = time allowed for that subtask.)

This work was done by Eric E. Hird and Moira LeMay of Caltech for **NASA's Jet Propulsion Laboratory**.
NPO-16281 /TN

FOR ADDITIONAL INFORMATION: *Contact: Director, Technology Transfer Division, P.O. Box 8757, BWI Airport, MD. 21240; (301) 621-0100 Ext. 241*
REFER TO THE NUMBER LISTED AT THE END OF THE ARTICLE

NASA Tech Brief
National Aeronautics and Space Administration

Licensing Opportunity

Design Considerations for High-Speed Control Systems

Existing hardware can be integrated into a versatile, high-speed control system.

A report discusses five global design considerations to integrate array-processor, multimicroprocessor, and host-computer system architectures into versatile, high-speed controllers. Such controllers are capable of control throughputs as high as 36 MHz for 8-bit bytes and can maintain constant interaction with the non-real-time or user environment. As an application example, the architecture of a high-speed, closed-loop controller used to control helicopter vibration actively is briefly discussed.

Most modern computer-based control systems are represented by a rather straightforward integration of a central (host) computer with several unintelligent (i.e., nonprogrammable) peripheral devices. The host computer must supervise all actions of the peripheral devices and synchronize the operations of each one with the rest of the system. Therefore, it is usually sufficiently burdened that it cannot support heavy input/output or extensive interaction with the user and maintain control of the system at the same time. In applications where simultaneous high control throughput and numerical computations are required, a point is reached where the necessary control computations cannot be done if the data input/output operation frequency is too high.

These difficulties can be avoided through the following five system-hardware design modifications:

1. Array processors can be added to minicomputer-based control systems to increase system performance by freeing the host from intensive numerical calculations. This leaves the host computer free to coordinate more input/output transfer and to sequence events.
2. The array processor can be used to separate the non-real-time events from the real-time events. This decoupling allows the array-processor-based loop-processor subsystem to process data at extremely high rates, while the executive subsystem monitors the user or non-real-time environment.
3. Large executive computers can enhance control system performance by providing multitasking and multiuser environments necessary to synthesize flexible and versatile control systems.
4. The use of intelligent peripherals to share the real-time burden can increase system throughput by freeing the array processor from having to supervise the external devices.
5. Intelligent interfaces can provide high-speed data paths to maximize the speeds of communication and data transfer between the array processor and its external devices.

Unlike conventional control-system design, these design considerations are not aimed at optimally sizing the control-system components to fit a particular task. Rather they emphasize high throughput and flexibility.

This work was done by Stephen A. Jacklin, Jane A. Leyland, and William Warmbrodt of **Ames Research Center**.

"High- Speed, Automatic Controller Design Considerations for Integrating Array Processor Multi-Microprocessor, and Host Computer System Architectures,"

Inquiries concerning rights for the commercial use of this invention should be addressed to the Patent Counsel, Ames Research Center Refer to ARC-11670./TN

Ames Research Center
Technology Utilization Officer:
Laurance A. Milov
Mail Code 204-10
Moffett Field, CA 94035
(415) 694-5761
Patent Counsel:
Darrell G. Brekke
Mail Code 200-11
Moffett Field, CA 94035
(415) 694-5104

FOR ADDITIONAL INFORMATION: *Contact: Director, Technology Transfer Division, P.O. Box 8757, BWI Airport, MD. 21240; (301) 621-0100 Ext. 241*
REFER TO THE NUMBER LISTED AT THE END OF THE ARTICLE

Ada Language System (ALS), Version 3.0

The Ada Language System (ALS) is a complete programming environment with features which support the life cycle of software written in Ada. Its extensible tool set provides an open-ended environment. Configuration control is provided through a variety of features, including protected access to files and records of how objects are created. A key feature of the ALS design is support for portability. Rehosting is eased by the ALS KAPSE which provides a standard interface between the host machine and the rest of the programming environment. The tools and file system remain constant over different host machines, aiding the ability of programmers to move from one environment to another. The ALS is also designed to produce programs which will execute on a variety of target machines. The tools have been designed so that the degree to which components need to be changed for retargeting is minimized. The three major components of the Ada Language System are: (1) A file structure called the environment database which stores all information relevant to a software project throughout its life cycle; (2) A set of tools which enable users to do their work. This tool set consists of predefined tools and user-defined tools. (3) A mechanism by which tools are invoked, called the command language. The command language is the language with which the user invokes tools.

Software Description: The system is written in the Ada, Bliss and Macro-II programming languages for implementation on a DEC VAX 11/780 computer under the VAX/VMS V.4.4 operating system. The system requires ALS Version 3.0 environment. Corc storage requirement is 8000K bytes. The system resides on seven magnetic tapes. Two of the tapes contain source code and are recorded in ASCII. The remaining five tapes are in object code.

For Additional Information:

For information about ordering this software, contact the
NTIS Computer Products Center, NTIS, 5285 Port Royal Road, Springfield, VA 22161; (703) 487-4763.

Refer to PB87-127346/NAC

Source tape is in the ASCII character set. This restricts preparation to 9 track, one-half inch tape only. Identify recording mode by specifying density only. Price includes 33 supporting documents, PB87-127015 thru PB87-127338. U.S. sales only.

Department of Energy

Technology Application

The Intergrated Reliability and Risk Analysis System (IRRAS-PC)

IRRAS software allows systems analysts to use the color graphics capability of a PC to view, graphically construct, modify, and automatically generate fault tree data for PRA. (A fault tree is a schematic analytical tool that shows the relationship of potential failures in a system being analyzed.) This allows more efficient and effective simulation and analysis of complex systems. Use of IRRAS software results in large time savings and improved accuracy in the output.

IRRAS allows fault tree PRA, formerly underutilized due to the large effort required to construct and analyze, to be used in the decision making process and analysis of safety issues at, e.g., nuclear plants. IRRAS allows the analyst to creat, modify, update, and reanalyze a plant PRA to keep the risk assessment current with the plant's configuration and operation. This allows a picture of the plant as it is now and not as it was sometime in the past. The fault trees are created and edited using the graphics capability of a PC and highly optimized reduction algorithms. A set of pop-up menus is incorporated to make the software user friendly. IRRAS lets the analyst easily create and maintain fault tree data and automates the formerly cumbersome process of converting the data to equations to be used in the analysis. With IRRAS, PRAs become "living" documents that reflect the current status of the system.

By using highly optimized reduction algorithms and integrated color graphics on a PC, the IRRAS software gives system analysts the ability to rapidly construct and modify complex fault tree diagrams with less risk of error and at a lower cost than previous methods. These algorithms eliminate the need to use mainframe computers in the fault tree analysis process. Prior to IRRAS, systems analysts used pencil and paper fault tree diagrams to model a system. This model was then converted to computer readable alphanumeric computer cards for use on mainframe computers. Mainframe computers were used because the large amounts of data generated by the fault trees required extensive computer memory. Besides being time consuming and error prone, the trend toward more complex automated systems made the pencil and paper method obsolete. Features of the IRRAS software include: use of the keyboard or a mouse to construct diagrams, use of monochrome or color graphics, editor functions grouped by category, predefined fault tree shapes, display functions (e.g., moving, copying, deleting) allows assignment of names and probabilities to events, disk storage and retrieval, hardcopy of the diagrams, and automatic conversion of the diagrams to alphanumeric codes for input to the final analysis system. No other comparable system or software exists.

IRRAS-PC was developed for use in the nuclear power plant PRAs. IRRAS-PC can be applied to all other industries which use fault trees for analysis of risk, reliability, availability or maintainability of systems. IRRAS-PC has been released to companies in the aerospace, chemical, defense nuclear power and computer industries, such as AT&T Bell Labs, Commonwealth Edison, JBF Associates, Sargent & Lundy Engineers, Morton Thiokol, and Science Applications International Corporation.

In almost all industries today the move is towards greater automation. This increased automation typically results in more complex systems with an associated increased concern for reliability and maintainability. IRRAS-PC provides the capability to perform analysis on these systems before they are constructed to ensure that the concerns are minimized and the long term effectiveness of the system is increased. Once in operation IRRAS-PC can be used to study proposed design or system modifications in light of these important factors. This software puts this important science in the hands of a much larger group than was previously possible with the complexity and cost of the computers required to operate existing software. Not only does this software increase the number of users of Probabilistic Risk Assessment, but it significantly improves the user interface and reduces the time and cost required to perform studies.

FOR ADDITIONAL INFORMATION: Contact:
Dr. Jane Welch
ORTA Office
Idaho National Engineering Laboratory
P. O. Box 1635
Idaho Falls, ID 83415
(208) 526-8318
Refer to DOE/INEL-018/TN

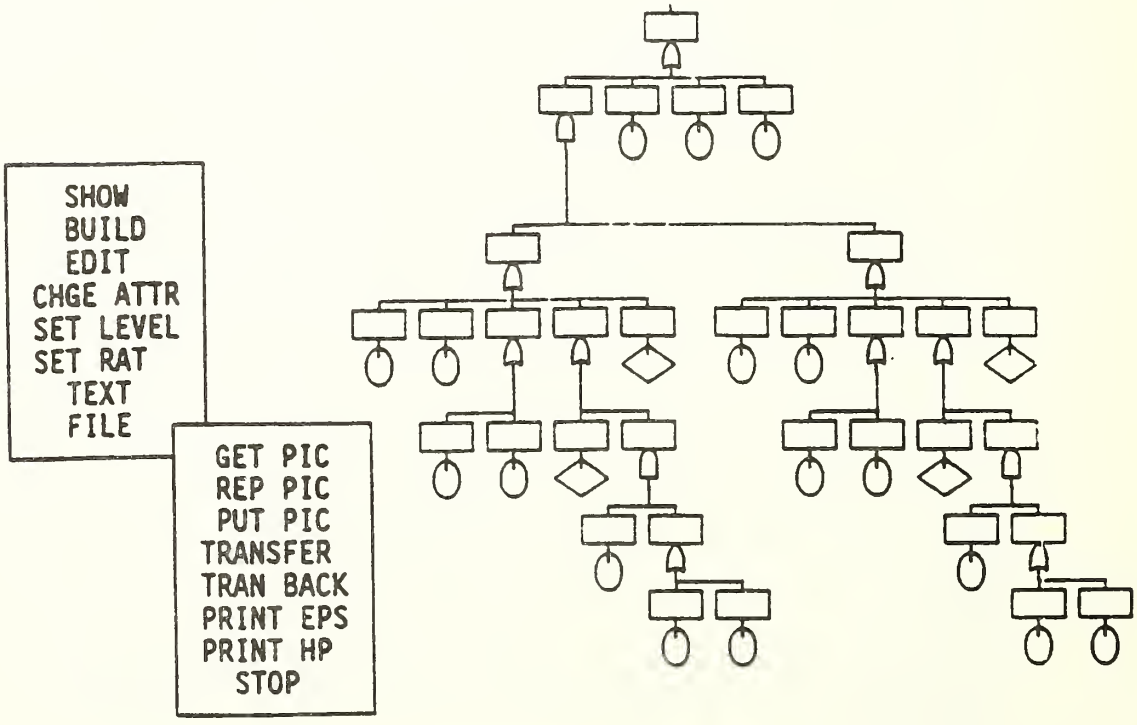

IRRAS Fault Tree with Pop-up Menus.

Electrotechnology

831 VHSIC/VHSIC-Like Reliability Modeling

832 Out-of-Band Response of Antenna Arrays

833 Optoelectronic Docking System — Sensors and computers control approach and coupling.

834 Theoretical Efficiencies of Microwave Diode Triplers — Simulations are conducted for 300- to 900-GHz units.

835 MOSFET's for Cryogenic Amplifiers — A study seeks ways to build transistors that function effectively at liquid-helium temperatures.

836 Radar Time-Base and Pseudonoise Generator — Long pulses are effectively compressed by a pseudonoise techique.

837 VLBI System for Satellite Navigation — A system is described, and its anticipated performance is analyzed.

838 Three-Axis Attitude Control With a Single Wheel — Internally gimbaled wheel plus reaction torquing combine to yield three-axis control. (Licensing Opportunity)

839 Switching Circuit for Shop Vacuum System — No internal connections to machine tools are required.

840 Overriding Faulty Circuit Breakers — A retainer keeps power on in an emergency.

Testing & Instrumentation

841 Microelectronic Parts Field Failures — A new project will help engineers avoid predominant failure mechanisms.

842 Effectiveness of Microcircuit Device Screening

843 Infrared Systems Developed to Test Gallium Arsenide Wafers

Other items of Interest

849 Improving Solar Cells with Polycrystalline Silicon — Thin layers arranged strategically would make cells more efficient.

U.S. Air Force
Reliability Analysis Center (RAC)
Rome Air Development Center, Griffiss Air Force Base, NY 13441

VHSIC/VHSIC-Like Reliability Modeling

IIT Research Institute has recently teamed with Honeywell to initiate a study under contract to RADC to develop VHSIC and VHSIC-like reliability prediction models. Since meaningful amounts of empirical field reliability data are not expected to be available for use in model development, these prediction methodologies will be based predominantly on information available during circuit fabrication.

The information to be used in this study is available from electronically addressable test structures used to monitor and control various fabrication processes. By using this information as a baseline, this study will correlate data on each failure mechanism to the applicable test structure data and then to macro level reliability performance. This is a radical departure from traditional techniques used to develop reliability prediction models in that extensive quantities of historical failure data are not required.

The intent of these models is ultimately for inclusion in MIL-HDBK-217, and therefore the models must be easy to use, easily updated and sensitive to the pertinent fabrication processes. To meet these goals and achieve prediction models acceptable to the user community, IITRI is currently seeking feedback from individuals knowledgeable in VHSIC/VHSIC-like fabrication, reliability, failure mechanism modeling, yield-reliability correlations, etc. Anyone wishing to discuss this effort is encouraged to call William Denson at (315) 336-2359.

NBS technology update

National Bureau of Standards
U.S. Department of Commerce
Gaithersburg, MD 20899

Out-of-Band Response of Antenna Arrays

The response of antennas to out-of-band frequencies plays an important role in interference and jamming problems. NBS has previously studied and reported on the out-of-band response of reflector antennas and now has continued the work by investigating antenna arrays. A new report analyzes arrays at out-of-band frequencies; effective aperture, directivity, and impedance mismatch are treated in detail. Near-field measurements made on two large arrays of slotted waveguides are reported, and the subject of sampling in frequency and space is considered.

FOR ADDITIONAL INFORMATION: Out-of-Band Response of Antenna Arrays (NBSIR 86-3047) is available from the National Technical Information Service, Springfield, VA 22161, for A03 prepaid. Order by PB87-125746/NAC

NASA Tech Brief
National Aeronautics and Space Administration
Lyndon B. Johnson Space Center, Houston, Texas

Optoelectronic Docking System

Sensors and computers control approach and coupling.

A proposed optoelectronic system with no moving parts would automatically control the approach of two spacecraft as they closed from a distance of about 1 km to within a few cm. The system concept could probably be modified for use on Earth in robotic assembly, to control the docking of large ships, or to guide the placement of large structural components.

Through light emitters, sensors, and microcomputers on the approaching vehicle, the control system detects and computes the relative position, orientation, and velocity of target retroreflectors on the approached vehicle (see figure). The velocity and roll (spin along the docking axis) of the approaching vehicle are set in response to these computed quantities, starting with a rapid approach at long range along a direction that may be several degrees off target and ending with a slow, precise approach at close range as the two vehicles become aligned in both position and angle.

When the spacecraft are 1 km apart, the central processing unit of the optoelectronic system turns on a pulsed-laser ranging subsystem. The light from each of 20 GaAs laser diodes is formed by a cylindrical lens into a fan-shaped beam of 1° by 20°. The light reflected by the retroreflectors back to the sensor array is channeled into an array of 20 photodiode detectors by cylindrical lenses, along fan-shaped beams of 1° by 20° that are perpendicular to the transmitted beams. The emitting and detecting diodes are switched on in sequence so that the entire 20° by 20° field of view is sampled in the sequence of 1° by 1° overlaps of the transmitted and received beams. The direction to the target is thus determined to within the 1° by 1° sector that contains the target reflection, while the distance to the target is determined from the time of flight of the light pulses; the approach speed is calculated from the rate of change of the distance.

At a distance of 30 m, the approach-control task is handed to a continuous-wave-laser tracking subsystem, which distinguishes among the return signals from the three retroreflectors. In this case, the 20° by 20° field of view is still scanned by driving 20 transmitting and 20 receiving diodes in sequence, but the three target returns are detected in separate diodes, and the distance (within about ±3 cm) to each retroreflector is computed by measurement of the relative phase, in the return signal, of a 3-MHz modulation imposed on the transmitted signal.

From the three range signals, the system computes the average target distance and the orientation of the target relative to the line of sight. The coordinates of the return signals are also processed to compute both the direction to the target and the target roll angle and roll rate.

A charge-coupled-device-television/pulse-ranging system takes over at distances of less than 3 m: from 3 m to 1 m,

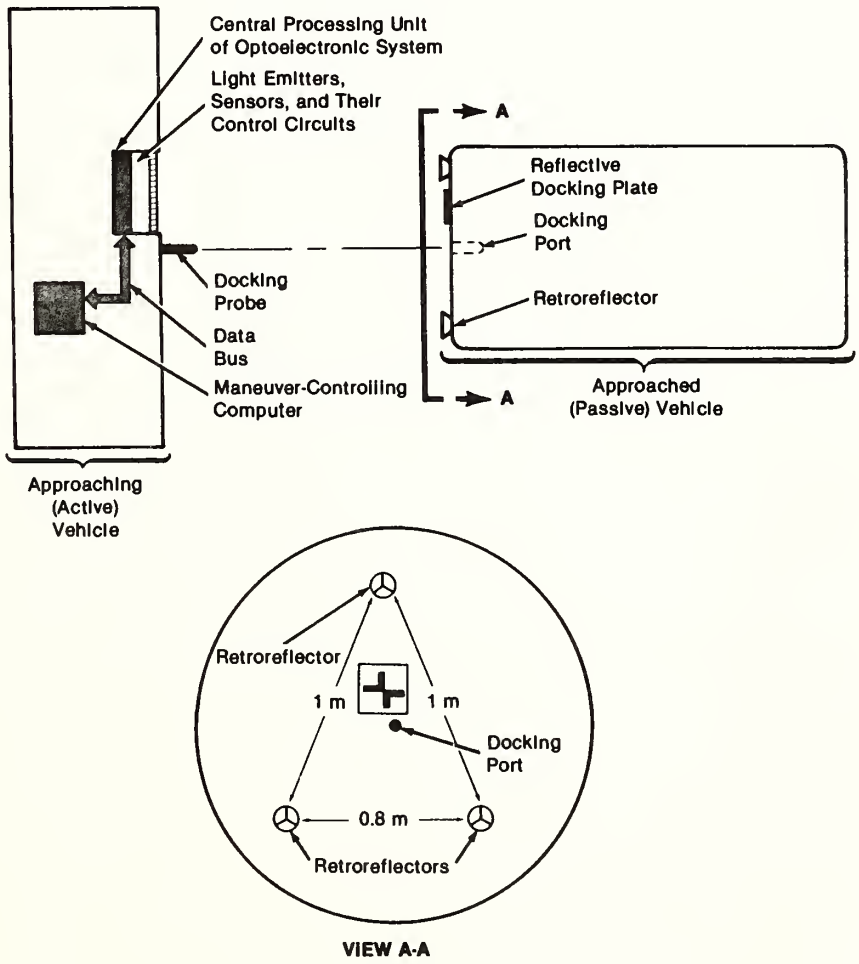

The **Optoelectronic Docking System** automatically controls the approach of an active vehicle or mechanism to a passive vehicle or object. The maneuvers of the approaching vehicle are controlled in response to the optoelectronically sensed relative position of the approached vehicle.

the system processes the outline of the reflective docking plate in the television image to determine the target pitch and yaw; at 1 m, the docking-plate image exceeds the camera field of view and the system begins to seek alignment between four laser beams and the converging edges of the dark pattern in the docking plate; at a distance of 35 cm, the docking probe enters the docking port; and at 20 cm, the probe closes a hard-docking indicator switch, which deactivates the system.

This work was done by Steven M. Ward of Energy Optics, Inc., for **Johnson Space Center**. *MSC-21159 /TN*

FOR ADDITIONAL INFORMATION: *Contact: Director, Technology Transfer Division, P.O. Box 8757, BWI Airport, MD. 21240; (301) 621-0100 Ext. 241*

REFER TO THE NUMBER LISTED AT THE END OF THE ARTICLE

NASA Tech Brief
National Aeronautics and Space Administration

Theoretical Efficiencies of Microwave Diode Triplers

Simulations are conducted for 300- to 900-GHz units.

A report discusses computer simulations of 300- to 900-GHz triplers using nonideal GaAs Schottky diodes operating in the varistor mode. The nonlinear boundary-value problem posed by the diode state equations cannot be solved in closed form. Consequently, such computer simulations are needed to optimize the tripler configuration and operating conditions.

Even though varistors have series resistance, they are more efficient than varactors at the frequencies of interest because they have greater cutoff frequencies. Therefore, in this analysis the diode is considered to operate in the forward-bias (varistor) mode. The mathematical model of the tripler includes the diode series resistance, the dc bias current, the pump-oscillator input, the harmonic outputs, the voltage-dependent portion of the diode resistance, the junction capacitance (which is approximated as constant at the zero-bias value), and the network of impedances representing the diode mount.

To facilitate an iterative solution, the model also includes a lossless transmission line at the interface between the diode junction and the mount. The transmission-line length is set to an integral number of wavelengths at the pump frequency (300 GHz) so that the steady-state waveforms remain unaffected by this artifice. A dynamic boundary condition poses an unbalanced transmission-line system, for which the settling behavior is well defined. Part of an initial wave propagating toward the diode is reflected back toward the mount, part of the back-reflected wave is reflected by the mount toward the diode, and so forth. When the waves in both directions have settled down to equal magnitudes, the steady-state solution has been attained.

At the beginning of a computation, the pump power and diode bias are set at the desired operating levels. The mounting-network impedances are set to arbitrary design values at the harmonics to be considered. The computer then iterates the reflection cycle until the system converges to the operating point. At the pump frequency, the computer adjusts the mount impedance so that the pump power is completely absorbed. Thus, the pump-frequency impedance becomes an output of the program, and each operating-point calculation represents a different mount design.

A series of calculations was done using a set of parameters typical of a state-of-the-art mixing diode. The pump power was set at 40 mW, a level representative of the outputs of carcinotrons at 300 GHz. The dc bias current was systematically varied from run to run over the range of 3 to 25 mA. In runs corresponding to the optimum value of the imaginary component of mount impedance at 900 GHz, the maximum computed efficiency was about 7 percent. (An ideal varistor would exhibit about 11 percent efficiency.)

This work was done by Margaret A. Frerking and Katherine Benson of Caltech for **NASA's Jet Propulsion Laboratory**. *"Theoretical Efficiency for Triplers Using Non-Ideal Varistor Diodes at Submillimeter Wavelengths," NPO-16749 /TN*

FOR ADDITIONAL INFORMATION: *Contact: Director, Technology Transfer Division, P.O. Box 8757, BWI Airport, MD. 21240; (301) 621-0100 Ext. 241*
REFER TO THE NUMBER LISTED AT THE END OF THE ARTICLE

NASA Tech Brief
National Aeronautics and Space Administration

MOSFET's for Cryogenic Amplifiers

A study seeks ways to build transistors that function effectively at liquid-helium temperatures.

A report discusses the physics of metal-oxide/semiconductor field-effect transistors (MOSFET's) and the performances of these devices at cryogenic temperatures. MOSFET's are useful in highly sensitive cryogenic preamplifiers for infrared astronomy.

Astronomers would like to improve the signal-to-noise ratios of receivers by operating the preamplifiers at the same temperature as the detectors — as low as 1.4 K. Currently available MOSFET's are designed to operate primarily at room temperature but perform well at temperatures as low as 60 K. Below that, however, the performance degrades rapidly as the temperature decreases.

The report discusses electrical measurements of p-channel, enhancement-mode MOSFET's over the temperature range from 300 to 4.3 K. Current-versus-voltage measurements were made as a function of temperature on MOSFET's on integrated-circuit chips, each of which contained four transistors. The average channel lengths of the four transistors on each chip were 3.27, 5.68, 8.37, and 11.39 μm, respectively. The devices were made on (1,1,1)-plane silicon wafers doped with phosphorus to a level of 2.5×10^{16} cm^{-3}. The p^+ source and drain wells were formed by boron diffusion.

The devices with shorter channels performed better in the range of 4 to 20 K than those with longer channels. Additional testing will be done down to 1.4 K, with various channel-dopant levels.

The report explains carrier freeze-out, which is the principal mechanism that degrades performance at low temperatures. It discusses how the mechanism might be circumvented by increasing impurity concentrations. MOSFET's with p-channels can be made in p-type silicon wafers so that the gap between acceptor and valence bands is much less than 0.04 eV. Such devices will not operate at room temperature but may operate well at very low temperatures.

This work was done by Robert DeHaye of **Marshall Space Flight Center** *and Carl A. Ventrice of Tennessee Technological University. "Electrical Performance of Semiconductor Devices at Cryogenic Temperatures," MFS-27111 /TN*

FOR ADDITIONAL INFORMATION: *Contact: Director, Technology Transfer Division, P.O. Box 8757, BWI Airport, MD. 21240; (301) 621-0100 Ext. 241*
REFER TO THE NUMBER LISTED AT THE END OF THE ARTICLE

NASA Tech Brief
National Aeronautics and Space Administration
NASA's Jet Propulsion Laboratory, Pasadena, California

Radar Time-Base and Pseudonoise Generator

Long pulses are effectively compressed by a pseudonoise technique.

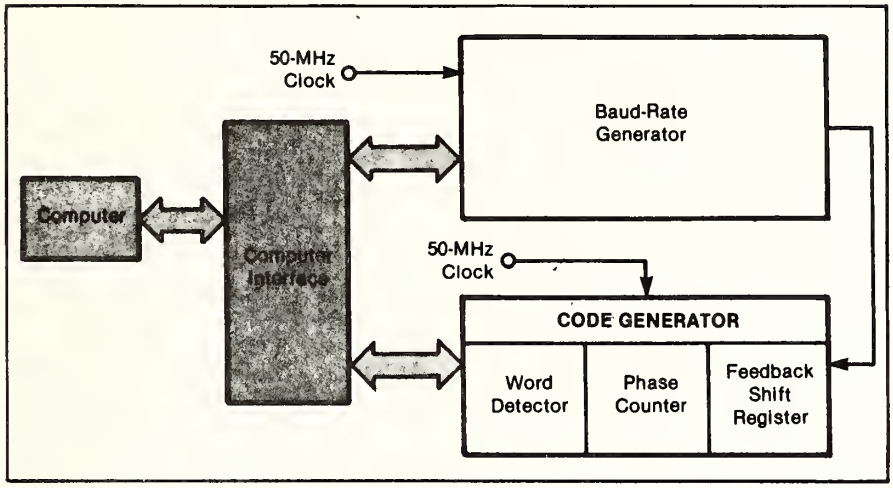

The **Polynomial-Driven Time-Base and Pseudonoise Generator** produces a polynomial binary code sequence in a receiver to track that of the received signal within 20 ns.

A computer-controlled, polynomial-driven time-base and pseudonoise generator (see figure) will enable a radar system to achieve a range resolution of about 80 m with radar pulses of 1-s duration. Normally, an unmodulated 1-s pulse would have a relatively coarse range resolution of several thousand kilometers. However, this radar system effectively compresses a modulated pulse into one of the 100-ns pseudonoise-modulating pulses. Intended primarily for use with interplanetary radar, the time-base/pseudonoise concept may also prove useful in test instruments or in time-base correction for video recording.

As in other spread-spectrum systems of the same general type, the pseudonoise modulation is derived from maximal-length binary codes that yield an optimum correlation function with minimum side lobes and with the lowest possible signal-to-clutter ratio. The code sequence is specified by a polynomial that is implemented by feedback shift registers. In the radar receiver, a pseudonoise generator similar to that of the transmitter is used for the coherent detection (cross correlation) of the received modulated pulses.

In the return signal, both the carrier frequency and the modulation are expanded or contracted in time by the Doppler shift caused by the relative motion between the station and the target. For coherent detection, it is necessary to vary the time base of the receiver pseudonoise generator to match that of the pseudonoise modulation of the return signal.

In the receiver, a 50-MHz clock is synchronized with the precise 1-s transmitter pulses. The time base (shifting rate) for the shift register in the pseudonoise generator is set by the baud-rate generator, which operates on the 50-MHz clock signal to produce a clock signal of 10 MHz plus or minus a small increment. This skewed clock signal is used in tracking the time shifts in the return signal caused by the relative motion between the station and the target.

In the code-generator portion of the pseudorandom-noise generator, the feedback taps on the shift register are selected for the desired code by a programmable read-only memory. Codes up to 2^{24} in length are available. A word detector and a phase counter are used to determine the precise elapsed time between the most recent 1-s pulse and the detection of a word. The starting time of the receiver pseudonoise signal is set accordingly. The receiver pseudonoise signal tracks the correct phase within ±20 ns over the entire code length.

This work was done by Stanley S. Brokl of Caltech for **NASA's Jet Propulsion Laboratory**. *NPO-16361 /TN*

FOR ADDITIONAL INFORMATION: *Contact: Director, Technology Transfer Division, P.O. Box 8757, BWI Airport, MD. 21240; (301) 621-0100 Ext. 241*
REFER TO THE NUMBER LISTED AT THE END OF THE ARTICLE

NASA Tech Brief
National Aeronautics and Space Administration

VLBI System for Satellite Navigation

A system is described, and its anticipated performance is analyzed.

A report discusses a proposed low cost very-long-baseline interferometric (VLBI) system dedicated for use with the Tracking and Data Relay Satellite System (TDRSS) in determining the orbits of user satellites. The theoretical accuracies of the orbits to be measured by the new system are compared with similar orbital determinations by other satellite-navigation systems, based on the anticipated state of the VLBI art in the year 1990.

Ideally, the VLBI system would include four 1-m antennas for each TDRS at the ends of orthogonal 6,000-km baselines, with the TDRS centered above the intersection of the baselines. It is also possible to use three antennas at the corners of an equilateral triangle with the TDRS located above the centroid. The system would measure the differential one-way range to a satellite station from the two antennas at the opposite ends of each baseline, using quartz clocks with a system noise temperature of 300 K. A special receiver would be used to calibrate the ionospheric and clock offsets, using the dual L-band signal transmitted by the Global Positioning System (GPS) satellites. Calibrations would be performed at each differential one-way measurement.

One set of instrument errors of the proposed system is based on the capabilities of the portion of the GPS system scheduled to become available about now. A second set of errors is based on the assumed deployment, around the year 1990, of the complete 18-satellite GPS and the SERIES/X radiometric system of geodetic receivers for tracking satellites in low orbits around the Earth. The ephemeris error is assumed to be 5 meters in the supposed present system and is expected to decrease to less than 1 meter with the 1990 system.

The performance of the VLBI system was evaluated using the assumed instrument errors in an ideal four-antenna configuration. First, the TDRSS navigation accuracy was assessed in terms of the maximum position error during a 24-hour period, assuming the acquisition of differential one-way ranges from both baselines every two hours. Next, error analyses were conducted for a Topex satellite in a circular orbit at an altitude of 1,330 km and an inclination of 65°, in which the predominant dynamic errors are expected to be due to the uncertainty of the geopotential field. Another analysis was conducted for a Space Shuttle at 280 km altitude and 28° inclination.

Based on the assumed 1990 VLBI system, the TDRSS orbit-determination accuracy is expected to improve by a factor of about 20. This translates into accuracy-improvement factors ranging from 3 to 10 for typical TDRSS users. Such error sources as instrument biases and uncertainties in station locations can be independently calibrated in the VLBI system. Other advantanges of the VLBI system are that it is susceptible to evolutionary improvements without additions to the basic system elements, that it reduces the sampling frequency and the volume of tracking data for TDRSS navigation, and that the loading requirements on the TDRSS Multiple-Access forward link are reduced.

This work was done by Jordan M. Ellis of Caltech for **NASA's Jet Propulsion Laboratory**. *"Performance of a Dedicated VLBI system for TDRSS Navigation,"*
NPO-16319 /TN

FOR ADDITIONAL INFORMATION: *Contact: Director, Technology Transfer Division, P.O. Box 8757, BWI Airport, MD. 21240; (301) 621-0100 Ext. 241*
REFER TO THE NUMBER LISTED AT THE END OF THE ARTICLE

NASA Tech Brief
National Aeronautics and Space Administration
Goddard Space Flight Center, Greenbelt, Maryland

Licensing Opportunity

Three-Axis Attitude Control With a Single Wheel

Internally gimbaled wheel plus reaction torquing combine to yield three-axis control.

A single-device attitude-control system provides stabilization along three axes. Conventionally, some combination of devices has been used for multiaxis control. For example, a system might include three low-speed reaction wheels, one for each axis, or two control-moment gyros, each of which can control two axes. These multiple device systems can be replaced by a multifunction device with a single moving element, having lower mass and potentially higher reliability.

The new system includes a flywheel driven by an electronically-commutated dc motor and supported by a torque-producing active magnetic bearing (see figure). This arrangement allows both the free rotation of the motor and flywheel about the central axis and limited angular torsional deflections of the flywheel about two orthogonal axes perpendicular to the central axis.

The bearing is a radially-servoed, permanent-magnet device that can produce cross-axis torques on the flywheel. The operation of the bearing, including the production of cross-axis torques, is described in "Magnetic Bearing With Radial and Angular Control," (GSC-12957) in this issue of *NASA Tech Briefs*. Three body-attitude sensors (for pitch, yaw, and roll) generate command signals along three orthogonal axes (x, y, and z, respectively). The signals energize coils that produce torques and the consequent limited angular excursions about the x and y axes, and control the speed of the flywheel about the z axis.

The flywheel turns at high speed of about 1,000 rad/s so that it can develop high gyroscopic torques with limited angular excursions. An energy-recovery system operates during the deceleration of the motor. This regenerative braking system makes high rotational speed practical. Without it, too much energy would be lost when the flywheel must be decelerated in response to control signals.

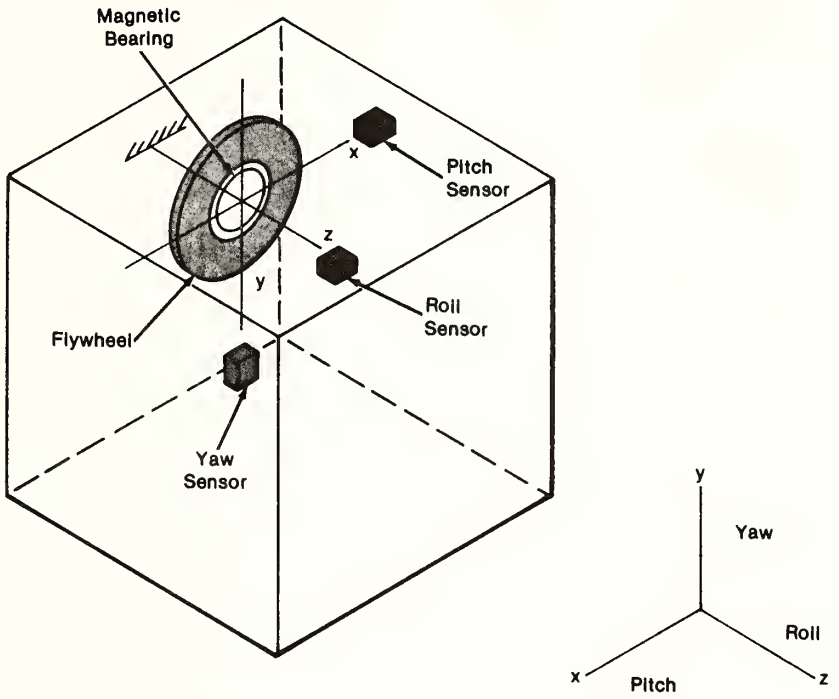

A **Flywheel Connected to an Electronically Controlled Motor** rotates on a magnetic bearing. At high rotational speed, small angular displacements about the x and y axes (in response to control signals) enable the storage of relatively large amounts of angular momentum. Angular momentum about the z axis is stored in changes in the rotational speed.

This work was done by Philip A. Studer of **Goddard Space Flight Center.**

This invention is owned by NASA, and a patent application has been filed. Inquiries concerning nonexclusive or exclusive license for its commercial development should be addressed to the Patent Counsel, Goddard Space Flight Center Refer to GSC-12970 /TN

Goddard Space Flight Center
Technology Utilization Officer:
Donald S. Friedman
Mail Code 702-1
Greenbelt, MD 20771
(301) 286-6242
Patent Counsel:
John O. Tresansky
Mail Code 204
Greenbelt, MD 20771
(301) 286-7351

NASA Tech Brief
National Aeronautics and Space Administration
Marshall Space Flight Center, Alabama

Switching Circuit for Shop Vacuum System

No internal connections to machine tools are required.

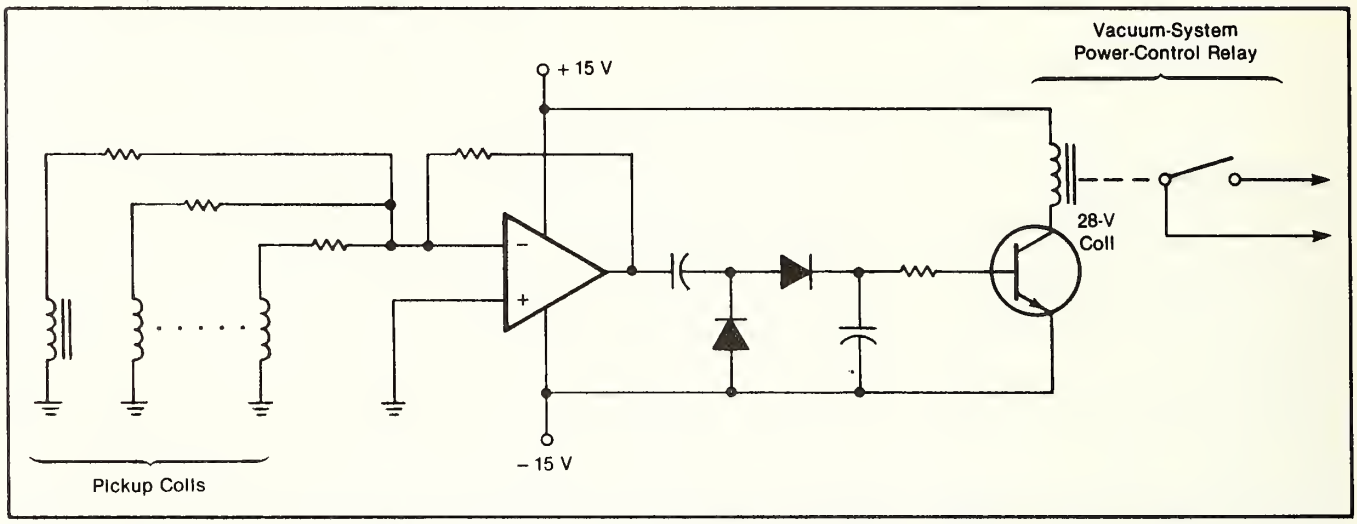

The **Pickup Coils Sense the Alternating Magnetic Fields** just outside the operating machines. A signal from any coil or combination of coils causes the vacuum system to be turned on.

A switching circuit controls a vacuum system that draws debris from grinders and sanders in a machine shop. The circuit automatically turns on the vacuum system whenever at least one sander or grinder is operating. Thus, debris are safely removed, even when the operator neglects to turn on the vacuum system manually.

The circuit was devised for a shop in which different sanders and grinders operate at different voltages. The installation of a conventional control for an automatic vacuum system would be expensive because of the complexity of the equipment needed to accommodate the different voltages.

The switching circuit is simple, inexpensive, and easy to install. No internal electrical or mechanical connection has to be made to any of the shop machinery other than the vacuum system. A small inductor is glued to the outside of the motor housing of each machine to pick up the small alternating magnetic field transmitted through the housing during operation.

The coil output is amplified 10^4 times, rectified, filtered, and applied to the base of a switching transistor (see figure). The transistor controls the current to the vacuum-system power relay. Since the pickup coils are wired in parallel, the system switches on whenever at least one of them puts out an "on" signal. (To assure reliable operation with any combination of one or more machines operating, it may be necessary to orient all coils for the same polarity.)

This work was done by Richard K. Burley of Rockwell International Corp. for **Marshall Space Flight Center.** *No further documentation is available.*
MFS-29153 /TN

FOR ADDITIONAL INFORMATION: *Contact: Director, Technology Transfer Division, P.O. Box 8757, BWI Airport, MD. 21240; (301) 621-0100 Ext. 241*
REFER TO THE NUMBER LISTED AT THE END OF THE ARTICLE

NASA Tech Brief
National Aeronautics and Space Administration
Lyndon B. Johnson Space Center, Houston, Texas

Overriding Faulty Circuit Breakers

A retainer keeps power on in an emergency.

A simple mechanical device can be attached to a failed aircraft-type push/pull circuit breaker to restore electrical power temporarily until the breaker can be replaced. The device holds the push/pull button in the closed position, making it unnecessary for a crewmember to hold the button in that position by continual finger pressure.

The circuit breaker normally operates in the closed position, which is maintained by an internal mechanism unless the breaker is intentionally opened or trips because of an overcurrent. If the mechanism malfunctions or breaks, a spring on the actuator opens the breaker and keeps it open. This type of mechanical failure is overcome by the retaining device.

The retaining device consists of an internally threaded sleeve and a threaded plug (see figure). One end of the sleeve fits over the circuit-breaker button and is screwed onto the threads that extend from the circuit-breaker mounting nut. The plug is screwed into the open end of the sleeve. As the plug is sufficiently advanced into the sleeve, it pushes the button, closing the circuit breaker. Left in this position, the plug maintains a closed circuit.

The plug can be inserted in the sleeve after a failure, or it can be held in the sleeve and tightened when a failure occurs. If the plug end of the sleeve is left unthreaded, the plug cannot be removed from the sleeve and therefore cannot be lost. When the plug is turned fully counterclockwise, it clears the circuit-breaker button; in this configuration the device serves as a guard to prevent the circuit-breaker button position from being changed accidentally.

The retaining device does not interfere with the electrical function if the circuit breaker is of the "trip-free" type: an overcurrent will still trip the breaker to the open position even though the device is holding it closed.

This work was done by Richard L. Robbins of Rockwell International Corp. and Thomas E. Pierson of Ford Aerospace for **Johnson Space Center**. *MSC-20583 /TN*

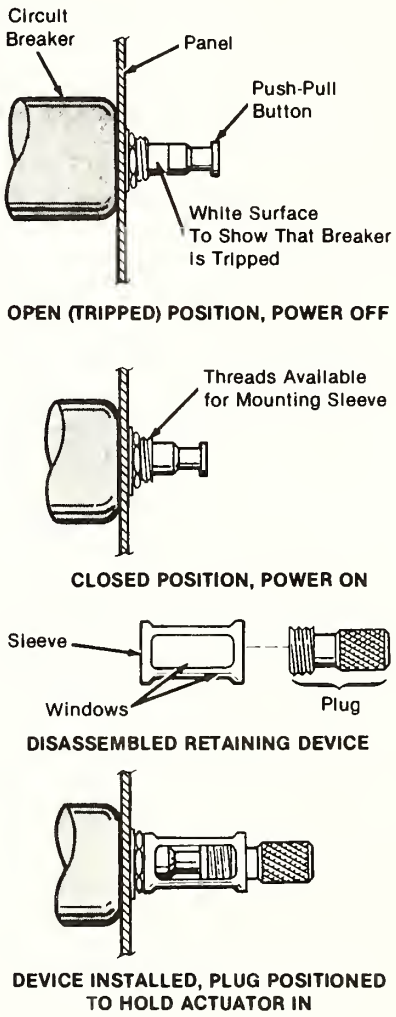

A Sleeve and a Plug Hold the Button In, overriding a mechanical failure in the circuit breaker. Windows in the sleeve show the button position.

FOR ADDITIONAL INFORMATION: *Contact: Director, Technology Transfer Division, P.O. Box 8757, BWI Airport, MD. 21240; (301) 621-0100 Ext. 241*
REFER TO THE NUMBER LISTED AT THE END OF THE ARTICLE

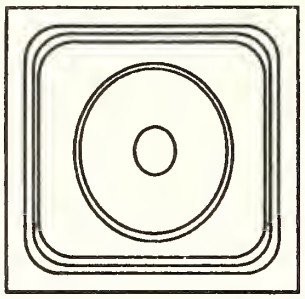

U.S. Air Force
Reliability Analysis Center (RAC)
Rome Air Development Center, Griffiss Air Force Base, NY 13441

Microelectronic Parts Field Failures

A new project will help engineers avoid predominant failure mechanisms.

There is a serious lack of useful part field failure data available to industry/government personnel. The existing failure information database is deficient in terms of analyzing failure causes or the relative makeup of failure modes and mechanisms. Rarely is a defect found in the field, examined, failure mechanism noted, and the cause of failure determined.

The purpose of this in-house project is to analyze microelectronic parts that have failed in the field, specifically to identify the part failure mode, failure mechanism and cause of failure and to develop a useful data base of confirmed field failures.

The results will help the engineers design in features to avoid the predominant failure mechanisms. Part manufacturers will better understand the workmanship flaws that are most prevalent in the field and can so reevaluate their own processes and take corrective actions. And finally, the government can use the results to fine-tune the part standards/specifications system.

If you are interested in the project or would like more information please call Project Officer: Capt. Thomas J. Green, RADC/RBRE, (315) 330-4029.

U.S. Air Force
Reliability Analysis Center (RAC)
Rome Air Development Center, Griffiss Air Force Base, NY 13441

Effectiveness of Microcircuit Device Screening

Experience shows that a newly constructed equipment fails more often during its early life (i.e., during assembly and testing) than later during use in the field. This indicates that piece parts received from suppliers contain a certain number of weak devices which tend to fail during the initial testing of subassemblies or complete equipments.

The relatively large number of failures witnessed early in the lifetime of some parts is normally attributable to the natural variability found in production processes. The unavoidable manufacturing variations in materials and processes cause a distribution of strengths to develop within a component population. These variations introduce weaknesses into some parts and not in others and consequently the weak parts have the potential to develop into failures which occur early in the population's lifetime.

Manufacturing deviations at the piece part level are precipitated as process defects which become the dominant cause of rework, scrap and yield losses. In order to eliminate the incipient failures from the manufacturing process, quality and screening tests can be employed. Specifically to accommodate these manufacturing insufficiencies, most manufacturing operations have included progressive inspection sequences, rework stations and repair loops as integral elements in the manufacturing process. However, screening is often a controversial issue since in the short-run its intrinsic value conflicts with economic considerations.

Parts screening, especially burn-in for semiconductors, is a key factor in removing defective parts. The purpose of a screen is to rapidly precipitate an adequate proportion of contained defects or flaws. The term "screening" can be defined as the application of a stress test or tests to electronic devices which will reveal inherent weaknesses (and thus incipient failures) without destroying the integrity of the device. This procedure, when applied equally to a group of similar devices manufactured by the same processes, is used to identify sub-par members of the group without impairing the structure or functional capability of the "good" members of the group.

Subjecting microelectronic devices to a battery of tests throughout their development is intended to identify and eradicate potential weaknesses which may exist in a component population. In the preliminary stages of product development, certain tests can precipitate failures that have been induced by the product design or in the manufacturing processes. The tests are designed to surface problem areas requiring rework and process verification to establish a baseline reliability from which further developments can proceed. Ultimately, the tests will ensure that the inherent reliability of a component population is of an acceptable level to produce a quality item.

The acute attention developing in the manufacturing community toward "doing it right the first time" attests to a prevailing attitude that building quality into a product is not only respectable but also profitable.

However, the use of testing as an avenue to greater product reliability becomes hotly debated when well-established and mature technologies are subjected to the same rigorous testing as newly emerging ones are. Theoretically, continued testing on a product that has been fine-tuned through years of successful production should yield minimal impact on improving overall quality. This, however, is not always substantiated by the field reliability and is therefore cause for debate.

The Reliability Analysis Center's most recent study focuses on the relative effectiveness of microcircuit screening. It is believed that a potentially reliable design is ultimately only as reliable as its manufactured quality will allow; however, reliability design and testing each make important contributions to the achievement of improved field reliability. **MDR-22, "Microcircuit Device Screening Data and Analysis"**, is the latest in the series of device reliability documents offered by the RAC. Additionally, the detailed data portion of the book will be available on floppy disks. The "floppy copy" allows users with IBM-compatible PCs to utilize the data to create custom analyses to fit individual needs.

For further information concerning **MDR-22 Microcircuit Device Screening Data and Analysis** please contact: Donald E. Rash, (315) 336-2359.

NBS technology update

National Bureau of Standards
U.S. Department of Commerce
Gaithersburg, MD 20899

Infrared Systems Developed to Test Gallium Arsenide Wafers

Detecting flaws in gallium arsenide (GaAs) semiconductor materials should be easier with two polarized infrared light systems developed by NBS Semiconductor Electronics Division researchers. Both are non-destructive methods wafer manufacturers can use to screen materials before marketing. One system can examine an entire wafer, while the other employs a 75- to 600-X microscope to view isolated wafer portions. Both systems allow digital storage of images and the use of false-color graphics to represent wafer characteristics such as variations in the transmitted infrared intensity, which could indicate potential problems. GaAs wafer applications in high-speed electronic and opto-electronic devices are growing rapidly, but production of the near-perfect GaAs crystals needed for optimum performance is not as advanced as with the older silicon technology. The two NBS systems can aid in production control by pinpointing wafer flaws and inhomogeneities. Bureau researchers are using the infrared techniques in-house, but will also assist industries in setting up their own systems.

FOR ADDITIONAL INFORMATION:

To discuss this effort further, contact:
Dr. Michael Bell
Technology Bldg., Room A-305
National Bureau of Standards
Gaithersburg, MD 20899
(301) 975-2081

Energy

844 Ceramic Two-Cycle Engine Development

845 CACS Conservation Actions in Small Commerical Building

846 Cooling Season Performance of an Earth-Sheltered Office/ Dormitory Building

847 Residential Photovoltaic/Thermal Energy System — A proposed system would supply a house with both heat and electricity.

848 A Surface-Controlled Solar Cell — The open-circuit voltage and the cell efficiency may be increased. (Licensing Opportunity)

849 Improving Solar Cells with Polycrystalline Silicon — Thin layers arranged strategically would make cells more efficient.

Other items of Interest

854 Elastic Hinge for Solar-Cell Array — A lightweight, compact hinge provides part of its own closing torque. (Licensing Opportunity)

911 More Oil and Gas May Be Recovered by Using New Fracture Mapping Tool

MANUFACTURING TECHNOLOGY NOTE

U.S. ARMY MATERIEL COMMAND

Ceramic Two-Cycle Engine Development

The U.S. Army Tank-Automotive Command RD&E Center has a long-term plan for the evaluational development of ceramic engines. Part of this effort has involved a program to evaluate and demonstrate the potential benefits of a range of ceramic materials for diesel engine technology, and increase the experience baseline for component fabrication, product reliability and nondestructive evaluation (NDE).

The program has consisted of three basic tasks: Manufacture Prototype Ceramic Components; Conduct Single Cylinder Rig Tests; and Demonstrate Product Reliability.

The project effort has focused around evaluating the friction horsepower performance of a single cylinder, two-stroke, opposed piston diesel engine fabricated from conventional metal components, and with the substitution of ceramic components for the cylinder liner and pistons.

So far they have:

- Conducted baseline studies on a metal engine;
- Performed thermal and stress analyses for various ceramic material designs;
- Designed and fabricated alternative ceramic materials;
- Performed preliminary ceramic engine evaluations;
- Selected optimum ceramic component materials;
- Performed engine durability tests (goal 100 hours);
- Fabricated pistons by injection molding;
- Evaluated piston quality nondestructively.

FOR ADDITIONAL INFORMATION:

Their efforts have been reported in "Adiabatic End Systems" available from the Society of Automotive Engineers, 400 Commonwealth Ave., Warrendale, PA 15096; (412) 776-4841. Ask for publication, SP-700, costing $50.

"Fabricational Testing of a Ceramic Two-Cycle Diesel Engine" available from NTIS, Springfield VA 22161, (703) 487-4650. Ask for AD-A175229/NAC, price code A08.

To discuss these efforts further, contact Mr. Ernest Schwartz, Project engineer, U.S. Army Tank Automotive Command, ATTN: AMSTA-RGRD, Warren MI 48397-5000; (313) 574-5656.

CACS CONSERVATION ACTIONS IN SMALL COMMERCIAL BUILDINGS

The energy savings and cost effectiveness of single and multiple retrofit energy conservation actions in small commercial buildings has been examined. The information derived from these studies is useful to state governments and to utilities as they develop audit procedures under the Commercial and Apartment Conservation Service (CACS) Program. Four small commercial building models, prototypical of those covered by CACS, were defined. The four buildings were simulated using DOE-2.1, a computer program that calculates energy flows and equipment requirements on an hour-by-hour basis. CACS Program conservation measures and procedures that could be handled by DOE-2.1 were then incorporated into each building model, and the calculations were repeated for six different climates.

Reduced lighting levels, addition of local switches, and automatic controls for heating and air conditioning systems were found to be cost effective (simple payback period <5 years in all climates). Building envelope retrofits such as ceiling and wall insulation and caulking/weatherstripping were generally cost effective (or nearly so) in colder climates but only slightly so in the warmest climates; storm/thermal windows and doors were not cost effective in any climate considered.

Additional information:

Office of Technology Applications
Information Service
Martin Marietta Energy Systems, Inc.
P.O. Box X
Oak Ridge, TN 37831
Telephone: (615) 574-4192; FTS 624-4192

R. J. Kedl and T. K. Stovall, *Cost-Effectiveness of Single and Multiple CACS Conservation Actions in Small Commercial Buildings,* ORNL/CON-176, Oak Ridge National Laboratory (August 1985).

R. J. Kedl and T. L. Bircher, *Energy Conservation Case Studies for Model Commercial Buildings Covered by the CACS Program,* ORNL/CON-133, Oak Ridge National Laboratory (March 1985).

energygram®

COOLING SEASON PERFORMANCE OF AN EARTH-SHELTERED OFFICE/DORMITORY BUILDING

Continuous, detailed, hourly thermal performance measurements were taken from February 1982 to October 1984 in and around an occupied, underground, 4000-ft^2 office/dormitory building at the Oak Ridge National Laboratory. This building has a number of energy-saving features that have been analyzed with regard to their performance in a southeastern United States climate and with respect to overall commercial building performance. The analysis documents cooling season performance, effects of earth contact, interior thermal mass, an economizer cycle, and interface of an efficient building envelope with a central three-ton heat pump.

The earth-sheltered structure achieves a cooling energy savings of about 30% compared with an energy-efficient, above-grade structure and has the potential to save as much as 50%. The proper installation of the overhang, interior thermal mass, massive supply duct system, and earth contact team up to prevent summertime overheating. From May through September, this building costs a total of $300 (at 5.7 ¢/kWh) to cool and ventilate 24 hours a day. In addition, extensive data show that at least 90% of the occupants are comfortable all of the time.

An earth-contact shelter provides a stable thermal environment, enhances thermal comfort, blends well into the natural landscape, allows a quiet environment, reduces peak energy demands, and has the potential for very low maintenance requirements.

Innovative materials and construction techniques are needed to reduce first costs, and a means must be found to increase public acceptance of the concept, but it has great potential for such purposes as tornado or civil defense shelters.

Additional information:

Office of Technology Applications
Information Service
Martin Marietta Energy Systems, Inc.
P.O. Box X
Oak Ridge, TN 37831
Telephone: (615) 574-4192; FTS 624-4192

J. E. Christian, *Cooling Season Performance of an Earth-Sheltered Office/Dormitory Building in Oak Ridge, Tennessee,* ORNL/CON-151, Oak Ridge National Laboratory (July 1984).

J. E. Christian, *Thermal Envelope Field Measurements in an Energy-Efficient Office and Dormitory,* ORNL/TM-8571, Oak Ridge National Laboratory (April 1983).

J. E. Christian, *Detailed Thermal Performance Measurements and Cost Effectiveness of Earth-Sheltered Construction: A Case Study,* ORNL/CON-186, Oak Ridge National Laboratory (September 1985).

NASA Tech Brief
National Aeronautics and Space Administration

Residential Photovoltaic/Thermal Energy System

A proposed system would supply a house with both heat and electricity.

A pair of reports describes a concept for a self-sufficient heating, cooling, and power-generating system for a house. Panels on the walls of the house would provide hot water, space heating, and heat to charge a heat-storage system, and would generate electricity for circulation pumps and fans. Roof panels would generate electricity for the household, operate a heat pump for summer cooling, and provide supplementary winter heating via the heat pump, using the solar-cell cooling-fluid loop.

The wall panel includes a pair of glass sheets with an airspace between them and tiltable solar-cell boards on the outside. Banks of louvers between the glass sheets are rotatable like venetian blinds to expose an appropriate surface to the outside; a silvered side to reflect heat rays in summer and an oxidized copper side to absorb them in winter. In the heating season, a fan circulates room air over the louvers to extract their heat.

The exterior solar-cell boards are mounted at gaps between the louver banks so as not to cast shadows on them. The boards are tilted at an angle that changes with the season so that the boards face the Sun squarely and absorb a maximum of available light. In winter or summer, water for domestic use is pumped through a thin finned tube in the airspace to absorb heat. Vents at the tops and bottoms of the panels open the airspaces to the inside or outside of the house, depending on the season.

The roof panel includes asymmetric V-trough concentrators and photovoltaic strip modules. A photovoltaic strip runs along a tube at the bottom of a trough. Water or another coolant flowing at the base of a strip absorbs heat generated by the photovoltaic cells as they produce electricity. The householder would reverse the north/south orientation of the trough on the first days of spring and fall to ensure the maximum capture of sunlight.

The wall and roof panels can be used independently. A homeowner could elect to install wall panels only, roof panels only, or both wall and roof panels.

This work was done by M. Kudret Selcuk of Caltech for **NASA's Jet Propulsion Laboratory**. *"A Combined Photovoltaic-Thermal Energy System for Residential Applications" and "Analysis and Two Years of Testing of the Vee-Trough Concentrator/Evacuated Tube Solar Collector," NPO-15013 /TN*

FOR ADDITIONAL INFORMATION: *Contact: Director, Technology Transfer Division, P.O. Box 8757, BWI Airport, MD. 21240; (301) 621-0100 Ext. 241*
REFER TO THE NUMBER LISTED AT THE END OF THE ARTICLE

NASA Tech Brief
National Aeronautics and Space Administration
NASA's Jet Propulsion Laboratory, Pasadena, California

Licensing Opportunity

A Surface-Controlled Solar Cell

The open-circuit voltage and the cell efficiency may be increased.

A proposed technique for controlling the recombination velocity on solar-cell surfaces could provide cells of increased efficiency and open-circuit voltage. In present cells, uncontrolled surface recombination velocity degrades the open-circuit voltage and the efficiency. In a cell using the proposed technique, a transparent conducting layer, insulated from the cell contacts, would be biased (see figure) to enable variable control of the surface recombination velocity.

The fabrication process for one of the new solar cells includes the following two steps:

1. A solar cell with isolated junctions is made by use of oxide-masking and photolithographic techniques. Contacts to the junctions are made by the usual photolithographic metallization.
2. A thin, passivating oxide is grown at the surface (everywhere except at the junctions). On this oxide layer is superimposed a very thin, slightly absorbing layer of metal or of transparent and conducting oxide or polymer. This transparent conducting layer serves as an antireflective coating and also can be biased to alter the surface properties of the cell.

By the application of a suitable voltage with very little power consumption, the surface can be put in the enhancement mode to repel the minority carriers from the surface. This should enhance carrier collection at the junctions and increase the open-circuit voltage and the efficiency of the solar cell.

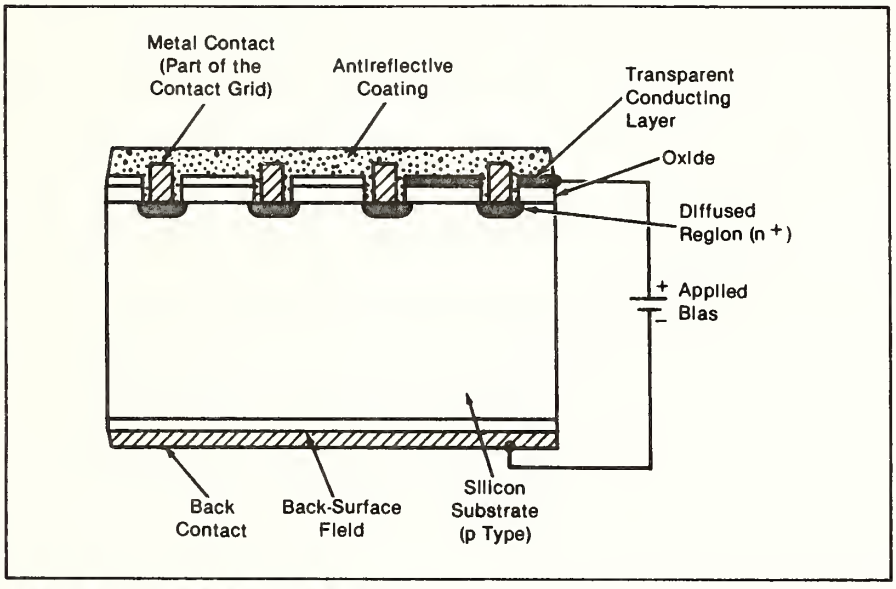

Biasing a Thin, Transparent Coating on a solar cell could enhance carrier collection at the junctions, increasing the open-circuit voltage and the efficiency.

This work was done by Taher Daud and Gerald T. Crotty of Caltech for **NASA's Jet Propulsion Laboratory.** *NPO-16430 /TN*

FOR ADDITIONAL INFORMATION: *Contact: Director, Technology Transfer Division, P.O. Box 8757, BWI Airport, MD. 21240; (301) 621-0100 Ext. 241*
REFER TO THE NUMBER LISTED AT THE END OF THE ARTICLE

NASA Tech Brief
National Aeronautics and Space Administration
NASA's Jet Propulsion Laboratory, Pasadena, California

Improving Solar Cells With Polycrystalline Silicon

Thin layers arranged strategically would make cells more efficient.

In a proposed solar-cell design, layers of polycrystalline silicon would be grown near the front metal grid and the back metal surface. The net electrical effect should increase the open-circuit voltage and the short-circuit current, resulting in greater cell power output and energy-conversion efficiency.

The figure shows the differences between the existing and proposed cell configurations. In the emitter region, a single-crystal layer of n^+-doped silicon, 0.3 μm thick, would be replaced by a 0.2-μm n^+ polycrystalline layer and a 0.1-μm n^+ single-crystal layer. This could be done by depositing first the polycrystalline layer on the p-doped base, then forming the n^+ region by diffusion through the polycrystalline layer. The polycrystalline layer should decrease recombination and reverse-saturation emitter current. In a typical surface-passivated cell with low base resistivity, high bulk lifetime, and a high ratio of reverse-saturation emitter current to reverse-saturation base current, the result should appreciably increase open-circuit voltage.

A second layer of n^+ polycrystalline silicon would be established under the metal of the front-surface contact grid. Although a typical grid covers only 5 percent of the front surface, it attracts many charge carriers from the surrounding regions, causing them to recombine at the metal/silicon interface. The interposition of the new doped polycrystalline layer creates a new polycrystalline/single-crystal contact interface with a recombination velocity much lower than that of the metal/silicon interface. To reduce the range of influence of the metal grid and thereby increase cell performance, the thickness of the polycrystalline layer should exceed the minority-carrier diffusion length in that layer.

To reduce recombination in the back-surface-field region, a p^+-doped polycrystalline layer would be added between the p^+ back-surface-field layer and the back metal contact. The decrease in recombination in the back-surface-field region should reduce the recombination at the p/p^+ interface, in turn reducing the base contribution to the total reverse saturation current. The net effect should appreciably increase open-circuit voltage in a cell that has a high-resistivity, low-lifetime base with a high ratio of reverse-saturation base current to reverse-saturation emitter current, or in a cell in which the polycrystalline layers have reduced the emitter recombination so much that the open-circuit voltage is limited mainly by recombination in the base side.

Experience with metal oxide/semiconductor devices has shown that polycrystalline layers can act as getter materials to remove impurities from the adjacent silicon during oxidation or high-temperature processing, consequently increasing carrier lifetimes from microseconds to milliseconds. Since the polycrystalline silicon layers in the improved solar cell are to be doped by high-temperature diffusion, similar increases in the bulk lifetimes of the solar cell are anticipated. Although this entails the gathering of impurities and defects into the polycrystalline layers, it has little adverse effect on cell performance because the polycrystalline layers are meant to be heavily doped (and therefore to have short lifetimes) in the first place.

This work was done by Ajeet Rohatgi, Robert B. Campbell, and Prosenjit Rai-Choudhury of Westinghouse Electric Corp. for **NASA's Jet Propulsion Laboratory.** *NPO-16820 /TN*

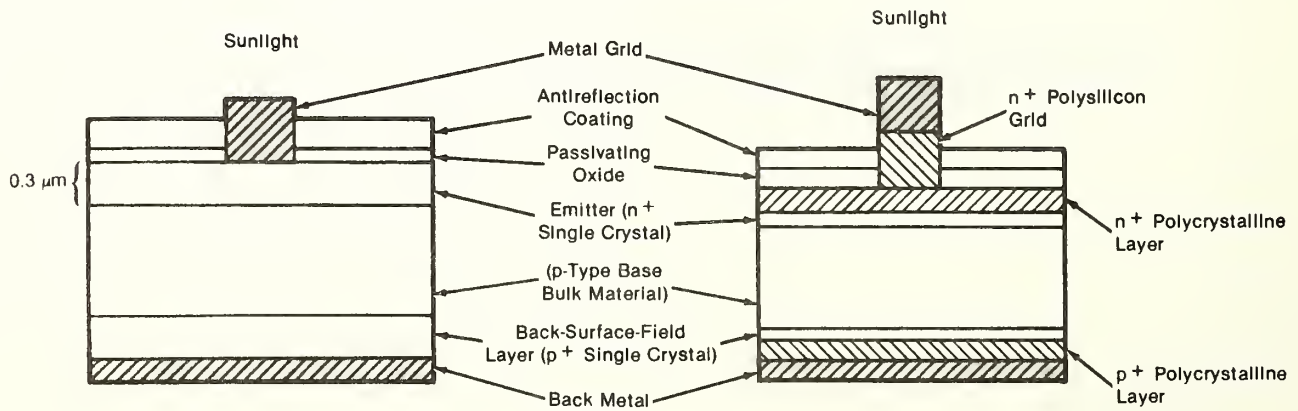

The **Proposed Solar-Cell Configuration** differs from the existing one in that layers of doped polycrystalline silicon are added to reduce recombination in the emitter and back-surface-field regions.

FOR ADDITIONAL INFORMATION: *Contact: Director, Technology Transfer Division, P.O. Box 8757, BWI Airport, MD. 21240; (301) 621-0100 Ext. 241*
REFER TO THE NUMBER LISTED AT THE END OF THE ARTICLE

Engineering

850 New Standard for Safety Colors

851 Water Purification Production Doubles in Desert

852 Locating Sonic Lines in Transonic Nozzles — New formulas predict accurately the line location in advanced convergent/ divergent nozzles.

853 Design Improvement for Airplane-Engine Nacelles — Better streaming reduces drag. (Licensing Opportunity)

854 Elastic Hinge for Solar-Cell Array — A lightweight, compact hinge provides part of its own closing torque. (Licensing Opportunity)

858 Increasing Maintainability of a Wastewater-Recovery Unit — A modified system leaks less and is easier to disassemble for maintenance.

Software

855 Interactive Computer Model for Calculating V-I Curves in Electrostatic Precipitators

856 Analysis of Scramjet Inlets — Viscous flow can be accounted for in the computations.

857 Buckling Analysis of Rectangular Plates With Holes — Loads and deflections are predicted for a variety of cutouts.

Testing & Instrumentation

859 Large-Area Radiation Portal/Personnel Monitor — A faster, more sensitive personnel monitoring system

860 Side-Looking Viewer for Crevices — Gaps only 1 mm wide are inspected with a thin metal mirror.

861 Measuring Thicknesses of Wastewater Films — A sensor resists excessive film buildup.

862 Large Wire Strain Gauges — Wires yield data on average strains over distances ranging from inches to many feet.

NBS technology update

National Bureau of Standards
U.S. Department of Commerce
Gaithersburg, MD 20899

New Standard for Safety Colors

As a result of several years of studies, researchers in the NBS Center for Building Technology have recommeded a new set of standard safety colors that can be identified more accurately under different types of lighting. The NBS researchers found that the current ANSI standard safety colors were not accurately identified under many common light sources. Fifty-eight safety colors were viewed under seven different light sources. Subjects had particular difficulty identifying colors under two types of sodium lights and clear mercury lights. The researchers found that the current ANSI orange and red often are not recognized accurately, and are confused with each other and with yellow. They have recommended a set of new colors, including fluorescent red and orange, which are more accurately recognized. The findings have been reported to the Occupational Safety and Health Administration. The American National Standards Institute (ANSI), which is currently revising its standard for safety colors, will consider including the NBS recommendations.

FOR ADDITIONAL INFORMATION: A report is available from the National Technical Information Service, Springfield, VA 22161.

NTIS price code: A07, prepaid

Order Safety Color Appearance Under Selected Light Sources

NTIS order number: PB87-152294/NAC

Water Purification Production Doubles in Desert

Temperatures perked to 110° under a scorching sun. But the well never ran dry for more than 20,000 thirsty Marine and Army personnel participating in simulated but realistic war games on the steamy Mojave Desert near Twenty Nine Palms, California.

All the drinking water they needed or wanted—more than one million gallons—was readily available during the six-day Gallant Eagle training exercise that finished in August.

This "on demand" water supply was generated by a series of water treatment systems that introduced the newly redesigned, more efficient, Reverse Osmosis Water Purification Unit (ROWPU), capable of producing 2,000 gallons of potable (drinkable) water an hour from the brackish water found in the desert. The new ROWPU also can produce 1,200 gallons of potable water an hour from seawater sources.

After three years of research and testing, the Naval Civil Engineering Laboratory (NCEL), Port Hueneme, California, successfully tested the larger and improved ROWPU designed for Marine Corps field combat operations. One singular advantage of the new unit is that it produces twice the amount of potable water as the original 600-gallon-per-hour purification system. Although it doubles water production, the NCEL design retains the same size of the earlier model.

For Additional Information:

Backup material on this effort is available from:

Navy Domestic Technology Fact Sheet
Reader Reply Service
Code E211
Naval Surface Weapons Center
Dahlgren, VA 22448-5000
(703) 663-8921

Refer to 120201/TN

NASA Tech Brief
National Aeronautics and Space Administration
Marshall Space Flight Center, Alabama

Locating Sonic Lines in Transonic Nozzles

New formulas predict more accurately the line location in advanced convergent/divergent nozzles.

A new set of formulas for the positions of sonic lines enables the more accurate determination of pressures, heat transfers, and flow-discharge coefficients in advanced convergent/divergent nozzles. Older, closed-form approximate solutions of the Sauer type were used to determine the best position. However, in advanced nozzles with shorter transonic fields, such approximations are no longer adequate.

The Sauer solution is described in A. H. Shapiro, *The Dynamics and Thermodynamics of Compressible Flow*, vol. 2, pp. 826—836, Ronald Press Co., 1953. The Sauer approximation for a two-dimensional (flat) nozzle is as follows:

$$\Delta x/y = -[(\gamma+1)R_T/9R_U]^{1/2}$$

For an axisymmetric nozzle, the approximation is the following:

$$\Delta x/y = -[(\gamma+1)R_T/32R_U]^{1/2}$$

In both cases Δx is the axial displacement of the sonic line, y is the distance from the axis to the point on the wall where Δx is measured, R_U is the radius of curvature of the nozzle throat in a plane that includes the axis, R_T is the distance from the axis to the throat at the narrowest part, and γ is the ratio of the specific heat of the flowing gas at constant pressure to that at constant volume. The minus sign indicates a displacement upstream.

Where R_U/R_T lies between 1 and 5, the new approximations are as follows:

$$\Delta x/y = -[(\gamma+1)R_T/140R_U]^{0.4}$$

for round nozzles and

$$\Delta x/y = -[(\gamma+1)R_T/40R_U]^{0.4}$$

for flat nozzles.

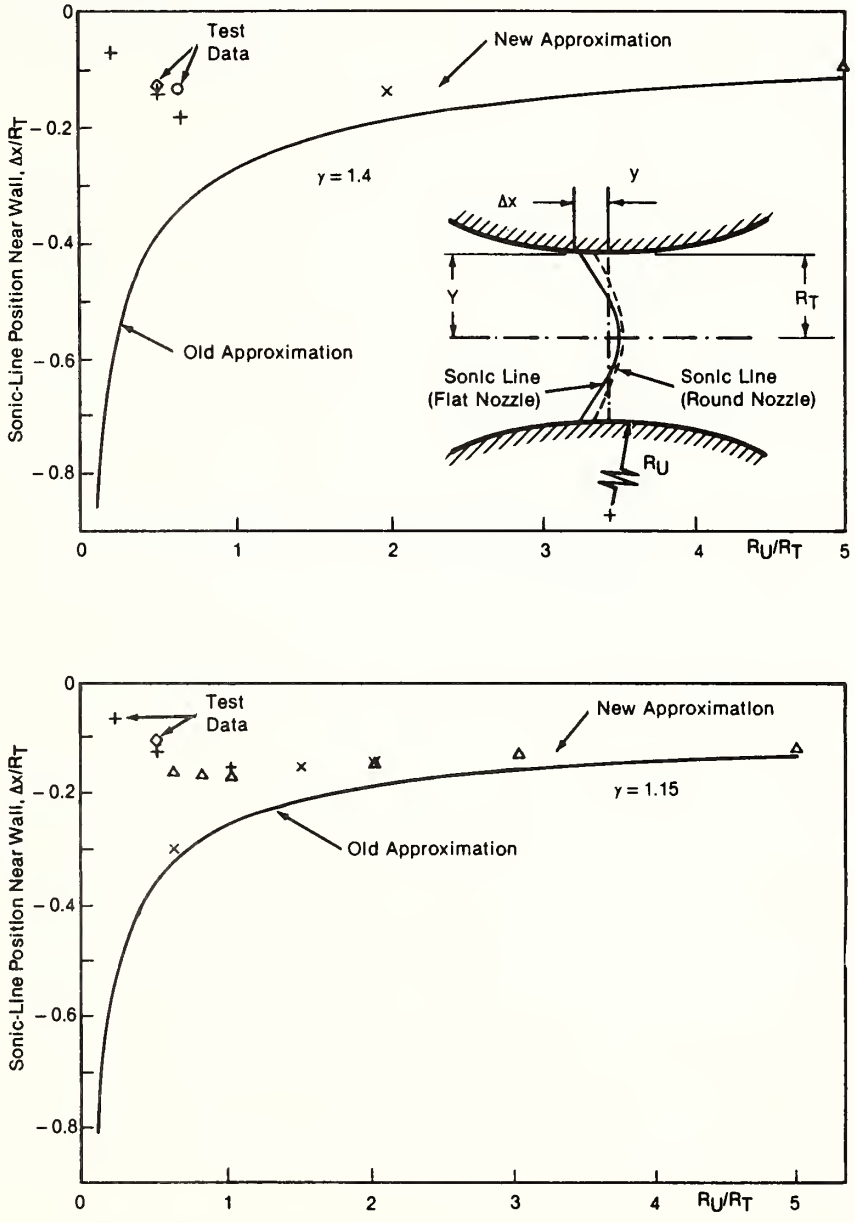

Figure 1. **Plots Compare Positions** of sonic lines computed by old and new methods (solid and dashed lines, respectively). The plot for the new method is much closer to measured data points (dots).

Where R_U/R_T lies between 0 and 1, the new approximations are

$$\Delta x/R_T = -[0.09R_U/(\gamma + 1)R_T]^{0.5}$$

for round nozzles and

$$\Delta x/R_T = -1.88[0.09R_U/(\gamma + 1)R_T]^{0.5}$$

for flat nozzles.

Figure 1 compares the old and new approximations with measurements taken on the round nozzle shown in Figure 2.

This work was done by William R. Wagner, Frank F. Lepore, and Bernard J. Ostermier of Rockwell International Corp. for **Marshall Space Flight Center**. *No further documentation is available.*
MFS-29163 /TN

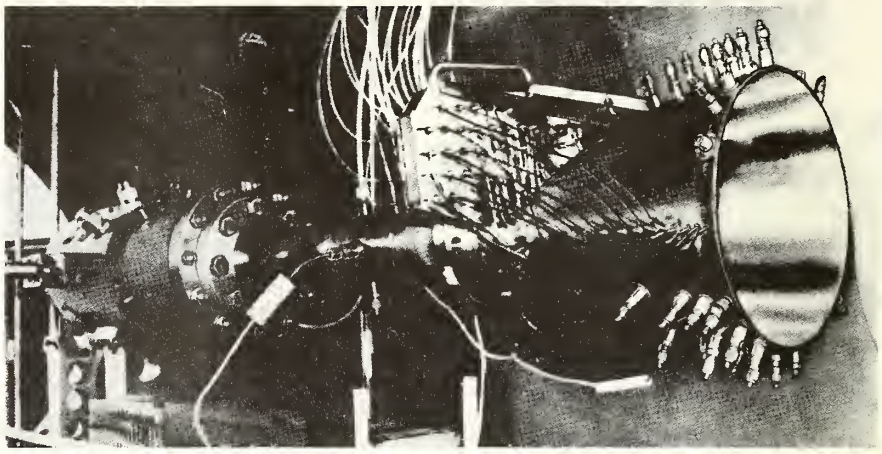

Figure 2. This **Sharp-Radius-Throat Test Nozzle** for the Space Shuttle main engine was used in experiments to verify the new equations.

FOR ADDITIONAL INFORMATION: *Contact: Director, Technology Transfer Division, P.O. Box 8757, BWI Airport, MD. 21240; (301) 621-0100 Ext. 241*
REFER TO THE NUMBER LISTED AT THE END OF THE ARTICLE

NASA Tech Brief
National Aeronautics and Space Administration
Ames Research Center, Moffett Field, California

Licensing Opportunity

Design Improvement for Airplane-Engine Nacelles

Better streamlining reduces drag.

An advanced three-dimensional transonic design routine for wing-mounted engine nacelles has been modified to include the effects of propellers and wing sweep. The resulting new nacelle shapes will introduce less airflow disturbance and, therefore, less drag.

Before the modification, the routine had been used to calculate wing airfoil shapes that satisfy boundary conditions imposed as chordwise pressure distributions. The improvement consists of the introduction of boundary conditions in the form of nonuniform onset flow in the area of the wing washed by the propeller slipstream.

The improved routine generates the nacelle shape as a series of cross sections that are swept, relatively to the unperturbed flow, as a function of wing shape. The collection of points defining the centroids of the nacelle cross sections is made to conform to a line representative of the local flow field. The figure shows a wing with a nacelle shape designed by this method.

This work was done by David F. Vernon, Gregory S. Page, and H. Robert Welge of McDonnell Douglas Corp. for **Ames Research Center**.

Inquiries concerning rights for the commercial use of this invention should be addressed to the Patent Counsel, Ames Research Center. Refer to ARC-11580/TN

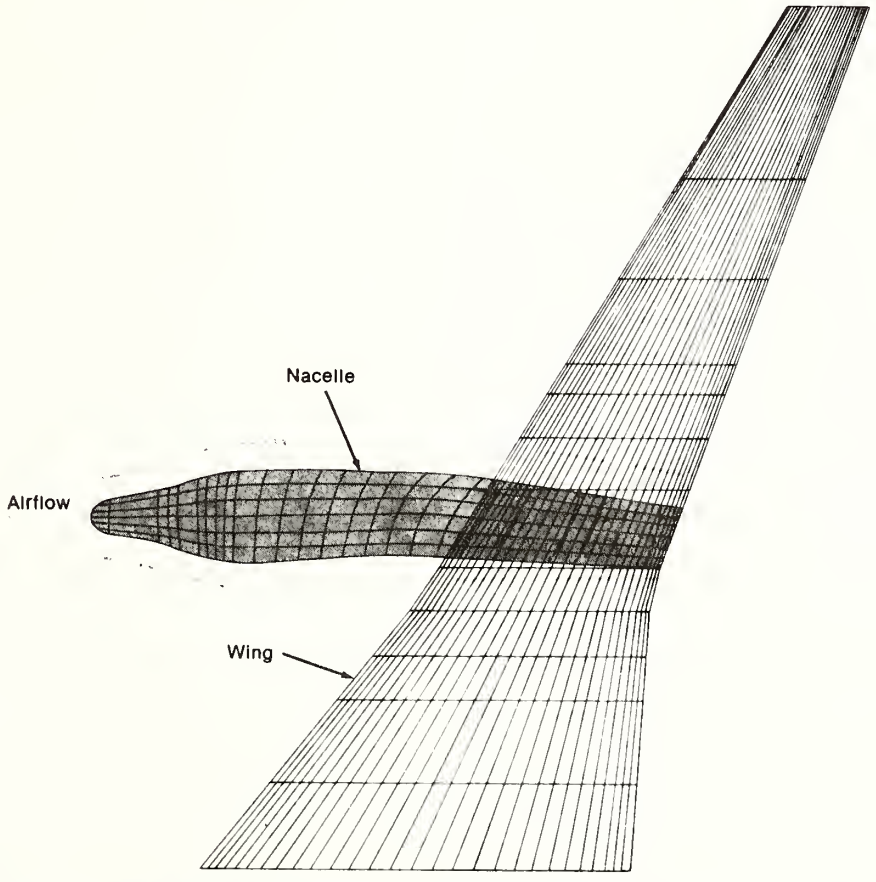

An **Engine Nacelle on a Wing** has a shape that is swept to conform more closely to the local airflow streamlines. This shape is for an engine and propeller with up-outward rotation.

Ames Research Center
Technology Utilization Officer
Laurance A. Milov
Mail Code 204-10
Moffett Field, CA 94035
(415) 694-5761
Patent Counsel:
Darrell G. Brekke
Mail Code 200-11
Moffett Field, CA 94035
(415) 694-5104

FOR ADDITIONAL INFORMATION: *Contact: Director, Technology Transfer Division, P.O. Box 8757, BWI Airport, MD. 21240; (301) 621-0100 Ext. 241*
REFER TO THE NUMBER LISTED AT THE END OF THE ARTICLE

NASA Tech Brief
National Aeronautics and Space Administration
Marshall Space Flight Center, Alabama

Licensing Opportunity

Elastic Hinge for Solar-Cell Array

A lightweight, compact hinge provides part of its own closing torque.

An elastic hinge folds to a small thickness, allows easy replacement of the panels attached to it, and provides part of the torque for refolding without additional springs. The hinge is being developed for foldable modules for solar-cell panels.

Fourteen modules, each 9.5 by 14.6 in. (24.1 by 37.1 cm), are attached to a row of hinges 12 ft (3.66 m) long on hinge-stiffener strips. The hinge allows opposing pairs of modules (see figure) to fold together so that the assembly is no more than 0.052 in. (1.32 mm) thick.

The hinge is assembled by inserting the loops of the lower hinge elements through slots in the hinge stiffeners and slots in the upper hinge elements. A pin inserted through the hinge loops captures the stiffeners and the hinge elements.

When the panels are unfolded for use, one panel wing must travel through an arc of 180° relative to the other panel wing. This is done by bending opposing hinge elements through 90° each. The panel wings are then held in tension in the open position. When the panels are to be refolded, the hinge, with its residual elasticity, helps in turning the panels toward each other.

The hinge elements are made of molybdenum foil. This material was selected for its stiffness, and because its coefficient of thermal expansion closely matches that of the glass modules.

This work was done by Richard M. Mills of Lockheed Missiles and Space Co., Inc., for **Marshall Space Flight Center.**

Inquiries concerning rights for the commercial use of this invention should be addressed to the Patent Counsel, Marshall Space Flight Center Refer to MFS-28133. /TN

George C. Marshall Space Flight Center
Technology Utilization Officer:
Ismail Akbay

Code AT01
Marshall Space Flight Center,
AL 35812
(205) 544-2223
Patent Counsel:
Leon D. Wofford, Jr.
Mail Code CC01
Marshall Space Flight Center,
AL 35812
(205) 544-0014

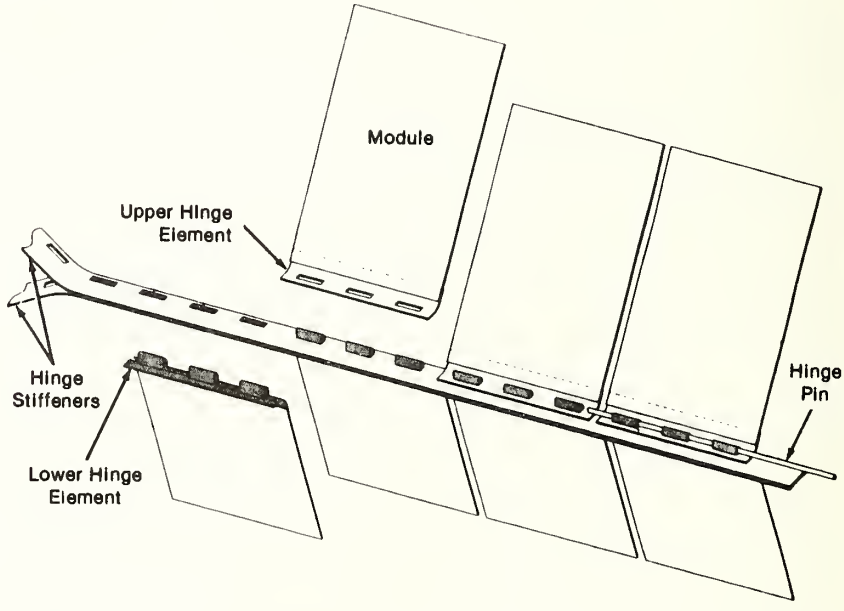

The **Elastic Hinge Holds Modules** of a solar-cell array. The modules are kept in the open position shown here by an external restraint (not shown). When the restraint is removed, the elasticity of the molybdenum hinge elements helps to fold the facing modules together.

FOR ADDITIONAL INFORMATION: *Contact: Director, Technology Transfer Division, P.O. Box 8757, BWI Airport, MD. 21240; (301) 621-0100 Ext. 241*
REFER TO THE NUMBER LISTED AT THE END OF THE ARTICLE

United States
Environmental Protection
Agency

Research and Development

EPA

Project Summary

Interactive Computer Model for Calculating V-I Curves in Electrostatic Precipitators

Two microcomputer programs are written to estimate the performance of electrostatic precipitators (ESPs): the first, to estimate the electrical conditions for round discharge electrodes in the ESP; and the second, a modification of the EPA/SRI ESP model, to estimate the particle collection efficiency of the ESP operating with the electrical conditions predicted by the first program. Both programs, written in the BASIC computer language, are designed for the IBM-PC and compatible computers and the Tandy 2000 computer. The programs require Advanced BASIC and a color graphics adapter. The models are quite useful and allow rapid assessment of expected ESP performance under a wide variety of conditions.

Software description: The program is written in the Basic programming language for implementation on an IBM Tandy, PC, XT, AT 2000, using the PC-DOS (2.0) or higher or the MS-DOS (2.1) or higher operating systems.

For Additional Information:

For information about ordering this software, contact the NTIS Computer Products Center, NTIS, 5285 Port Royal Road, Springfield, VA 22161; (703) 487-4763.

Refer to PB87-126025/NAC

The software is contained on 5 1/4-inch diskette, double sided, double density compatible with the IBM PC XT/AT 2000 microcomputer. Diskettes are in the ASCII format. Price includes documentation, PB87-100046.

The principle investigators also may be contacted: L.E. Sparks, Air and Energy Engineering Research Lab., Environmental Protection Agency, Research Triangle Park, NC.

NASA Tech Brief
National Aeronautics and Space Administration

Analysis of Scramjet Inlets

Viscous flow can be accounted for in the computations.

The NASCRIN program analyzes two-dimensional flow fields in supersonic-combustion ramjet (scramjet) inlets. It solves the two-dimensional Euler or Navier-Stokes equations in conservative form by an unsplit, explicit, two-step finite-difference method. A more recent explicit/implicit, two-step scheme has also been incorporated for the analysis of viscous flow. An algebraic, two-layer eddy-viscosity model is used for the turbulent-flow calculations.

NASCRIN can analyze both inviscid and viscous flows with no struts, one strut, or several struts embedded in the flow field. It can be used in a quasi-three-dimensional sense for some scramjet inlets under certain simplifying assumptions. Although developed for supersonic internal flow, NASCRIN may be adaptable for other flow problems. In particular, it should be readily adaptable to subsonic inflow with supersonic outflow, supersonic inflow with subsonic outflow, or fully subsonic flow.

The NASCRIN program is available in vectorized as well as scalar form. The vectorized version, developed in 1983, is written for CDC CYBER 205 computer, whereas the scalar version, developed in 1985, can be run on CRAY or other scalar computers. The code has a central-memory requirement of approximately 300K words for a grid size of about 3,000 points.

These programs were written by Ajay Kumar of **Langley Research Center**. *LAR-13297 and LAR-13559 /TN*

FOR ADDITIONAL INFORMATION

CONTACT:

COSMIC®
112 Barrow Hall
University of Georgia
Athens, GA 30602
(404) 542-3265

NASA Tech Brief
National Aeronautics and Space Administration

Buckling Analysis of Rectangular Plates With Holes

Loads and deflections are predicted for a variety of cutouts.

BUCKO is a computer program developed to predict the buckling of a rectangular compression-loaded orthotropic plate with a centrally located cutout. The plate is assumed to be a balanced, symmetric laminate of uniform thickness. The cutout shape can be elliptical, circular, rectangular, or square. The BUCKO package includes sample data that demonstrate the essence of the program and its ease of use.

BUCKO uses an approximate one-dimensional formulation of the classical two-dimensional buckling problem following the Kantorovich method. The boundary conditions are considered to be simply supported unloaded edges and either clamped or simply supported loaded edges. The plate is loaded in uniaxial compression by either uniformly displacing or uniformly stressing two opposite edges of the plate.

The BUCKO analysis consists of two parts: the calculation of the stress distribution in the plane prior to buckling, and the calculation of the plate axial load and displacement at buckling. The user input includes the size and shape of the plate planform and cutout, the plate membrane and bending stiffnesses, finite-difference parameters, boundary-condition data, and loading data. The results generated by BUCKO are the pre-buckling strain energy, in-plane stress resultants, buckling-mode shape, critical end shortening, and average axial and transverse strains at buckling.

BUCKO is written in FORTRAN V for batch execution and has been implemented on a CDC CYBER 170-series computer operating under NOS with a central-memory requirement of approximately 343K of 60-bit words. This program was developed in 1984.

This program was written by Michael P. Nemeth of **Langley Research Center.**
LAR-13466 /TN

FOR ADDITIONAL INFORMATION

CONTACT:
COSMIC®
112 Barrow Hall
University of Georgia
Athens, GA 30602
(404) 542-3265

NASA Tech Brief
National Aeronautics and Space Administration

Increasing Maintainability of a Wastewater-Recovery Unit

A modified system leaks less and is easier to disassemble for maintenance.

The redesign of a wastewater-recovery system that separates water from urine has improved operation and made the system easier to maintain. The details of the redesign, which chiefly affected the hollow-fiber-membrane evaporator, are described in a report.

Previously, the evaporator had to be removed as a unit and partly disassembled so that maintenance could be done on the 1,656 evaporator tubes grouped into 18 bundles. During 1,650 hours of operation, defects developed in the membrane bundle headers and in the steam-shell seals, forcing the shutdown of the system. The correction of the defects involved the disassembly of the evaporator — in a difficult, time-consuming procedure that often caused damage to parts and thereby necessitated further repair.

The major criteria for the redesign were the following:

- The new unit had to be completely interchangeable with the old unit;
- Leakage at the O-ring seals had to be reduced;
- The membrane-tube section had to be more maintainable; and
- While keeping the same membrane area, the number of tube-bundle headers had to be reduced to simplify assembly and maintenance while increasing reliability.

The most significant departure from the old arrangement was the reduction in the number of tube-bundle headers from 36 to 6. The length of each bundle was increased from 0.38 m to 2.29 m to provide adequate membrane area. The number of tube-to-header connections was reduced from 3,312 to 552, making it easier to remove them for maintenance. At the same time, reliability was increased. The perforated metal retainers that prevented the tube-bundle headers from being forced through the header manifold were no longer needed; with their elimination, the header plug now forms a facial seal (in addition to the inherent radial seal) with the header manifold.

Among other changes, O-ring seals were made compressive between mating flange sections instead of radial between cylindrical sections. The compressive face-type seal is much less subject to leakage from expansion, contraction, and distortions in the mating surfaces.

Mating parts were fabricated from a single material, titanium, instead of polysulfone and titanium as before. The differing rates of thermal expansion and contraction between the two materials in the old unit had contributed to leakage around the radial seal.

This work was done by Gerard F. Dehner and Harlan F. Brose of United Technologies Corp. for **Johnson Space Center**. *Further information may be found in NASA CR-171823 [N85-16468/NSP], "Addendum Development of a Preprototype TIMES Wastewater Recovery Subsystem."*

Copies may be purchased from the National Technical Information Service, Springfield, Virginia 22161, [A06] MSC-20984 /TN

FOR ADDITIONAL INFORMATION: *Contact: Director, Technology Transfer Division, P.O. Box 8757, BWI Airport, MD. 21240; (301) 621-0100 Ext. 241*
REFER TO THE NUMBER LISTED AT THE END OF THE ARTICLE

Large-Area Radiation Portal/Personnel Monitor

A faster, more sensitive personnel monitoring system

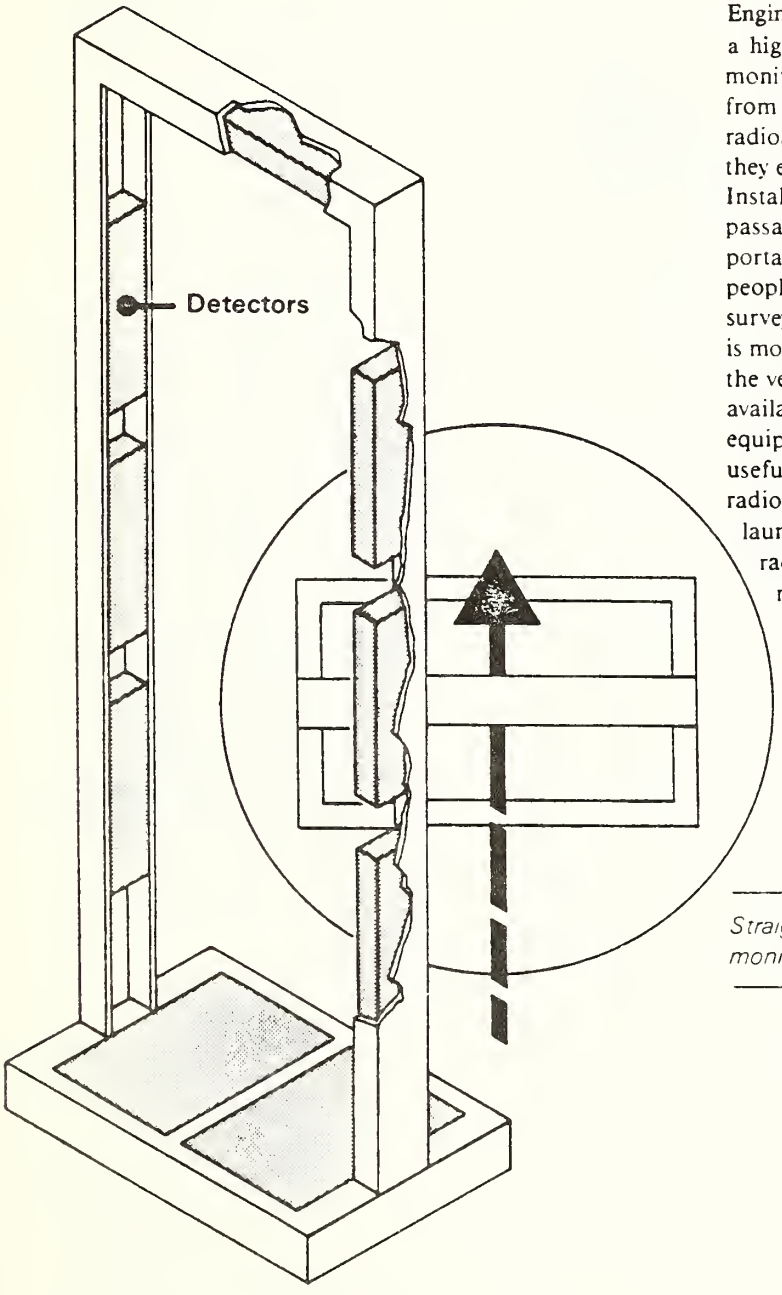

Straight-through portal monitor model

Engineers at the INEL developed a highly sensitive portal monitor that surveys personnel from head to toe for radioactive contamination as they enter and leave a facility. Installed in doorways or passageways, the large-area portal monitor allows more people to be whole-body surveyed in a shorter time, and is more sensitive than all but the very best commercially available monitoring equipment. The system is useful in nuclear power plants, radioactive waste facilities and laundries, and wherever radioactive contamination must be controlled.

INEL engineers designed the portal monitoring system to meet stringent specifications that were not available in the marketplace. In the past five years, about 50 units have been operated successfully at the INEL and Three Mile Island.

Conventional ways of surveying personnel for radioactive contamination are time consuming and are not always as accurate or as sensitive as desired. For example, a person with a hand-held Geiger or scintillation counter can complete a whole body survey in about 15 minutes, and even the best available walk-through monitors require the individual to stand for a time while the equipment completes the survey and processes the data. Both monitor types are sensitive to gamma radiation, which in some applications is considered background noise that reduces sensitivity to beta radiation.

The system's proportional counters used in the thin-walled detectors are more sensitive and discriminating than the commonly-used Geiger or scintillation counters, making the INEL system suitable for detecting beta radiation as well as alpha and gamma radiation.

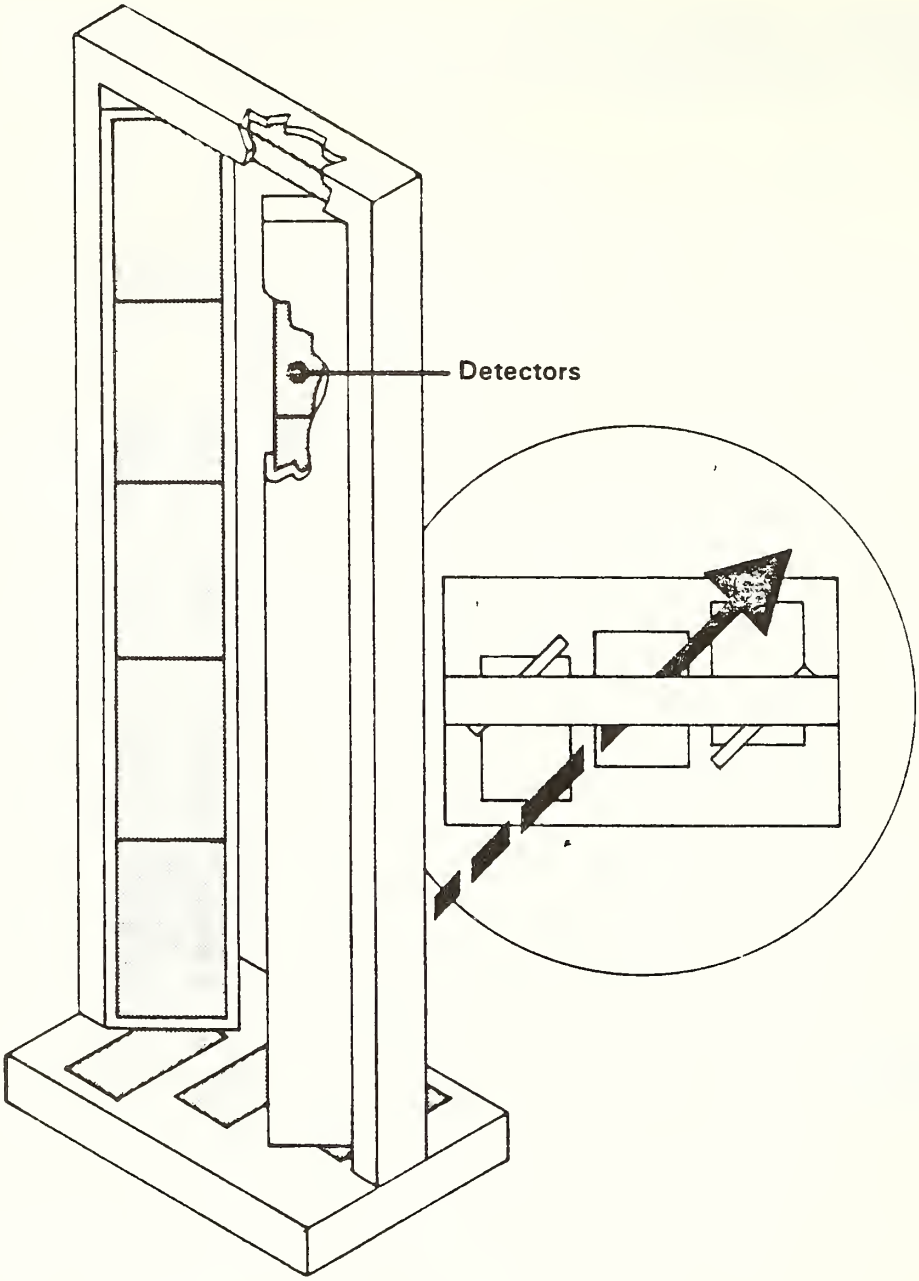

Slanted portal monitor model directs personnel closer to detectors for greater detection capability

The portal monitor frame contains nine large-area detectors—three on each side, one on top, and two in the base. The electronic circuitry, all within the portal frame, contains eight channels, each with an alarm light on the frame to make it easier to pinpoint and remove contamination. A motion detector senses when the portal is occupied. When unoccupied, the background radiation reading is updated every two-tenths of a second and averaged over a 20-second interval. This background reading is used to set the system's lower detection threshhold on the control panel. When occupied, the system compares the radiation background reading (plus a setable multiple of the standard deviation) to the personnel reading every 50 to 200 milliseconds as set on the control panel's time switch. If desired, the detectors can be mounted in two pivoted "wings" set at an angle like louvers to direct personnel closer to the detectors for even greater detection capability.

The large area radiation portal/personnel monitor is fully developed and tested. The system is not patented, and is available for private-sector manufacture and marketing. An operation and maintenance manual is included.

For Addtional Information

Contact:

Dr. Jane Welch
ORTA Office
Idaho National Engineering Laboratory
P.O. Box 1635
Idaho Falls, ID 83415
(208) 526-8318

Refer to DOE/INEL-014/TN

NASA Tech Brief
National Aeronautics and Space Administration
Lyndon B. Johnson Space Center, Houston, Texas

Side-Looking Viewer for Crevices

Gaps only 1 mm wide are inspected with a thin metal mirror.

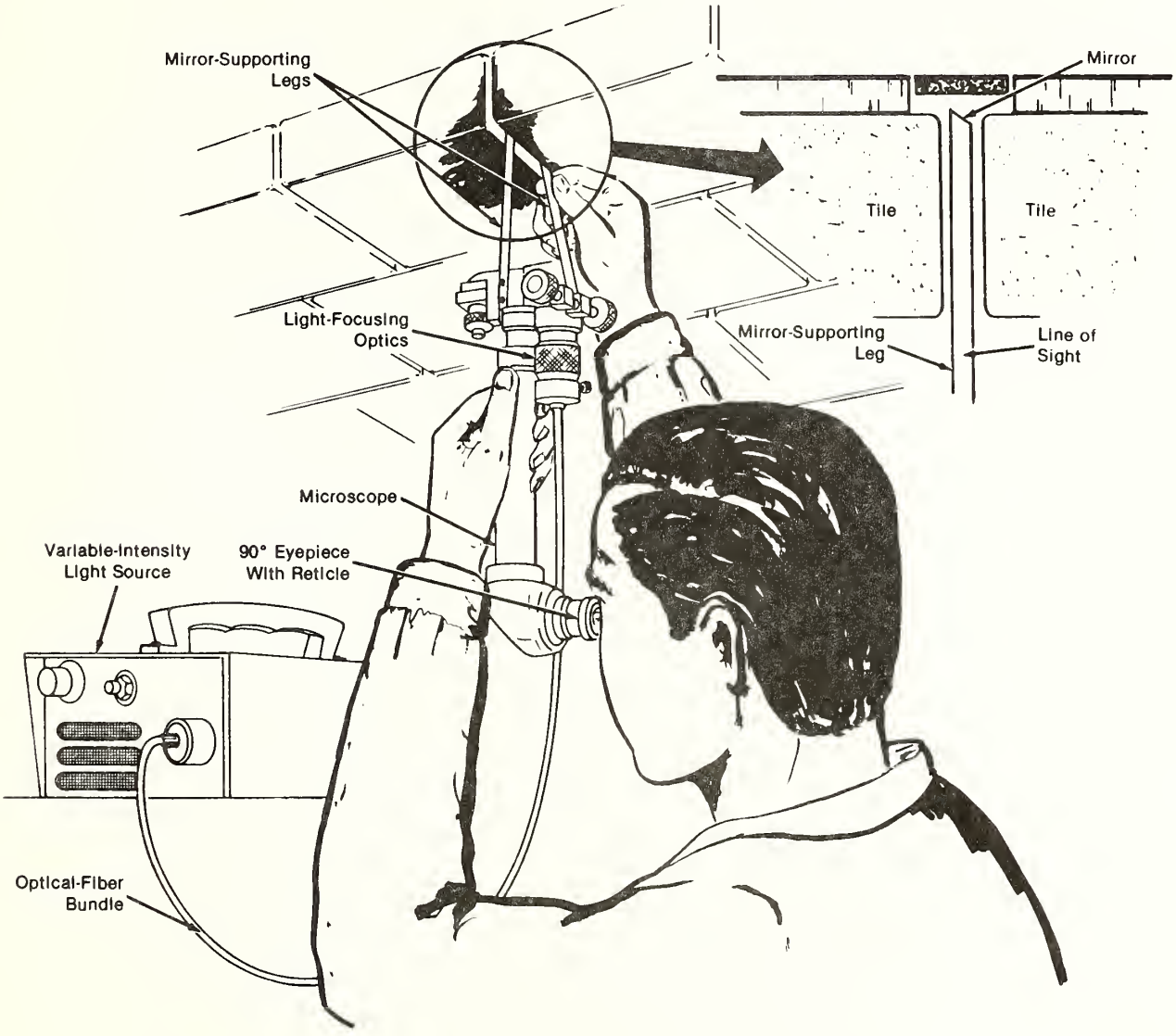

An Observer Inspects the gap between a pair of tiles, using the side-looking optical viewer. A long, narrow metal mirror in the gap reflects an image to the microscope.

A side-looking optical viewer can be inserted into a gap 1 mm wide to a depth of 10 cm. The instrument allows a human observer to inspect small crevices from a comfortable viewing angle (see figure).

A small mirror atop a pair of thin, flat legs is inserted into the gap. The mirror reflects an image of the gap wall or other object into a microscope, which magnifies the image 20 times. A quartz/halogen lamp in a separate unit provides light to illuminate the gap via an optical-fiber bundle. The observer can look directly through the microscope or can attach a photographic or video camera without disturbing the setup.

The mirror is made from hardened, polished tool steel. It is soldered to the two legs to give a viewing angle of 102°, 90°, or 86° with respect to the microscope axis. A mirror can thus be selected

to look at the interior of the gap either perpendicularly to the line of entry or from a slightly inward or slightly outward direction. The legs, made of stainless-steel strips 0.032 in. (0.81 mm) thick, hold the mirror 4.5 in. (11.4 cm) from the microscope objective lens. The legs are mounted in a crossbar at the base of the microscope.

The microscope, a commercial model, was modified in several ways. An extension was added in front of the erecting prism to provide the proper working distance for the 80-mm objective lens. Internal baffles and nonreflective surfaces were installed in the microscope tube to reduce the glare caused by the intense illumination in the gap.

The intensity of light from the lamp can be controlled. The 72-in. (1.83-m) fiber bundle carries the light to a lens near the base of the mirror-supporting legs. The lens projects the light into the gap.

For direct viewing, any of three eyepieces can be selected for greatest viewing comfort in various working positions: a straight eyepiece, a 60° eyepiece, and a 90° eyepiece. The last two contain erecting prisms that provide an uninverted image. Their angles are convenient for overhead work. Each eyepiece contains a reticle graduated in 0.002-in. (0.05-mm) divisions so that the observer can estimate dimensions.

A single-lens reflex camera was modified so that its viewfinder can look through the straight eyepiece. The camera is supported for its 5- to 20-second exposures by a tripod consisting of a bipod plus an adjustable stop on one of the mirror legs.

A small, lightweight video camera provides a high-quality color picture for remote viewing or recording. Because the camera uses a charge-coupled device instead of a vidicon tube, ghosts and blooming do not mar the image.

This work was done by George R. Hagen of Rockwell International Corp. for **Johnson Space Center**.
MSC-20610 /TN

FOR ADDITIONAL INFORMATION: *Contact: Director, Technology Transfer Division, P.O. Box 8757, BWI Airport, MD. 21240; (301) 621-0100 Ext. 241*
REFER TO THE NUMBER LISTED AT THE END OF THE ARTICLE

NASA Tech Brief
National Aeronautics and Space Administration
Lyndon B. Johnson Space Center, Houston, Texas

Measuring Thicknesses of Wastewater Films

A sensor resists excessive film buildup.

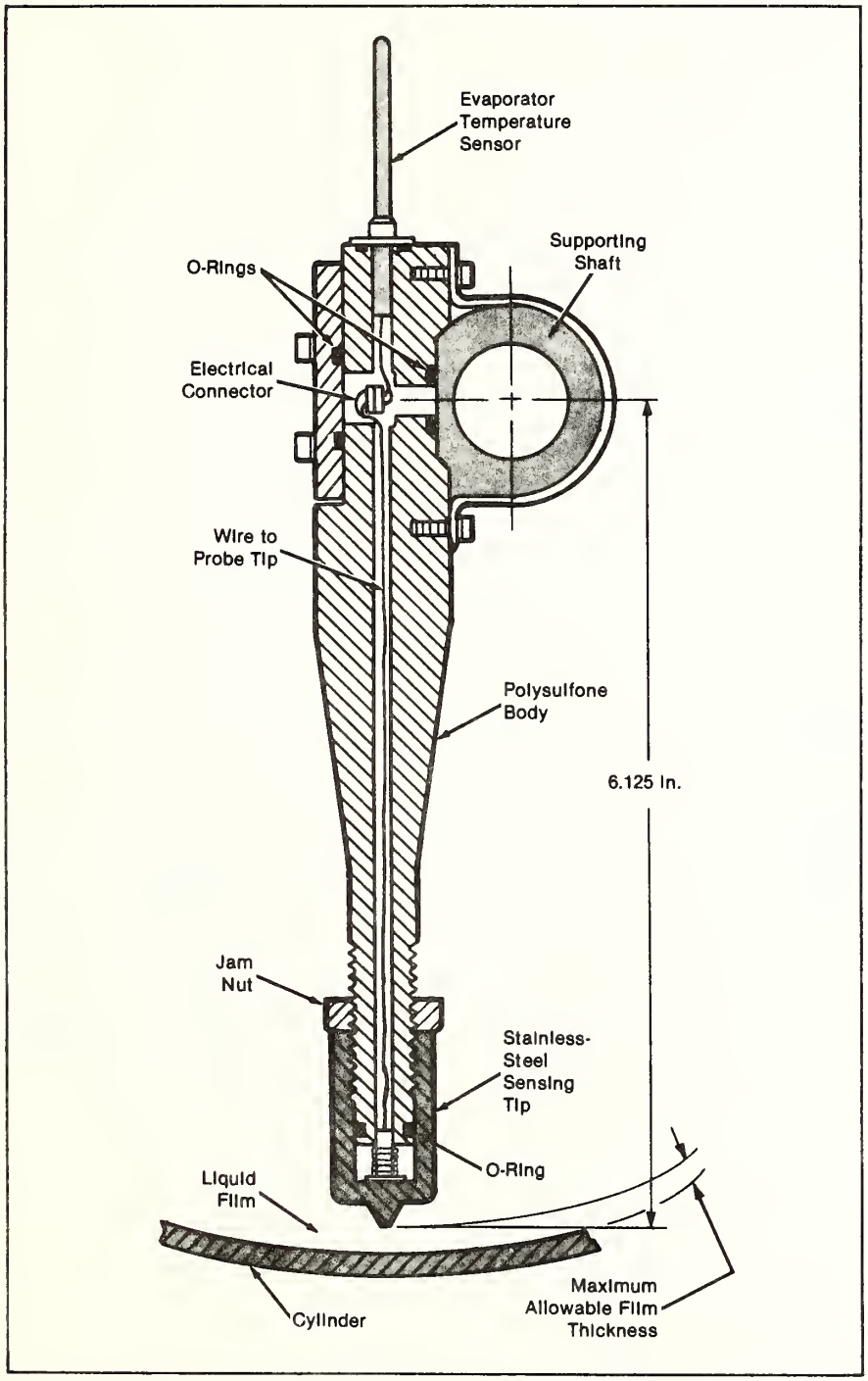

Mounted on a Shaft in a Rotating Cylinder, the liquid-thickness sensor extends toward the cylinder wall so that its tip almost touches. The sensor body also accommodates a probe that measures the temperature of the evaporated water in the cylinder.

A sensor determines when the thickness of a film of electrically conductive wastewater on a rotating evaporator drum exceeds a preset value. The sensor is a simple electrical probe that makes contact with the liquid surface. It is made of materials that are resistant to chemicals in the liquid.

The sensor was developed for equipment that reclaims potable water from astronauts' urine wastewater. The equipment is based on vapor-compression distillation, in which a film of the pretreated wastewater flows over the internal surface of a rotating cylinder, as in a centrifuge. Water evaporates from the film, leaving unwanted minerals behind. The vapor is then condensed.

If the liquid film becomes too thick, water production drops because less heat is transferred from the cylinder wall to the film surface. More seriously, wastewater would eventually accumulate in the cylinder, flood it, and perhaps spill into the product side of the equipment. The film-thickness sensor helps to prevent these occurrences.

The sensor consists of a passivated stainless-steel sensing tip in a polysulfone body. Electrical wiring and connections are hermetically sealed within the body (see figure). The sensing tip is positioned a predetermined distance [usually 0.06 inch (1.5 millimeter)] from the surface containing the film. When the liquid thickness equals or exceeds the distance between the surface and the tip, the liquid touches the tip, thereby closing an electrical circuit between the tip and the surface. This activates controls that cause the removal of the excess liquid.

The materials selected for the sensor are immune to chemical attack from the urine in the wastewater as well as from the sulfuric acid used to pretreat it. In addition, the geometry and materials of the tip and body prevent the sensor from becoming fouled by mineral residue.

This work was done by Franz H. Schubert and Ronald J. Davenport of Life Systems, Inc., for **Johnson Space Center.** *MSC-20915 /TN*

FOR ADDITIONAL INFORMATION: *Contact: Director, Technology Transfer Division, P.O. Box 8757, BWI Airport, MD. 21240; (301) 621-0100 Ext. 241*

REFER TO THE NUMBER LISTED AT THE END OF THE ARTICLE

NASA Tech Brief
National Aeronautics and Space Administration
Marshall Space Flight Center, Alabama

Large Wire Strain Gauges

Wires yield data on average strains over distances ranging from inches to many feet.

Long constantan wires can be used to measure average strains over distances characteristic of vehicles or buildings. Connected in a bridge circuit, the wires measure strain accurately (within 1 percent) and linearly (within 0.1 percent). The wires have been stretched as much as 0.15 percent and still returned to zero residual strain after release.

A strain gauge, for example, might be constructed with four enameled wires laid side by side (see figure). Two straight wires 0.005 in. (0.13 mm) in diameter are bonded with strain-gauge adhesive to the structure to be measured so that they elongate or shorten along with the surface of the structure. The two remaining wires, of 0.0125-in. (0.32-mm) diameter, are loosely taped nearby in a zigzag pattern so that they do not respond to the strain. The zigzag wires compensate for temperature variations of the electrical resistances of the strain-sensing (straight) wires. The four wires are connected in a bridge circuit.

The wires can be used in a variety of ways; for example, they can be wrapped around the circumference of a pressure vessel at intervals along its length. The strain gauges thus give data on the variation (if any) of strain and internal pressure along the vessel wall.

The wires can be used to average out the small local strain variations caused by cracking; for example, cracking of the resin in a wound-filament vessel. In such a case, it might suffice to use a single-wire gauge without temperature compensation, with a gauge factor obtained from a lot calibration.

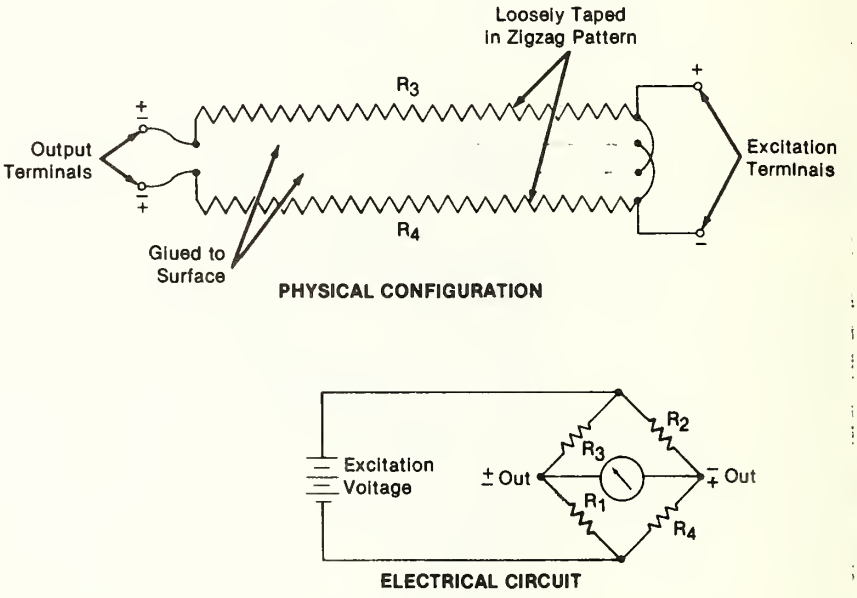

Long Constantan Wires Form a Bridge for the measurement of strain. R_1 and R_2 are the sensing wires. R_3 and R_4 are temperature-compensating sections.

A long wire can be tapped at intervals so that the total or average strain measured over the total length between the end taps can be compared with the strains measured between intermediate taps. A wire can also be stretched tightly between end points and not bonded in between, to measure accurately small changes in length over distances of 100 ft (30 m) or more. The wire can be calibrated in place by use of a micrometer to measure a change in distance between the end points. The calibration is accurate if the wire is maintained free of encumbrances between the end points.

This work was done by Boyd D. Bryner of Thiokol Chemical Corp. for **Marshall Space Flight Center**. *No further documentation is available.*
MFS-28062 /TN

FOR ADDITIONAL INFORMATION: *Contact: Director, Technology Transfer Division, P.O. Box 8757, BWI Airport, MD. 21240; (301) 621-0100 Ext. 241*
REFER TO THE NUMBER LISTED AT THE END OF THE ARTICLE

Environmental Science & Technology

863 GETS, A Simulation Model for Dynamic Bioaccumulation of Nonpolar Organics by Gill Exchange — A User's Guide

864 Removing Welding Fumes — A duct can be placed quickly where it is needed.

Software

866 Water Quality Models Used By the Corps of Engineers

867 Geotechnical Analysis for Dike Stability (GARDS)

868 Software Evaluates Liquid Waste Soil Liners

869 Integrated Air Pollution Control System Cost Model Version 2 (IAPCS2) — Program estimates costs and performance for coal-fired utility boilers

Testing & Instrumentation

870 Groundwater-Level Monitoring System

United States
Environmental Protection
Agency

Environmental Research
Laboratory
Athens GA 30613

Research and Development

EPA

Project Summary

GETS, A Simulation Model for Dynamic Bioaccumulation of Nonpolar Organics by Gill Exchange

A User's Guide

A FORTRAN program that estimates the absorption and depuration of a chemical across fish gills is described. The program is based on a set of diffusion and forced convection differential equations. Gill morphometric parameters are computed by the program via its own internal database. This database spans approximately 20 species. The program requires that the user input 12 relatively easily obtainable parameters.

This Project Summary was developed by EPA's Environmental Research Laboratory, Athens, GA, to announce key findings of the research project that is fully documented in a separate report of the same title (see Project Report ordering information at back).

Introduction

When fish are exposed to dissolved organic chemicals, such substances are accumulated within the fish by diffusive transport across its gills. During acute exposures, chemical exchange across the gill is the fish's prevailing route of exposure. During chronic exposure in the environment, exposure through contaminated food can become increasingly important or even greatly exceed direct gill uptake. Nevertheless, gill exchange still reciprocally controls the fish's body concentrations by determining the fish's excretory rates of the chemical.

Ultimate levels of organic toxicants in aquatic organisms can be explained in large measure as thermodynamic partitioning between toxicant in the aqueous environment and hydrophobic components of the organisms (primarily lipid). Reports of exceptions to this simple rule are numerous, however, particularly for chemicals having high partition coefficients. The frequency with which these exceptions have been noted has often led to questions of the reliability and utility of the relationship between bioconcentration factors (BCF) and thermodynamic partitioning. Based on our review of reported results for both laboratory and field investigations of BCF, uptake, and depuration, we have concluded that such results are both expected and explainable on an essentially thermodynamic (but not equilibrium) basis. Furthermore, we have developed a thermodynamically based kinetic model called GETS, which predicts whole-body burdens and concentrations of organic chemicals in fish.

GETS (Gill Exchange of Toxic Substances) is a FORTRAN simulation model that predicts a fish's whole body concentration (i.e., ppm = μg chemical [g live weight fish]$^{-1}$) of a nonmetabolized, organic chemical which is exchanged across a fish's gill by thermodynamic concentration gradients. These concentration dynamics are calculated algebraically after simulating a fish's total body burden of the chemical, Bf = μg chemical fish^{-1}, and its live weight, W = g live weight fish^{-1}. The temporal dynamics of these two quantities are generated by the system of coupled differential equations

$$\frac{dBf}{dt} = S^{*}kw^{*}(Cw - [PL^{*}KL]^{-1}CF) \quad (1)$$

$$\frac{dW}{dt} = \text{gamma} * W \qquad (2)$$

where S is the fish's total gill area (i.e., cm^2), kw is the chemical mass conductance through the interlamellar gill water (i.e., cm/day), Cw is the chemical's environmental concentration (i.e., ppm = mg l^{-1}), PL is the fish's lipid content as a fraction of its total live weight, KL is a lipid to water partition coefficient (i.e., [mole chemical/g lipid]/[mole chemical/g water]), Cf = Bf/W is the fish's whole body concentration of the chemical, and gamma is the fish's specific growth rate (i.e., g/g/day).

Conclusion

GETS enables internal fish concentrations of an organic chemical to be related dynamically to the chemical's environmental concentration. This capability is important when chemical exchange between fish and their environment is kinetically limited either by the physicochemical properties of the chemical (e.g., high log P or low water solubility) or by allometric properties of the fish (e.g., dynamic surface to volume ratios) since it is actually the chemical's concentration within the fish at specific or nonspecific sites of action that elicit potentially adverse ecological or physiological responses.

Similarly, the ability of GETS to predict the dynamics of bioaccumulation of organic chemicals in fish offers a powerful tool to assess potential food chain exposure for terrestrial fish-eating organisms. For example, if the use of a particular chlorinated organic pesticide were banned within a river basin, when might the pesticide's concentration no longer pose a health risk to man or an environmental threat to bald eagles or other piscivorous birds in the region?

The EPA authors Luis A. Suarez, M. Craig Barber, and Ray R. Lassiter are with the Environmental Research Laboratory, Athens, GA 30613.

The complete report, entitled "GETS, A Simulation Model for Dynamic Bioaccumulation of Nonpolar Organics by Gill Exchange," (Order No. PB 87-132 791/AS; Cost: $13.95, subject to change) will be available only from:

National Technical Information Service
5285 Port Royal Road
Springfield, VA 22161
Telephone: 703-487-4650

The EPA authors can be contacted at:

Environmental Research Laboratory
U S Environmental Protection Agency
Athens, GA 30613

NASA Tech Brief
National Aeronautics and Space Administration
Marshall Space Flight Center, Alabama

Removing Welding Fumes

A duct can be placed quickly where it is needed.

A portable exhaust duct for machining and welding shops removes oil mist, dust, smoke, and fumes. The duct was made especially for welding in a room with a low ceiling (see Figure 1). The room exhaust system could not remove pollution from the welding process; hazardous gases tended to accumulate overhead.

The portable duct is used with a shop exhaust system, the inlets of which are placed at various convenient locations in the shop floor (see Figure 2). The duct includes a 12-in. (30.5-cm) diameter flexible tube, about 14 ft (4.3 m) long, mounted on a swivel and a wheeled base. The base is rolled to the exhaust inlet near the welding station, and the swiveled end of the tube is positioned over the work. The suction in the exhaust system under the floor carries the fumes into the duct and the exhaust system.

The portable duct was built for about $112 in labor and $150 in material (1985 prices). A more-elaborate commercial system would cost almost 10 times as much.

This work was done by Lloyd J. Moore and Vandel L. Hall of **Marshall Space Flight Center.** *No further documentation is available.*
MFS-28106 /TN

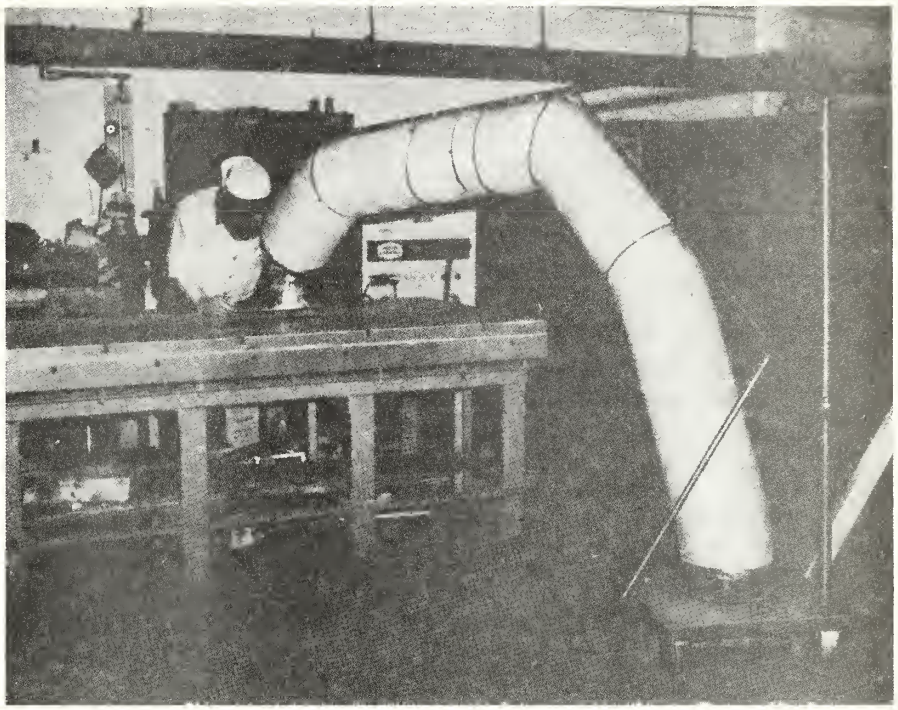

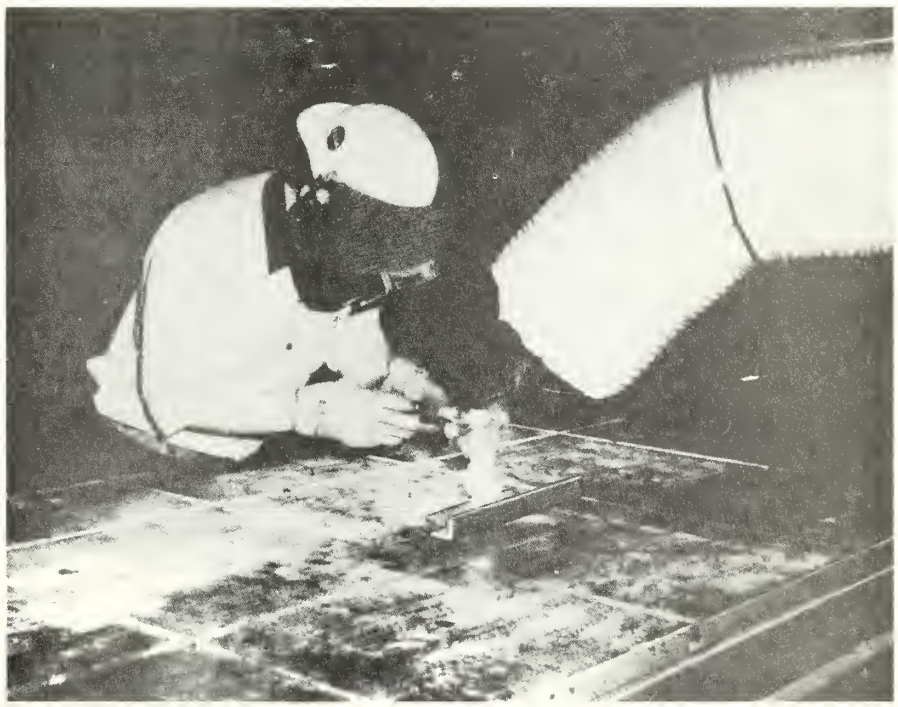

Figure 1. The **Exhaust Duct Scoops Up** welding fumes at one end and passes them to the exhaust system at the other.

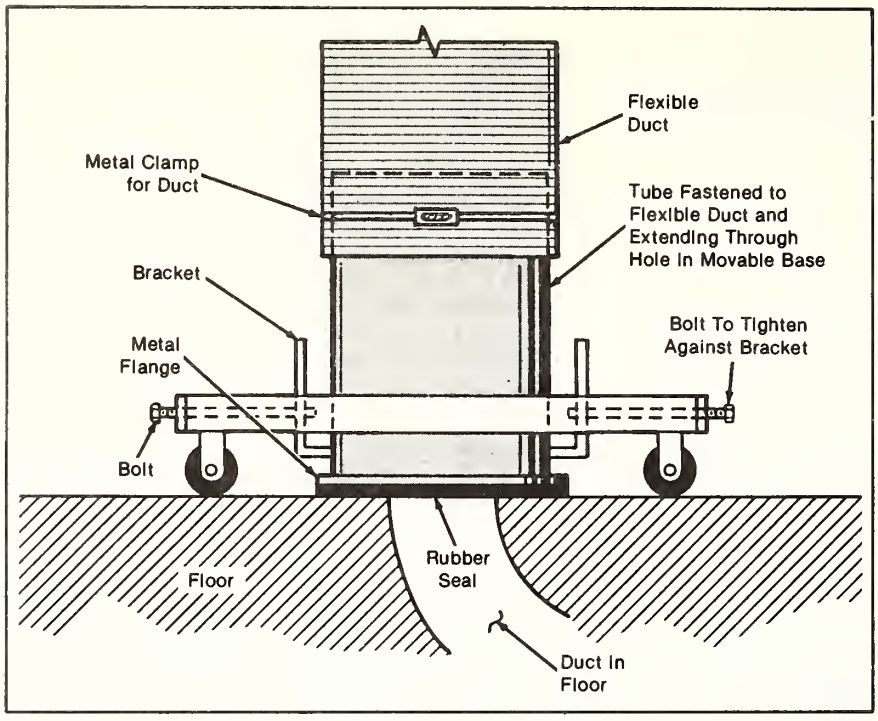

Figure 2. A **Flanged Connector** on the underside of the wheeled base links the flexible tube to the exhaust system under the floor.

FOR ADDITIONAL INFORMATION: *Contact: Director, Technology Transfer Division, P.O. Box 8757, BWI Airport, MD. 21240; (301) 621-0100 Ext. 241*

REFER TO THE NUMBER LISTED AT THE END OF THE ARTICLE

US Army Corps
of Engineers

Technology Transfer Opportunity

Waterways Experiment Station

Water Quality Models Used By the Corps of Engineers

During and following the Environmental and Water Quality Operational Studies (EWQOS) Program, a variety of water quality models for inland surface waters were identified/developed to help evaluate the effects of Corps of Engineers (CE) water-resources activities. These models vary widely in their purposes, assumptions, and capabilities. There is no single model that is best suited for all applications, rather one should select the most appropriate model for a particular application.

Model selection is the most important step of the model-application process. Selection should include consideration of such factors as model availability, study issues, characteristics of the system to be modeled, and time and budget constraints. A table has been prepared which highlights the major features and capabilities of water quality models used by the CE. It should help with the model-selection process. Although the table appears to contain a significant amount of information, it is actually quite abbreviated when compared with the total information available for each model. The user manuals and documentation should be reviewed to gain a better appreciation for model features. Potential users can also obtain additional information from the points-of-contact listed in the table.

FOR ADDITIONAL INFORMATION: Contact:
Environmental Laboratory, ATTN: J. L. Mahloch
U.S. Army Engineer Waterways Experiment Station
P.O. Box 631
Vicksburg, MS 39180-0631
(601) 634-3635

United States
Environmental Protection
Agency

Research and Development

EPA

Project Summary

Geotechnical Analysis for Dike Stability (GARDS)

A user-friendly, interactive computer program developed for the stability analysis of dikes (GARDS) has been developed. The GARDS program is designed to guide a geotechnical non-specialist (EPA regulatory personnel) through the customary steps of earth dike analysis considering slope stability, settlement, liquefaction, hydraulic flow and pressure conditions, and piping. The GARDS package is designed for use on the IBM-PC/XT microcomputer. User documentation consists of a combined Handbook/User's Manual (under development) which presents basic theory, program operational procedures, and example long hand and computer solutions for each analysis.

Software Description: The program is written in the FORTRAN program language for implementation on an IBM-PC AT, XT or compatible microcomputer using a DOS 2.1 or higher operating system. 512K bytes of core storage are required. Note: A hard disk is required; a color monitor is recommended.

For Additional Information:

For information about ordering this software, contact the NTIS Computer Products Center, NTIS, 5285 Port Royal Road, Springfield, VA 22161; (703) 487-4763.

Refer to PB87-130969/NAC

The software is contained on 5 1/4-inch diskette, double sided, double density compatible with the IBM PC ST AT microcomputer. Diskettes are in the ASCII format.

The principle investigators also may be contacted: D. C. Ammon, R. McCandless, and P. Cluxton; Hazardous Waste Engineering Research Lab., Environmental Protection Agency, Cincinnati, OH.

United States
Environmental Protection
Agency

Research and Development

EPA

Project Summary

Software Evaluates Liquid Waste Soil Liners

Among the provisions of the Hazardous and Solid Waste Amendments of 1984 are minimum technological requirements for hazardous waste landfills, surface impoundments and waste piles. These provisions are found in Sections 3004(o) and 3015 of the Resource Conservation and Recovery Act (RCRA) and further defined in the Part 264 regulation and associated guidance. Any new surface impoundment must install two or more liners and a leachate collection system between such liners. The lower liner must be designed, operated, and constructed to prevent breakthrough of constituents over the period of operation, including any post-closure care period. A computer program, SOILINER, has been developed to assist in the evaluation of these liners. The program is for an IBM PC/XT and IBM PC/AT or compatible personal computer.

Software description: The program is written in the Fortran programming language for implementation on IBM-PC-AT or XT or compatible using the DOS 2.1 (or higher) operating system. 256K bytes of core required. Hard disk required; Lotus 1-2-3 recommended for graphic output; Math co-processor chip and graphics board recommended.

For Additional Information:

For information about ordering this software, contact the NTIS Computer Products Center, NTIS, 5285 Port Royal Road, Springfield, VA 22161; (703) 487-4763.

Refer to PB87-126033/NAC

The software is contained on 5 1/4-inch diskette, double sided, double density compatible with the IBM PC XT, AT, microcomputer. Diskettes are in the ASCII format. Price includes documentation, PB87-100038.

The principle investigators also may be contacted: D. C. Ammon, A. Otte; Hazardous Waste Engineering Research Lab., Environmental Protection Agency, Cincinnati, OH.

Integrated Air Pollution Control System Cost Model Version 2 (IAPCS2)

Program estimates costs and performance for coal-fired utility boilers

The Integrated Air Pollution Control System (IAPCS) is a computerized simulation model developed for EPA's Air and Energy Engineering Research Laboratory (AEERL) to estimate the costs and predict the performance of sulfur dioxide (SO2), nitrogen oxides (NOx), and particulate matter (PM) emission control systems for coal-fired utility boilers. The model includes conventional and emerging technologies that effect pre-, in situ, and post-combustion emission control. The model can accept any combination of the technology modules built into the system. Alterations in the material balance are used to account for integrated performance and cost effects. The emission control technologies contained in IAPCS can be selected in either isolated or integrated configurations. The power of IAPCS lies in its ability to reflect integrated effects of various control configurations. This allows the analyst to identify synergistic interactions and thus optimize performance and cost in terms of integrated cost effectiveness.

Software Description: The program is written in the Fortran programming language for implementation on an IBM-PC AT or compatible microcomputer using the PC-DOS operating system. 512K bytes of core storage required. 1.5 Mbytes hard disk space; 80287 recommended.The software is contained on 5 1/2-inch diskette, double sided, double density compatible with the IBM PC AT microcomputer. Diskettes are in the ASCII format. Price includes documentation, PB87-127767/NAC, and PB87-127759/NAC.

For Additional Information:

For information about ordering this software, contact the
NTIS Computer Products Center, NTIS, 5285 Port Royal Road, Springfield, VA 22161; (703) 487-4763.

Refer to PB87-127775/NAC

energygram®

GROUNDWATER-LEVEL MONITORING SYSTEM

An automated system was designed to monitor groundwater fluctuations and the frequency with which groundwater came into contact with a group of experimental trenches. Fifteen on-site wells were equipped with portable liquid-level recorders; each recorder had a potentiometer that converted float level (i.e., water level) to an electrical resistance. A central power supply provided voltage to the potentiometers. The voltage from each well was fed to a single data logger preset to record at intervals from 16.67 s to 33.3 min onto a cassette tape. A series of computer routines was developed to process and analyze the data.

Although this system was designed specifically to meet the needs of the Engineered Test Facility, the hardware and computer routines have generic application to a variety of groundwater monitoring situations. Because data gathered by the system reflect both long-term trends in groundwater elevation and short-term responses to storms, they can be used in site characterization and as hydrological models to describe overall site water budget.

Additional information:

Office of Technology Applications
Information Service
Martin Marietta Energy Systems, Inc.
P.O. Box X
Oak Ridge, TN 37831
Telephone: (615) 574-4192; FTS 624-4192

J. D. Newbold and M. A. Bogle, *An Automated System for Monitoring Groundwater Levels at an Experimental Low-Level Waste Disposal Site,* ORNL/TM-9007, Oak Ridge National Laboratory (July 1984).

Manufacturing, Machinery, & Tools

871 Die-Target for Dynamic Consolidation of Powers

872 Robot to Transfer Wafers in New Integrated Circuit Facility

873 Corrosion and Load Transfer Effects on Fatigue of Mechanically Fastened Joints

874 Wet Winding Improves Coil Encapsulation — Voids are eliminated without special vacuum processing. (Licensing Opportunity)

875 Making Fillets by Electrical-Discharge Machining — A shaped graphite electrode eliminates many hours of hand work.

876 Quick-Release Panel Fastener — The twist of a handle activates and deactivates a clamp.

877 High-Pressure Valve With Controlled Seating Force — The poppet and seat are less likely to be damaged by faulty operation.

878 Magnetic Bearing With Radial and Angular Control — The rotor is stabilized magnetically with a feedback control system. (Licensing Opportunity)

879 Duplex Wrench — A special tool enables one worker to do a two-worker job.

880 Position Control for Nonlinear, Multiple-Link Robots — Several approaches to a complicated control problem are examined.

881 Optical Welding Torch — Arc welds can be viewed along the torch axis. (Licensing Opportunity)

882 Pultrusion Fabrication of Long Boom Models — Composite materials of quasi-isotropic strength are obtained.

883 Making Ceramic Parts by Laminating and Sintering Thin Sheets — The chemical composition can be varied as a function of depth.

884 Deep, Precise Etching in Semiconductors — Semiconductors can be made to accept precise etching after pretreatment.

885 Advanced Data Collection for Inventory Management — Bar-coding, radio-frequency, and voice-operated systems are selected.

886 Microprocessor-Based Valve Controller — A commanded mass-flow rate is maintained.

887 Inflatable Perimeter Seal — Inflatable tubing replaces gaskets or O-rings for sealing flat surfaces.

889 Low-Turbulence Valve — A valve promotes diffusion mixing of liquids rather than turbulence mixing. (Licensing Opportunity)

Testing & Instrumentation

888 Protecting a Ball-Bearing-Deflection Monitor — A thin barrier isolates a probe from liquid oxygon.

Other items of Interest

839 Switching Circuit for Shop Vacuum System — No internal connections to machine tools are required.

Department of Energy

Technology Application

Die-Target for Dynamic Consolidation of Powers

The Die-Target for Dynamic Powder Consolidation provides a new and improved method of consolidating metal monoliths from rapidly solidified powders (RSP). The method uses shock waves produced by detonation of explosive charges to consolidate the RSP. The die-target produces four fully consolidated monoliths for research test specimens which are fully dense and free from cracks. The die-target allows control of dynamic stress waves produced by detonation of high explosives to consolidate crack-free monolithic forms from RSP. This process does not produce high generalized temperatures in the powders which may seriously alter the microstructure and desirable properties of the RSP.

This technology is better than existing techniques which require substantial heating of powders. For rapidly solidified powders this could prove detrimental. Die-Target does not produce high temperatures.

FOR ADDITIONAL INFORMATION: Contact:
Dr. Jane M. Welch, Manager ORTA
Idaho National Engineering Laboratory
P.O. Box 1625
Idaho Falls, ID 83415
(208) 526-8318
Refer to DOE/INEL-019/TN
This technology is available for licensing

Consolidation techniques and the related processing parameters.

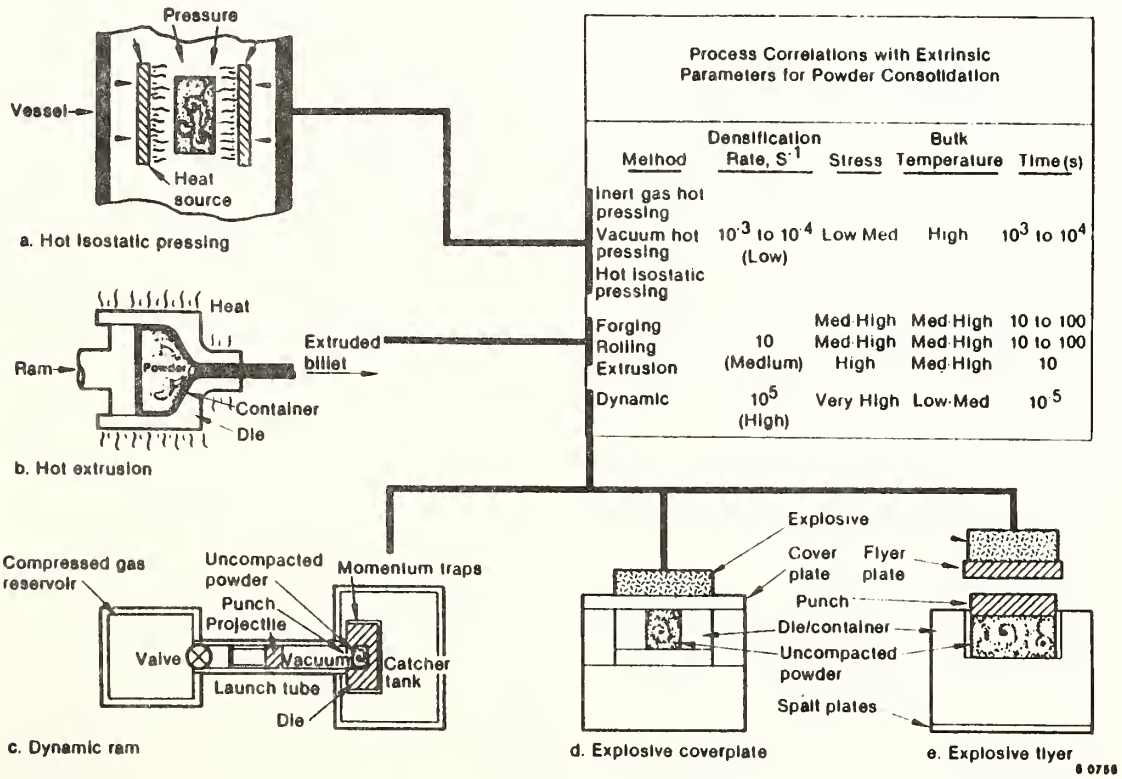

Robot to Transfer Wafers in New Integrated Circuit Facility

The new Radiation-Hardened Integrated Circuit (RHIC) facility, which is nearing completion at Sandia National Laboratories, will be the first U.S. integrated circuit research and prototype plant to use a robot in the entire fabrication process.

RHIC is the latest major addition to Sandia's Center for Radiation-Hardened Microelectronics (CRM). The CRM designs and builds microchips that continue operation even after receiving extremely high doses of radiation. Such microcircuits are used in nuclear weapon, space, and satellite systems as microprocessors, computer memories, and application-specific ICs.

The robot will travel RHIC's 300-ft-long clean room center aisle, accessing the 22 specialized processing bays (actually small clean rooms) that can be entered from that aisle.

Will move cassettes

It will home in on work in progress (WIP) stations and the plastic cassettes housed there that each hold 25 silicon wafers, called a lot. The robot will pick up the cassettes and move them to other processing bays.

The robot will select its travel route and actions based on information provided by the facility's computerized wafer fabrication operating system, and by following a reflective tape track that will be laid along floors throughout the 12,500-ft^2 clean room area.

"Other wafer fabrication lines have used robots," says Paul Plunkett, supervisor of Sandia's IC Interconnection & Deposition Division, "however, those robots have been confined to specific work stations. The case is the same, in fact, for the highly acclaimed robots that do much of the work along a modern automobile assembly line."

Besides being able to receive and execute instructions and to find its way around a large high-tech workplace, the CRM robot will display a new level of sophistication.

Sandia's Intelligent Machines Division has added a "force sensing" capability for the commercially available automated guided vehicle (AGV), the robot's formal name.

The work basically involved adding a commercially available strain-gauge-based sensor to the robot and developing algorithms and software that allow the robot to know whether it is being gentle enough with the wafer cassettes that are entrusted to it.

"A cassette of in-process CRM wafers is so valuable—nominally it represents a resource investment of up to $100,000—that we will take extreme measures to protect it during fabrication," Plunkett explains. "We simply can't have a robot mishandle a lot in any manner or form. We don't want it to drop a cassette. We don't want it to smash a cassette into a table or a piece of equipment.

"The know-how residing in our intelligent machines organization is helping us to determine other pitfalls of robot use in a wafer fab area, and to overcome or avoid those pitfalls," Plunkett says.

Just what does a robot add to a complex operation like IC fabrication? First, it ought to play a major role in keeping clean room contamination to a minimum. Every time a human process engineer or technician touches a cassette there is a contamination risk.

Reduces the risk

"That's a considerable risk when you consider that some 200 to 400 steps are involved in processing a wafer lot," says Bruce Draper, CRM robot project leader. "By simply using a robot to move wafers from bay to bay, instead of relying on people for that task, we'll significantly reduce the chances of contamination."

In addition, the fabrication line should display a greater degree of repeatability and control in executing processes. Finally, with the robot responsible for certain rather mundane tasks, the living, breathing workers in the RHIC facility can devote more of their time to completing the difficult engineering tasks that only they can do.

The heart of the RHIC facility is its 12,500-ft^2 Class 1 clean room where the robot will stay. This first large-scale Class 1 clean room will limit airborne particles in the work space to not more than one microscopic particle (0.12-micron size or larger) per cubic foot. Clean rooms use laminar air flow, the principle developed at Sandia in 1961, and now used worldwide to control airborne contamination.

FOR ADDITIONAL INFORMATION

Public Information Division,
Code 3161,
Dept. of Energy,
Sandia National Laboratories,
Albuquerque, NM 87185-5800
(505) 844-4207.
Refer to announcement 22, No. 3

NAVY
Domestic Technology Transfer Fact Sheet

Corrosion and Load Transfer Effects on Fatigue of Mechanically Fastened Joints

An aircraft structure consists of many components, which are connected mostly by mechanically fastened joints. Besides facilitating assembly and disassembly of structural components, the mechanically fastened joints transfer and distribute loads. Many aircraft structuralfailures are caused by fatigue cracking that originates at the fastener hole of a mechanically fastened joint. The fastener hole is a common site of load transfer and stress concentration. Therefore the fastener hole magnifies the local stress and influences the fatigue behavior of the joint.

To provide a technical basis for formulating a reliable service life prediction methodology of aircraft structures, it is essential to understand and quantify the load transfer effect on the fatigue behavior of mechanically fastened joints. The work was conducted to characterize the fatigue behavior of mechanically fastened joints and identifying the load transfer effect. With tests of low, medium, and high load transfer specimens of 7475-T7351 aluminum alloy, the fatigue crack initiation and growth, and the fracture behavior have been investigated, and the load transfer effect has been defined quantitatively. The results are compared to those of a zero load transfer specimen.

A $\frac{1}{4}$ in. thick plate of 7475-T7351 aluminum alloy was used as the specimen material. This was the same material that was employed in the study of the zero load transfer specimen. From the plate, reverse dogbone joint, $1\text{-}\frac{1}{2}$ dogbone joint, and double lap shear joint specimens were prepared in order to have low, medium, and high levels of load transfer, respectively, (figures 1-3). The longitudinal axis of the specimen was in the original plate rolling direction. In each specimen, a steel fastener of a protruding head (MS 20004) was installed in close tolerance fit holes (drilled and reamed), using a clamp-up torque of 20 in-lb.

FOR ADDITIONAL INFORMATION: A copy of the report is available from NTIS, Springfield, VA 22161; (703) 487-4600.

NTIS order number: AD-A173802/NAC

Price code: A03

To discuss this effort further, contact:
Dr. E.V. Lee
Aircraft Technology Directorate
Naval Air Development Center
Warminster, PA 18974
(215) 441-1663

Based on the study with mechanically fastened joint specimens of low, medium, and high load transfer levels, the following is concluded.

1. The load transfer levels, measured and calculated, are

	LOAD TRANSFER LEVEL	
SPECIMEN	MEASURED VALUE	CALCULATED VALUE
Reverse Dogbone Joint	0.06	0.068
1-1/2 Dogbone Joint	0.31	0.49

The load transfer level in the double lap shear joint specimen is obviously 1.0.

2. The fatigue crack initiation life, N_i, and the total fatigue life, N_f, decrease with increasing stress range, $\Delta\sigma$, and load transfer level, L. This relationship is defined by the equations.

$$\log N_i = 8.51 - 0.18\ \Delta\sigma - 2.26\ L^{1.48}$$

$$\log N_f = 8.19 - 0.15\ \Delta\sigma - 1.50\ L^{1.53}$$

3. The fatigue crack initiation life and total fatigue life of a joint specimen with some level of load transfer cannot be deduced from those of a zero load transfer specimen by merely adjusting the stress concentration factor at the fastener hole edge (or the crack initiation site).

4. The fatigue crack growth rate, da/dN, as a function of stress intensity factor range, ΔK, is

$$da/dN = (9.30 \times 10^{-9}) \cdot (\Delta K)^{2.89}\ \text{(in/cycle)}$$

5. The crack initiation portion of total fatigue life, N_i/N_f, decreases with increasing stress range, $\Delta\sigma$, and load transfer level, L, but increases with increasing total fatigue life, N_f. This relationship is defined by the equation.

$$\log (N_i/N_f) = [0.32 - (2.26 - 1.50\ L^{0.05})\ L^{1.48}] - 0.03\ \Delta\sigma$$

$$= \log [1 - U\ (N_f)^{-S}]$$

NASA Tech Brief
National Aeronautics and Space Administration
Marshall Space Flight Center, Alabama

Licensing Opportunity

Wet Winding Improves Coil Encapsulation

Voids are eliminated without special vacuum processing.

A wet-winding process encapsulates electrical coils more uniformly than do conventional processes. The process requires no vacuum pump and can be adapted easily to existing winding machines.

Encapsulation of electrical coils prevents electrical failures by protecting the coil wires against vibration and distortions due to temperature changes. Conventional methods of forcing potting materials into coil windings have often resulted in voids. Even impregnation in a vacuum does not completly eliminate the voids. The discontinuities resulting from these voids may degrade the coil performance or cause its failure under environmental loading. Coil wires, lead wires, wire-to-wire joints, and wire-to-pin joints can all break because of the inadequate support during vibration or because of cracking in conventional varnish coatings subjected to thermal cycling.

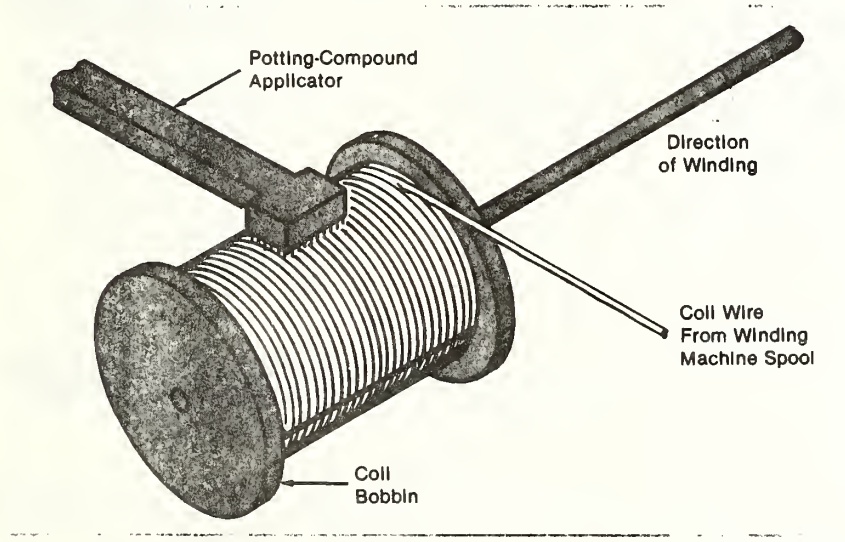

The **Encapsulant Is Applied** to each layer of wire as soon as it is added to the coil. This wet-winding process eliminates voids, giving a more uniformly encapsulated coil.

In wet winding (see figure) a brush or other suitable applicator is used to coat each layer of wire with the potting compound as soon as the layer is added to the coil. The coil is fully impregnated, and the joints between the coil wire and lead wires are encapsulated with the potting compound. In the original wet-winding application used on flow and speed sensors for fuel and oxygen turbopumps on the Space Shuttle, the potting compound was Hysol (or equivalent) epoxy.

This work was done by Arthur J. Hill of Rockwell International Corp. for **Marshall Space Flight Center**. *No further documentation is available.*

Inquiries concerning rights for the commercial use of this invention should be addressed to the Patent Counsel, Marshall Space Flight Center Refer to MFS-29174/TN

George C. Marshall Space Flight Center
Technology Utilization Officer:
Ismail Akbay
Code AT01
Marshall Space Flight Center,
AL 35812
(205) 544-2223
Patent Counsel:
Leon D. Wofford, Jr.
Mail Code CC01
Marshall Space Flight Center,
AL 35812
(205) 544-0014

FOR ADDITIONAL INFORMATION: *Contact: Director, Technology Transfer Division, P.O. Box 8757, BWI Airport, MD. 21240; (301) 621-0100 Ext. 241*
REFER TO THE NUMBER LISTED AT THE END OF THE ARTICLE

NASA Tech Brief
National Aeronautics and Space Administration
Marshall Space Flight Center, Alabama

Making Fillets by Electrical-Discharge Machining

A shaped graphite electrode eliminates many hours of hand work.

Fillets between tubes and a baseplate can be rounded to a small radius with a shaped electrode by electrical-discharge machining (EDM). The electrode was developed for finishing the base of the 600 injector posts in the Space Shuttle main engine. Previously, the hollow posts were finished manually with hand tools and a radius gauge. The procedure was time consuming, taking about 120 hours for one engine. With the new EDM electrode, all the posts are given fillets of 50-mil (1.27-mm) radius at their bases in only 10 hours.

The electrode is made by shaping it with a hardened-steel tool. The tool has a collar with the fillet that is to be impressed onto the corresponding internal lip of the electrode (see figure). The tool is brought to bear on the tip of the tubular graphite electrode and vibrated against it to produce the required fillet.

This work was done by R. K. Burley of Rockwell International Corp. for **Marshall Space Flight Center**. *No further documentation is available.*
MFS-19929 /TN

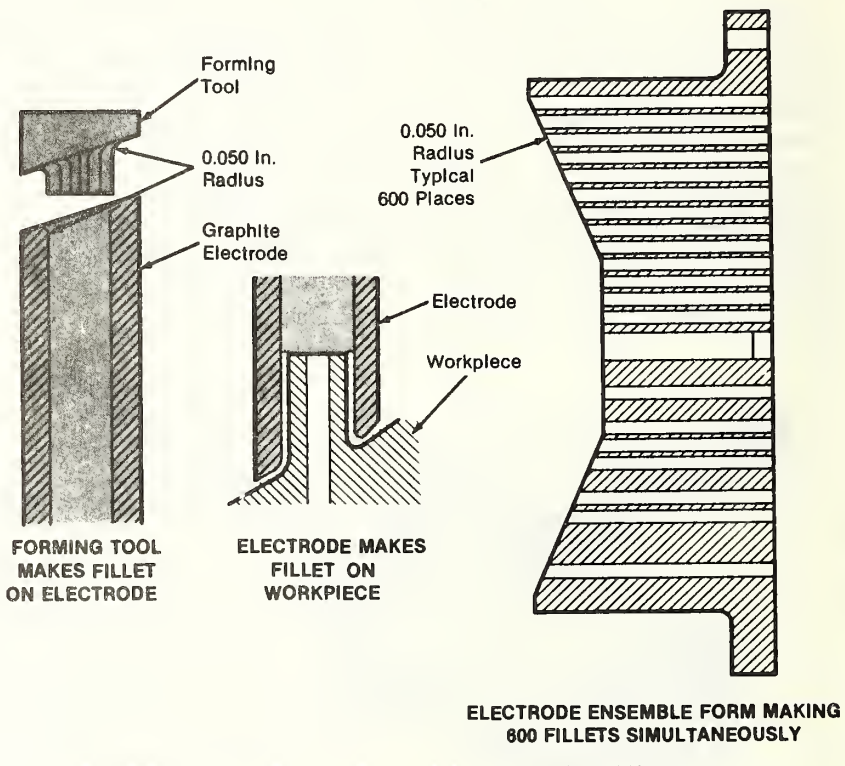

A Hardened-Steel Forming Tool Transfers Its Fillet Shape to the internal lip of an electrode. The lip shape is then transferred to the base of a post in the EDM procedure to form a fillet. An array of electrodes (right) can produce many fillets simultaneously.

FOR ADDITIONAL INFORMATION: *Contact: Director, Technology Transfer Division, P.O. Box 8757, BWI Airport, MD. 21240; (301) 621-0100 Ext. 241*
REFER TO THE NUMBER LISTED AT THE END OF THE ARTICLE

NASA Tech Brief
National Aeronautics and Space Administration
Lyndon B. Johnson Space Center, Houston, Texas

Quick-Release Panel Fastener

The twist of a handle activates and deactivates a clamp.

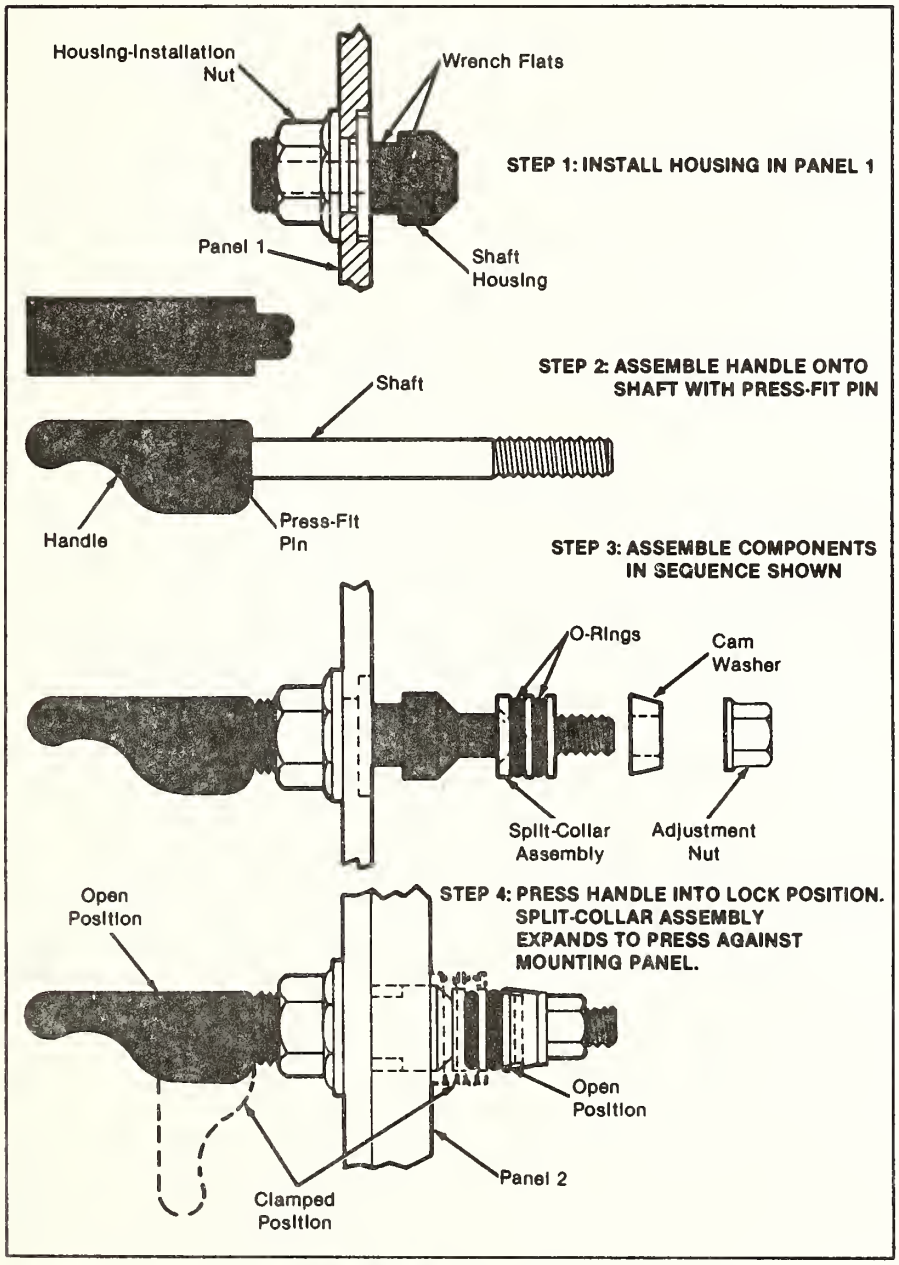

Installation of the Quick-Release Fastener is fast and easy. A 90° rotation of the handle after installation is all that is needed to clamp together or release a pair of panels.

A quick-release fastener for panels can be actuated with just one hand. The fastener has no loose parts, does not require mating hardware, and can be used in a blind hole in the mating panel.

The new panel fastener is a self-contained unit that extends through congruent holes in the two panels to be joined. The unit contracts to clamp the panels together and expands to release them.

The shaft housing of the fastener is installed in a counterbore in panel 1 and held there by a nut (see figure). A handle is attached to the shaft with a press-fit pin. The end of the shaft opposite the handle is inserted in the shaft housing, and a split-collar assembly with O-rings, a cam washer, and an adjustment nut are assembled on the shaft. The unit is then ready for use.

The shaft is inserted in panel 2, and the handle is turned so that its axis is perpendicular to the shaft axis. This action forces the adjustment nut and washer against the split-collar assembly, pushing the assembly up the taper of the shaft housing so that the split collar expands beyond the hole and clamps panel 2 against panel 1.

This work was done by David R. Fosdick and Robert C. Phillips of Rockwell International Corp. for **Johnson Space Center**. *MSC-20767 /TN*

FOR ADDITIONAL INFORMATION: *Contact: Director, Technology Transfer Division, P.O. Box 8757, BWI Airport, MD. 21240; (301) 621-0100 Ext. 241*
REFER TO THE NUMBER LISTED AT THE END OF THE ARTICLE

NASA Tech Brief
National Aeronautics and Space Administration
Lyndon B. Johnson Space Center, Houston, Texas

High-Pressure Valve With Controlled Seating Force

The poppet and seat are less likely to be damaged by faulty operation.

Improvements in a widely-used high-pressure valve increase the accuracy of preloading of the poppet. The redesigned valve also prevents metal shavings and other debris from developing during operation, installation, or removal. New features include a secondary seal in the cap.

In the previous version of the valve, the poppet was seated and preloaded by use of a torque wrench to apply a predetermined torque to a swivel nut that drove the poppet. However, this procedure sometimes damaged the valve seat if the torque wrench was not set properly or was poorly calibrated or because variations in valve properties or conditions altered the torque/preload relationship. The damage could spring a leak of pressurized gas or hydraulic fluid.

The new version of the valve uses the spring force of Belleville washers to apply, control, and limit the preload on the poppet seat. The length of the valve body is increased slightly to accommodate the washers, which are placed around the neck of the body (see figure). When the swivel nut is first tightened, the washer with the least stiffness will bottom out first, and the washer with the greatest stiffness will hardly be deflected. If the swivel nut is tightened further, the washer of medium stiffness will be the next one that deflects to preload the poppet. Still more tightening will cause the first two washers to bottom out, and the stiffest washer will then begin to deflect.

Thus, in a random sample of three washers, the washer that most closely matches the design stiffness can be selected, by progressive tightening, to be the one that provides the preload force. If that selected washer should fail, the bottomed-out washer will take over; the valve will still operate correctly but at a slightly lower preload.

If the swivel nut is tightened beyond the required preload, it comes into contact with the torque limiter, which is a washerlike device at the end of the valve body. The knurled face of the swivel nut scrapes against projections on the torque limiter, producing vibration and a screeching sound that alerts the installer. At the same time, the projections dig into the knurled surface, making further tightening of the swivel nut increasingly difficult.

The pressure-warning groove has a rounded contour in the new version; the sharp corners of the groove in the old valve design are eliminated. The new contour prevents metal particles from being cut from threads when the valve is assembled and operated. Such particles could lodge in the poppet seat or flow into the pneumatic or hydraulic system and cause harm.

The stem end is beveled in the new valve so that it sits tightly in a conical ring cavity in the valve cap. The stem and cap thus form a backup seal for the primary poppet seal.

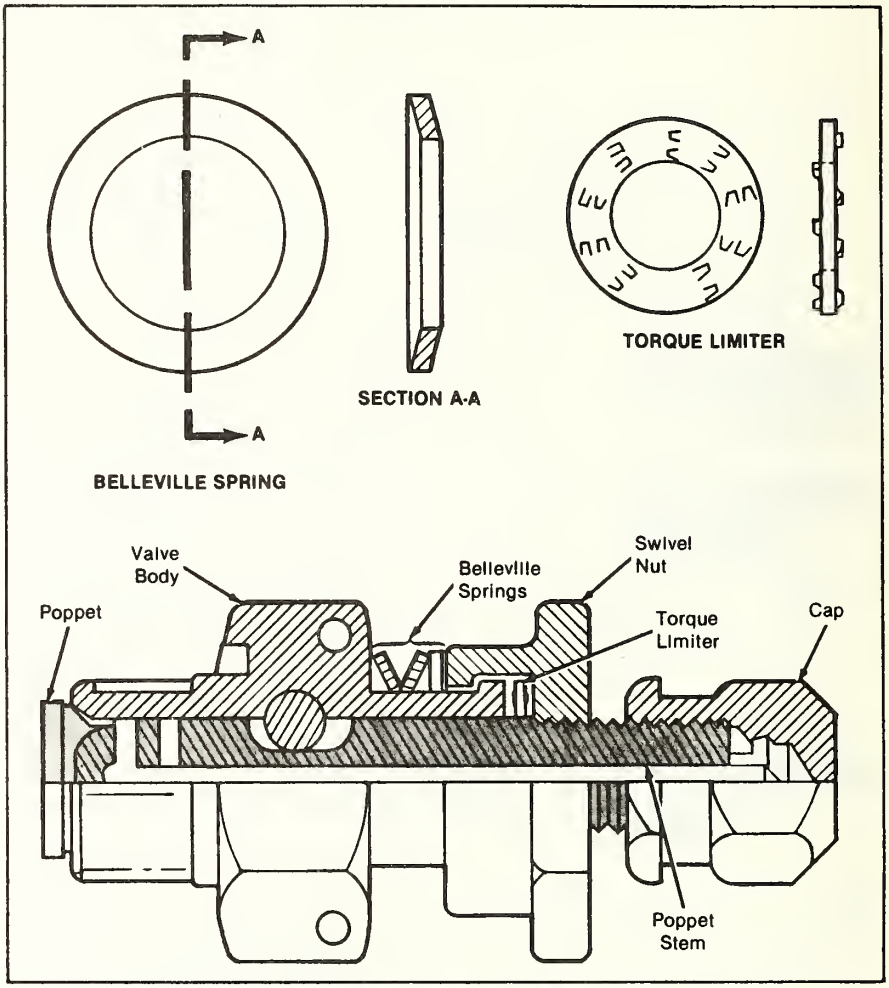

Belleville washers create a Precise Value of Seating Force. If an installer should attempt to exceed that force, the torque limiter gives tactile and aural warning and makes further force increases difficult.

This work was done by Raymond H. Bradley of **Johnson Space Center.**
MSC-20932 /TN

FOR ADDITIONAL INFORMATION: *Contact: Director, Technology Transfer Division, P.O. Box 8757, BWI Airport, MD 21240; (301) 621-0100 Ext. 241*
REFER TO THE NUMBER LISTED AT THE END OF THE ARTICLE

NASA Tech Brief
National Aeronautics and Space Administration
Goddard Space Flight Center, Greenbelt, Maryland

Licensing Opportunity

Magnetic Bearing With Radial and Angular Control

The rotor is stabilized magnetically with a feedback control system.

An active magnetic bearing stably levitates its rotor against radial (lateral) and axial motion and points the rotor axis in a controllable direction, yet allows the rotor to turn freely about its own axis. As in other magnetic-bearing systems, the rotor is the only moving part, and the absence of mechanical contact between the rotor and the stator assures long life. The adjustable magnetic bearing would be particularly useful in high-speed rotating devices, robotic joints, and supports for optical elements.

The bearing (see Figure 1) includes a stator equipped with permanent magnets and electromagnet coils. The rotor has a magnetically permeable ring that surrounds the stator. Three inwardly projecting rims on the rotor constitute magnetic pole pieces and face similar pole pieces on the stator.

The radial-control electromagnet coils on the opposite sides of the central permeable disk introduce a magnetic flux along the x axis (toward the left in the case of the figure). This flux aids the permanent-magnet flux on the right side while opposing it on the left side. Thus, the magnetic attraction between the rotor and stator pole pieces increases on the right and decreases on the left, thereby tending to pull the rotor to the left. Similarly, reversing the current in the radial-control coils forces the rotor to the right.

The angular-control electromagnet coils on the upper and lower permeable disk quadrants are connected to produce a magnetic flux circulating around the periphery of the magnetic path. When this flux circulates in the clockwise direction, as in the figure, it aids the permanent-magnet flux at the upper-right and lower-left airgaps and opposes the permanent-magnet flux in the lower-right and upper-left airgaps. This flux pattern does not introduce a net right or left force, but the inequalities of forces at the corner airgaps produce a net torque on

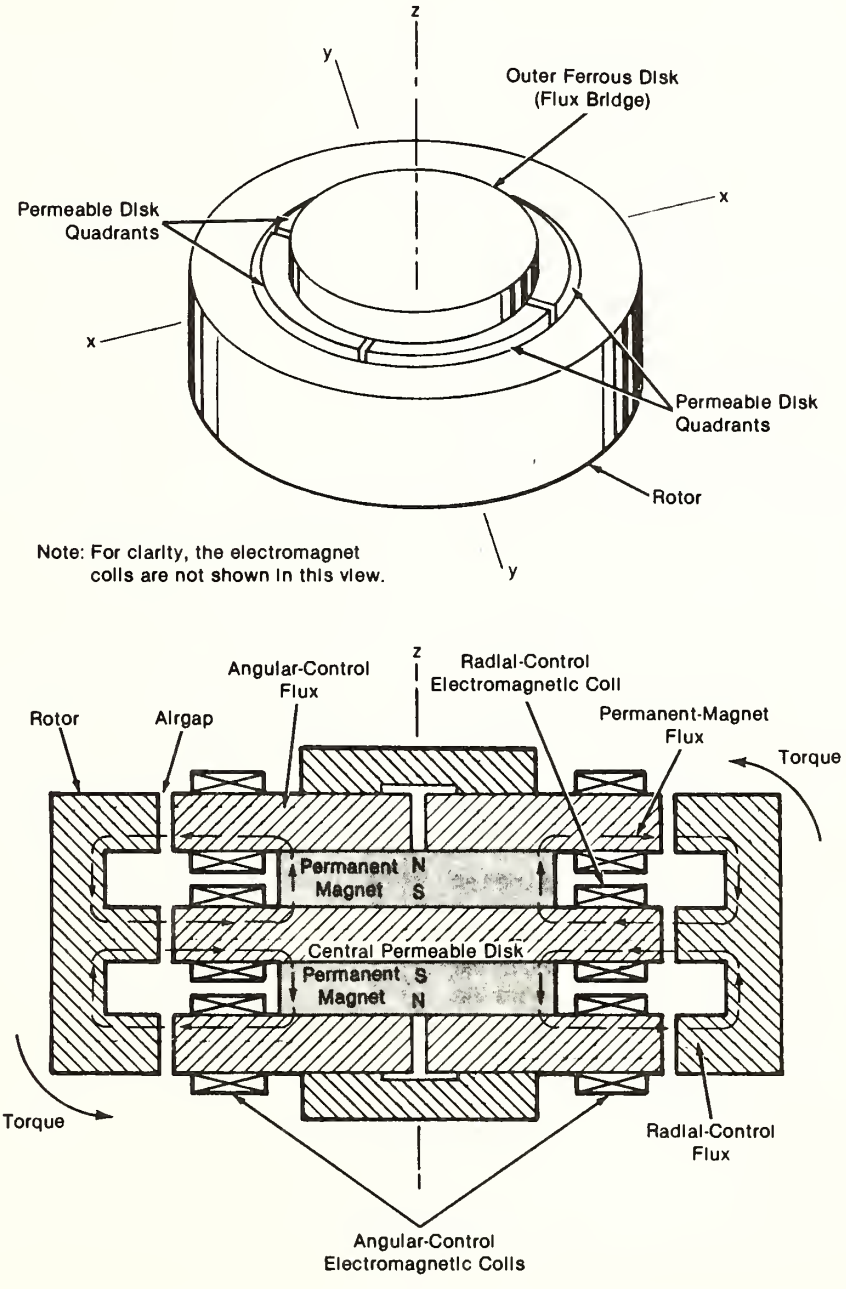

Figure 1. The **Active Magnetic Bearing** includes electromagnet coils that tilt the rotor clockwise or counterclockwise, or move it right or left.

the rotor, tilting it counterclockwise about the y axis. Of course, the rotor could be tilted clockwise by reversing the angular-control flux.

Similar electromagnet coils are placed in the y-z plane of the stator to control the rotor motion along the y axis and the rotor tilt about the x axis. No electromagnetic control is needed to steady the rotor along the z axis. The rotor continually seeks the z-axis position of minimum magnetic reluctance to the permanent-magnet field; because of the rotor and stator symmetries, this position is independent of the angular position of the rotor.

Figure 2 illustrates a feedback control system for one plane of the bearing. The control circuitry varies the currents in the radial- and angular-control coils in response to the outputs of the radial- and angular-position sensors. An angular-command bias to the angular differential amplifier sets the equilibrium angular position. In principle, a similar arrangement could be used to set an equilibrium radial position different from the z axis.

This work was done by Philip A. Studer of **Goddard Space Flight Center**.

This invention is owned by NASA, and a patent application has been filed. Inquiries concerning nonexclusive or exclusive license for its commercial development should be addressed to the Patent Counsel, Goddard Space Flight Center Refer to GSC-12957. /TN

Goddard Space Flight Center
Technology Utilization Officer:
Donald S. Friedman
Mail Code 702-1
Greenbelt, MD 20771
(301) 286-6242
Patent Counsel:
John O. Tresansky
Mail Code 204
Greenbelt, MD 20771
(301) 286-7351

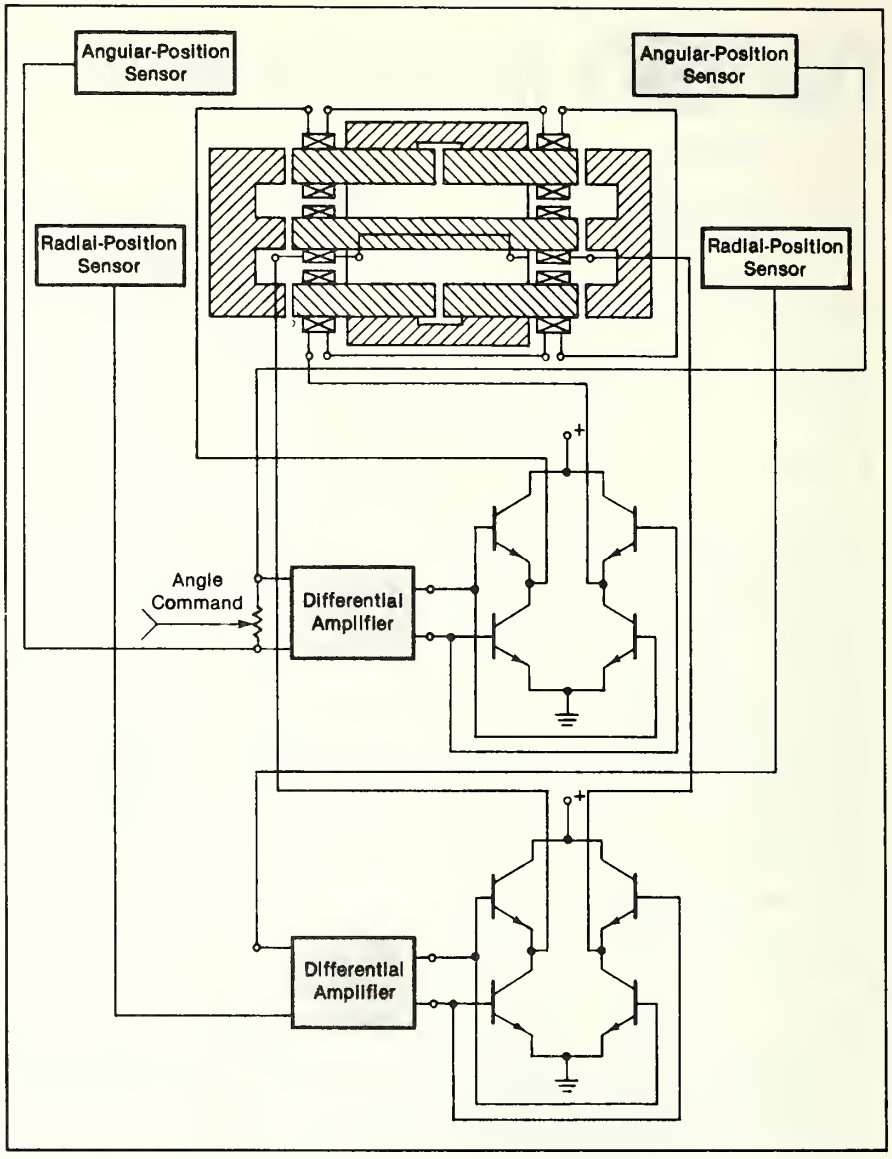

Figure 2. A **Feedback Control System** maintains the rotor at equilibrium radial and angular positions in response to signals from position sensors. No active control is needed to maintain the equilibrium axial position.

FOR ADDITIONAL INFORMATION: *Contact: Director, Technology Transfer Division, P.O. Box 8757, BWI Airport, MD. 21240; (301) 621-0100 Ext. 241*
REFER TO THE NUMBER LISTED AT THE END OF THE ARTICLE

NASA Tech Brief
National Aeronautics and Space Administration
Lyndon B. Johnson Space Center, Houston, Texas

Duplex Wrench

A special tool enables one worker to do a two-worker job.

A special wrench holds two nuts in place while a third nut, coaxial with the others, is turned. The wrench was developed for tightening delicate couplings on a gas-supply panel. With it, a single operator can restrain the coupling pressure cap and the connector body nut with one hand. The other hand is free to tighten the coupling nut with a torque wrench.

Previously, two operators using three wrenches were needed for the job. The operators often had difficulty coordinating their actions and sometimes damaged the parts. (The mating surfaces in the coupling must not be rotated on each other or else the seal will be broken, and costly repairs will be necessary.) The tightening operation was especially awkward in close quarters.

The wrench has two heads on a common shaft (see figure). The offset section secures the flats of the connector-body nut, which is flush against the panel. The straight section holds the pressure cap. Immobilizing these parts with the duplex wrench, the operator turns the coupling nut to the required tightness.

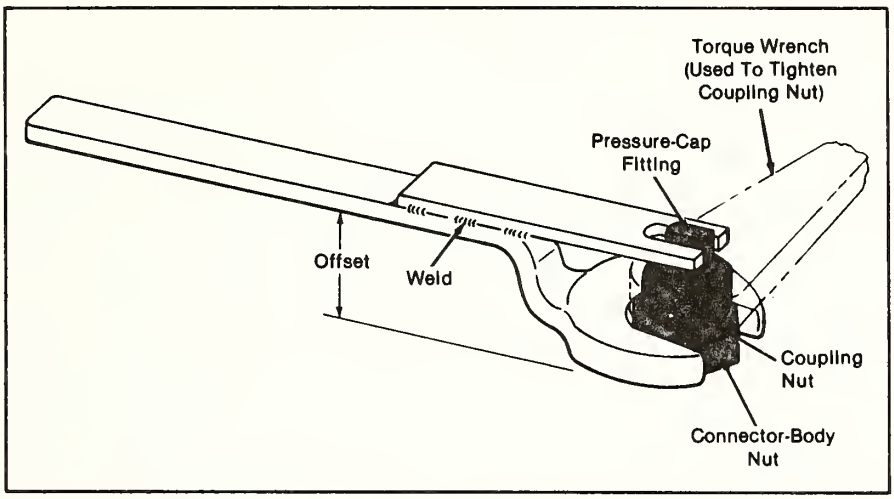

The Duplex Wrench Holds Two Parts of a pressure fitting while the nut between them is turned with another wrench. The concept can be adapted to other three-wrench operations on coaxial nuts.

This work was done by Charles N. Canada of Rockwell International Corp. for **Johnson Space Center**. *MSC-20585 /TN*

FOR ADDITIONAL INFORMATION: *Contact: Director, Technology Transfer Division, P.O. Box 8757, BWI Airport, MD. 21240; (301) 621-0100 Ext. 241*
REFER TO THE NUMBER LISTED AT THE END OF THE ARTICLE

NASA Tech Brief
National Aeronautics and Space Administration

Position Control for Nonlinear, Multiple-Link Robots

Several approaches to a complicated control problem are examined.

A report surveys methods for controlling the motion of robot manipulators. The report applies to coupled, highly nonlinear multiple-link robots.

The report notes that the position control of a robot involves the calculation of control inputs to the robot motors so that the response of the robot arm will be stable, the robot position will not deviate from the desired value even in the presence of disturbance inputs, and the robot arm will be able to follow desired trajectories with no errors. It is relatively easy to accomplish these objectives with linear, time-invariant systems.

However, a multiple-link robot is neither linear nor time-invariant because each link in the robot arm exerts varying torques on the other links as the configuration of the arm changes. The dynamic equations for a multiple-link manipulator are therefore highly nonlinear and coupled, and controlling such a manipulator is a very complicated task.

The report begins with an analysis of linear control for a single-link manipulator. It shows that the linear control methods can be applied to multiple-link manipulators with independent linear-position servos operating simultaneously at all the joints, because such systems can be approximated with linear systems once the nonlinearities due to the dynamic interactions among joints are taken into account.

In one control strategy, nonlinear state feedback is used to reduce the control of a robot system to a linear problem. For example, in the computed-torque technique, the coupling inertias, centrifugal torques, and Coriolis torques exerted by each link on the others are predicted, and the control of each link is then adjusted to compensate for them. An analogous method that provides position control of the last manipulator link only is called the "resolved-acceleration-control" technique.

The acceleration-feedback-control technique relies on high-gain feedback to minimize the effect of nonlinearities. A technique called "robust nonlinear control" is based on an inversion algorithm for the input/output map of a nonlinear system. It provides for close tracking of a required trajectory despite uncertainty in the payload.

The report ends by presenting an adaptive control technique based on a discrete linear model of the robot arm, obtained by linearizing the nonlinear dynamical equations about a nominal trajectory. The parameters of the model are calculated with an adaptive parameter-identification algorithm. Based on the system model, an optimal control input is computed using position and velocity feedback.

This work was done by Homayoun Seraji and Mary M. Moya of Sandia National Laboratories for **NASA's Jet Propulsion Laboratory**. *"Robot Control Systems: a Survey," NPO-16806 /TN*

FOR ADDITIONAL INFORMATION: *Contact: Director, Technology Transfer Division, P.O. Box 8757, BWI Airport, MD. 21240; (301) 621-0100 Ext. 241*
REFER TO THE NUMBER LISTED AT THE END OF THE ARTICLE

NASA Tech Brief
National Aeronautics and Space Administration
Marshall Space Flight Center, Alabama

Licensing Opportunity

Optical Welding Torch

Arc welds can be viewed along the torch axis.

A gas/tungsten-arc welding torch supports an electrode at its center while enabling the viewing of the weld area along the torch axis. The gas torch accommodates a lens and optical fibers — all part of a vision system for a welding robot.

The main component of the torch is the optical body — a square-cross-section copper part with internal bores that accept the various optical and welding components (see figure). A symmetrical spoked structure is machined in the optical body in its lower portion.

The optical body includes openings for coaxial viewing and support, electrical contact, and heat removal from the electrode, which is held by a collet screwed into the hub of the spoked structure.

Channels for cooling water are drilled through the optical body, close to the outer ends of the spokes. Cooling water enters through a vertical channel at a corner of the body and flows out through a channel at the opposite corner.

A lens above the spokes focuses a reduced image of the weld area, which is one-half to three-quarters of an inch (1.3 to 1.9 centimers) in diameter, onto the 5-millimeter-diameter end face of an optical-fiber bundle. The bundle is held by a brass supporting tube that sits in a bore at the top of the optical body. The tube also secures a stack of components: an iris diaphragm, the lens, a gas-injection spacer, and a filter window. A bundle-feedthrough nut atop the support tube can be loosened so that the bundle can be slipped up and down for focusing.

A copper gas-cup tube screws into the bottom of the optical body, and a ceramic gas cup screws into the gas-cup tube. The tube holds the cup on the center line of the torch and guides the flow of shielding gas to the cup. The tube can readily be removed and replaced if it is damaged.

The electrode is damped by a collet, which is mounted in a collet holder. The collet allows the electrode to be adjusted,

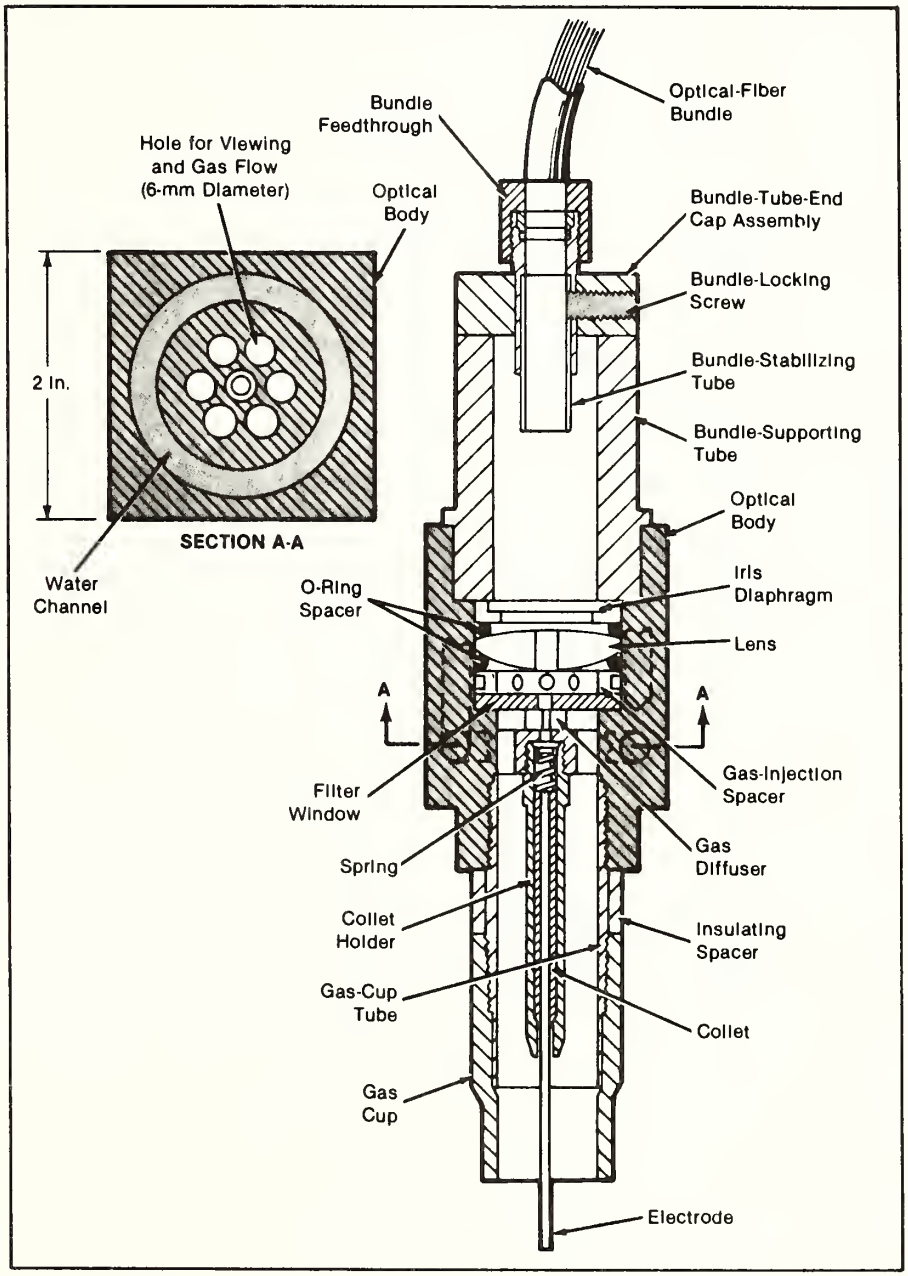

The **Welding Torch** includes a spoked structure in the central bore of the optical body. The structure supports the welding electrode, carries electric current to it, and takes heat away from it. The spokes are formed by drilling six holes 60° apart around the center line of the torch.

removed, and replaced conveniently. The collet holder must be tightened firmly against the torch body for good thermal contact and accurate alignment of the collet with the optical axis. A spring in the holder produces a downward thrust on the collet. The chamfered outer end of the collet seats against the chamfered inner end of the holder, forcing the collet inward to grip the electrode.

Shielding gas enters the optical body through a channel parallel to the cooling-water channels and passes through a gas-injection spacer in the bore. The spacer guides the flow smoothly around the periphery of the bore. The gas flows inward through radial holes in the spacer, then down through a central hole in the filter window (which stops unwanted light wavelengths from entering the vision system). Finally, the gas flows through a diffuser (which helps to prevent turbulence and entrainment of air at the weld site), through the holes in the spoked structure, and into the gas cup.

This work was done by Richard W. Richardson of Ohio State University for **Marshall Space Flight Center.**

In accordance with Public Law 96-517, the contractor has elected to retain title to this invention. Inquiries concerning rights for its commercial use should be addressed to

Richard W. Richardson
Ohio State University
1314 Kinnear Road
Columbus, OH 43212

Refer to MFS-26034 /TN

George C. Marshall Space Flight Center
Technology Utilization Officer:
Ismail Akbay
Code AT01
Marshall Space Flight Center, AL 35812
(205) 544-2223
Patent Counsel:
Leon D. Wofford, Jr.
Mail Code CC01
Marshall Space Flight Center, AL 35812
(205) 544-0014

FOR ADDITIONAL INFORMATION: *Contact: Director, Technology Transfer Division, P.O. Box 8757, BWI Airport, MD. 21240; (301) 621-0100 Ext. 241*
REFER TO THE NUMBER LISTED AT THE END OF THE ARTICLE

NASA Tech Brief
National Aeronautics and Space Administration
Langley Research Center, Hampton, Virginia

Pultrusion Fabrication of Long Boom Models

Composite materials of quasi-isotropic strength are obtained.

Pultrusion is a composite-fabrication method by which an extremely long fiber-reinforced polymer matrix material can be produced by pulling the fiber through a resin system for impregnation and then through a heated curing die. As the fiber/resin bundle travels through the curing die, polymerization occurs, and a composite structure emerges from the exit end of the die (see figure).

While pultrusion is not a new process, it is still in its infancy in the aerospace industry. At Langley Research Center, experiments with pultrusion are being conducted in advanced-composites technology with applications to aeronautical and space structures. In one such program, long flexible beams were required to establish ground vibration-test methods for very-low-frequency structures. The beams were fabricated by the pultrusion process using fiberglass for reinforcement and a thermoset polyester resin system for the matrix. These beams were rectangular in cross section [0.25 by 4.00 in. (0.64 by 10.16 cm)] and 32.81 ft (10.00 m) in length, each weighing 25.6 lb (11.6 kg).

The research applications of such tests are model space booms for the proposed MAST program and the space station. Because of the potential for lower cost, higher specific-strength and flexural properties, and dynamic-similarity considerations, pultruded-composite-beam models were selected as an option over extruded-aluminum structures. Continuous lengths up to 270 ft (82.3 m) were pultruded and later cut to the required lengths for dynamic testing.

The composite-reinforcement-materials approach used in the beam models was unique in that equal strength is provided in both the longitudinal (0°) and transverse (90°) directions. This was achieved by selective fiber orientation using knit-locked fabric. The availability of this new type of fabric makes possible the pultrusion fabrication of composite materials of quasi-isotropic strength using the conventional "wet-resin" technique. Furthermore, the potential for the precise orientation of fibers in any desired direction in pultrusion can now be realized by this approach to reinforcement materials.

Ultrasonic C-scans as well as SEM evaluations showed good wetting of fibers and bonding between plies. Physical and mechanical test results were compared with those of fiberglass unidirectional roving and continuous-strand-mat, conventional pultrusions, and with extruded 6061-T6 aluminum alloy.

This is an advancement in the state of the art of pultrusion technology in that the ability to duplicate any hand-layup fiber orientation, e.g., $(0°, +45°, -45°, 90°)_S$, and still use the "wet-resin" method of impregnation is now possible. This concept is not restricted to the fiberglass-reinforcement and polyester-matrix systems used in this program and should prove adaptable to other fiber/resin systems.

This work was done by Maywood L. Wilson and Robert Miserentino of **Langley Research Center**. *LAR-13441/TN*

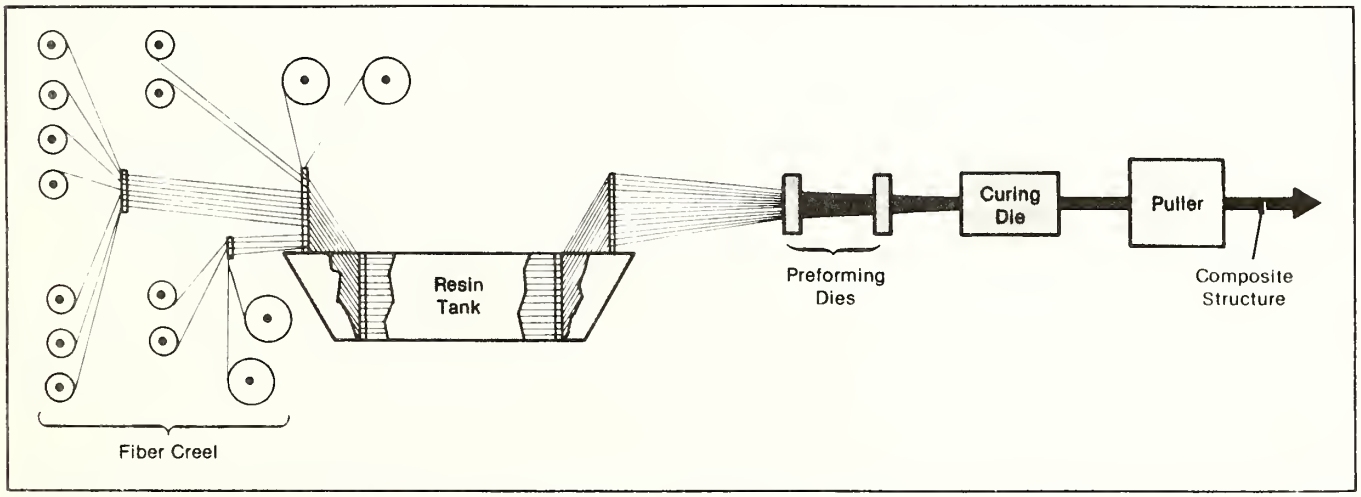

The **Fiber-Reinforced Polymer Matrix Material** is produced by pulling the fibers through the polymer resin system and then through preforming dies and a heated curing die.

FOR ADDITIONAL INFORMATION: *Contact: Director, Technology Transfer Division, P.O. Box 8757, BWI Airport, MD. 21240; (301) 621-0100 Ext. 241*
REFER TO THE NUMBER LISTED AT THE END OF THE ARTICLE

NASA Tech Brief
National Aeronautics and Space Administration
Lewis Research Center, Cleveland, Ohio

Making Ceramic Parts by Laminating and Sintering Thin Sheets

The chemical composition can be varied as a function of depth.

A technique has been developed to fabricate a monolithic ceramic component by sintering a laminated body made from thin sheets of green ceramic. This method allows discrete changes in chemistry to be effected across the monolith. A component that has a one-dimensional variation in material composition could be fabricated in this manner.

The thin sheets of ceramic can be made by "tape casting," in which a powder of the desired composition is placed in suspension and spread onto a hot surface. The liquid is evaporated, leaving a thin sheet of green ceramic. The sheet may be given flexibility through the incorporation of polymers (plasticizers) dissolved in the suspending liquid. Since the sheets are fabricated independently, the composition of any one sheet is independent of that of the others.

To construct the final part, the thin sheets are stacked in the appropriate order of desired chemical properties, compressed into a monolith, and sintered. Proof-of-concept tests have demonstrated that such parts can be made without bloating or delamination of the ceramic.

An example of the type of part that could be fabricated from this technique is an all-ceramic turbine-shroud seal for an advanced gas-turbine engine. The hot face of the seal could be made of material with good thermal-cycling and high-temperature characteristics, whereas the cold side could be made of material with high structural strength and high fracture toughness. One combination of materials would be (a) yttria/partially stabilized-zirconia (Y/PSZ) for the layers closest to the hot face of the turbine shroud seal and (b) magnesium/partially stabilized-zirconia (M/PSZ) for the "structural" layers.

This work was done by James D. Cawley of Ohio State University for **Lewis Research Center**. *Further information may be found in NASA TM-87078 [N85-32333/NSP], "Tape Casting as an Approach to an All-Ceramic Turbine Shroud Seal."*

Copies may be purchased from the National Technical Information Service, Springfield, Virginia 22161, [A02]
LEW-14361/TN

FOR ADDITIONAL INFORMATION: *Contact: Director, Technology Transfer Division, P.O. Box 8757, BWI Airport, MD. 21240; (301) 621-0100 Ext. 241*
REFER TO THE NUMBER LISTED AT THE END OF THE ARTICLE

NASA Tech Brief
National Aeronautics and Space Administration
NASA's Jet Propulsion Laboratory, Pasadena, California

Deep, Precise Etching in Semiconductors

Semiconductors can be made to accept precise etching after pretreatment.

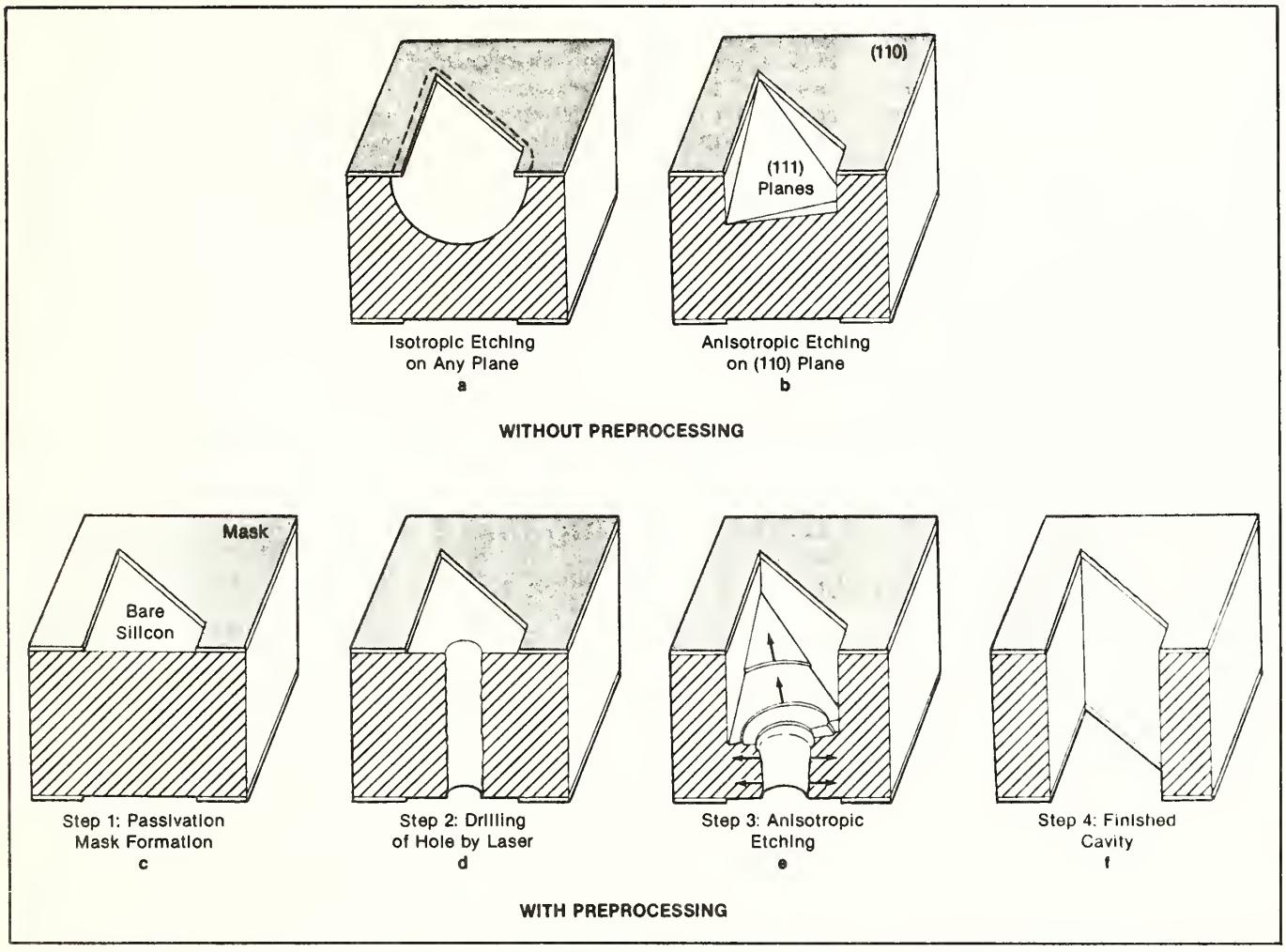

Anisotropic Etching of a Hole in a masked (110) silicon wafer yields a cavity of arbitrary depth bounded by perpendicular (111) planes. In contrast, conventional anisotropic etching produces a shallow, faceted cavity, and isotropic etching creates a hemispherical cavity.

A combination of material destabilization and anisotropic etching permits the formation of precise perpendicular-wall cavities in silicon wafers and other semiconductors. This new technique extends the capabilities of current micromachining technology to the fabrication of submillimeter waveguide arrays and filters.

"Micromachining" refers here to the fabrication of micromechanical devices, such as pressure sensors, bolometers, and switches, on silicon crystal wafers by combining the processes of VLSI (very-large-scale integration) technology (doping, masking, epitaxial deposition, oxidation, etc.) with anisotropic etching. Ordinary isotropic etchants attack all crystallographic planes indiscriminately, thereby forming hemispherical holes in masked wafers (see figure, a).

In contrast, anisotropic etchants of silicon crystals leave (111) planes unaffected but attack surfaces of any other orientation. Therefore, anisotropic etching ultimately produces cavities of atomically flat (111) planes bounded by concave edges (see figure, b). This permits the fabrication of precisely defined microscopic pyramidal cavities, slots, orifices, and similar mechanical elements.

This technology, however, does not permit the fabrication of perpendicular-walled deep holes, such as those needed for submillimeter waveguides, because of the early development of oblique (111) planes that stop the etchant from advancing deeper (see figure, b). In the new process, etching is preceded by the laser drilling of holes through the wafer (see figure, d). This insures that etch-sensitive convex edges will remain available for etchant attack until the perpendicular-walled rhombic cavity is etched completely through the wafer (see figure, f) or to a predetermined depth.

The pre-etching process of destabilizing the material to a given depth can be accomplished not only by laser drilling but also by any other process that renders the material unstable to the etchant. Alternatives include masking and etching from both sides so that the cavity bottom planes intersect each other, chemically milling or ion-etching central holes, or using an ion or laser beam to deform, recrystallize, or dope the central area of the desired cavity.

The pre-etching process is currently used to fabricate thin-walled arrays of submillimeter waveguides for use as dichroic bandpass filters. Other possible applications include the integration of sensor probes and processing of circuitry on the same silicon chip.

This work was done by Paul J. Shlichta of Caltech and Phillip W. Barth of Stanford University for **NASA's Jet Propulsion Laboratory**. *NPO-16562 /TN*

FOR ADDITIONAL INFORMATION: *Contact: Director, Technology Transfer Division, P.O. Box 8757, BWI Airport, MD. 21240; (301) 621-0100 Ext. 241*

REFER TO THE NUMBER LISTED AT THE END OF THE ARTICLE

NASA Tech Brief
National Aeronautics and Space Administration

Advanced Data Collection for Inventory Management

Bar-coding, radio-frequency, and voice-operated systems are selected.

A report discusses a study of the state-of-the-art in the automated collection of data for the management of large inventories. The study included a comprehensive search of the literature on data collection and inventory management, visits to existing automated inventory systems, and tours of selected supply and transportation facilities at the Kennedy Space Center. The information collected in these activities was analyzed in view of the needs of conceptual inventory-management systems for the Kennedy Space Center and for the manned space station and other future space projects.

Of the six technologies for automated data collection that were identified in the study, bar-coding, radio-frequency identification, and voice-operated systems were found to be viable considerations for the space station and Kennedy Space Center conceptual systems. Bar coding offers several advantages:

- It uses a computer-printable and computer-readable language.
- It is accurately and reliably readable.
- It is fast and easy to use.
- Equipment is readily available.
- The system is already in widespread use in the retail trades, and experience in the Department of Defense indicates that it saves money and improves the control and tracking of inventory.

A variety of radio-frequency identification systems are under development and in use, especially in the trucking and automobile-manufacturing industries. In such a system, a low-power transmitter/receiver irradiates a coded tag and reads the return signal, which is frequency modulated by the tag. There are both passive tags (which cannot be altered) and battery-powered active tags, which can be altered when irradiated with a signal containing a key code. An active tag can contain up to 8,000 bytes of information.

Voice systems (text-to-speech) would be used with bar coding or other systems to provide spoken guidance from a computer (test procedures, check lists, and the like) or audible alarms and warnings. Such systems are feasible because speech-synthesis techniques are relatively well developed. On the other hand, speech-recognition equipment has extremely limited capabilities. Consequently, a system for vocal data entry may not be available at a justifiable cost for several years.

The three technologies found unsuitable are optical character recognition, vision and image processing, and magnetic detection. Each was rejected for use in the conceptual systems because of the need for further adaptation to specific requirements, the need for further development, or limited utility.

This work was done by Gregory A. Opresko, Joel H. Leet, Daniel F. McGrath, and J. W. Eidson of **Kennedy Space Center**.

"Advanced Data Collection for Inventory Management," KSC-11349 /TN

FOR ADDITIONAL INFORMATION: *Contact: Director, Technology Transfer Division, P.O. Box 8757, BWI Airport, MD. 21240; (301) 621-0100 Ext. 241*

REFER TO THE NUMBER LISTED AT THE END OF THE ARTICLE

NASA Tech Brief
National Aeronautics and Space Administration
Marshall Space Flight Center, Alabama

Microprocessor-Based Valve Controller

A commanded mass-flow rate is maintained.

A flow controller uses a microprocessor to adjust a valve to maintain a commanded mass-flow rate in a gas stream. It operates the valve with a stepping motor instead of the usual servomotor. The new controller is simpler, more precise, and lighter than its predecessors. It repeatedly compensates for changing supply pressure and temperature.

The controller measures the flow pressure and temperature between the throttle valve and a venturi tube. (For a gas, a sonic venturi is used; for a liquid, the venturi is of a cavitating type.) The processor calculates the rate of mass flow from these measurements and compares it with the commanded flow rate. It corrects the rate by sending stepping pulses to the valve motor, which changes the valve opening accordingly. The controller makes a rate correction every 100 milliseconds (see figure).

The microprocessor determines the actual mass-flow rate from a simplified equation of state. It then calculates the flow-rate change per step of the valve motor by dividing the difference between the previous flow rate and the current flow rate by the number of steps in the previous correction. Finally, it calculates the number of steps, at the newly determined flow-rate change per step, needed to produce the desired flow rate.

The desired flow-rate setting can be changed as necessary. When a large change is required, the valve sometimes cannot make the required number of steps before the next correction, which would therefore be in error. To prevent this, the processor compares the number of steps in the previous correction with the maximum number of steps possible in the 100-ms interval between corrections. If the required number of steps exceeds the maximum possible, the controller uses the previously calculated change per step to determine the required number of steps.

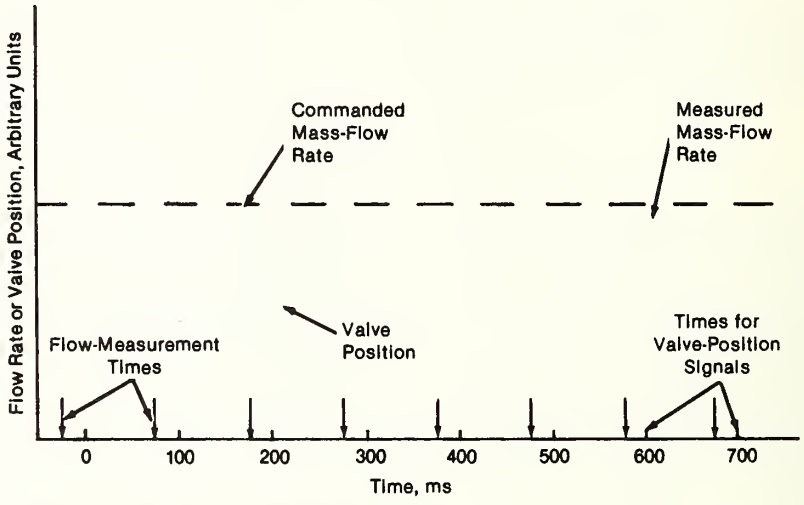

The Mass-Flow Controller Compensates for a changing supply pressure and temperature such as occurs when a gas-supply tank becomes depleted. By periodically updating its calculation of the mass-flow rate, the controller determines the correct new position for the valve and keeps the mass-flow rate nearly constant.

When the controller is started up, there is no previous flow-rate calculation available. At first, therefore, the present flow rate is checked against a predetermined minimum value. If the current flow rate is less than the minimum value, the processor calculates the change per step from an equation involving the supply pressure and temperature. It then calculates the required number of steps from this value and a correction factor found by an initial flow measurement.

Post-start-up oscillations can occur in the flow rate, depending on the system capacitance, the repetition rate of the calculations, and the valve speed. They can be eliminated or reduced to acceptable levels by simple programming techniques. Once the desired flow rate is attained, the controller is naturally stable, provided that the time between measuring pressure and temperature and sending the step pulses is short in comparison with the 100-ms update period.

This work was done by Arnold M. Norman, Jr., of Rockwell International Corp. for **Marshall Space Flight Center**. *MFS-29172 /TN*

FOR ADDITIONAL INFORMATION: *Contact: Director, Technology Transfer Division, P.O. Box 8757, BWI Airport, MD. 21240; (301) 621-0100 Ext. 241*
REFER TO THE NUMBER LISTED AT THE END OF THE ARTICLE

NASA Tech Brief
National Aeronautics and Space Administration
Lyndon B. Johnson Space Center, Houston, Texas

Inflatable Perimeter Seal

Inflatable tubing replaces gaskets or O-rings for sealing flat surfaces.

An effective, inexpensive pressure seal between two flat surfaces is formed from silicone rubber tubing. Resembling a refrigerator seal, the pressure seal is especially useful where the shape of the sealed region is irregular or subject to change. Unlike gaskets and O-rings, tubing seals require no machined grooves or custom-made parts and are not adversely affected by warpage of the sealed surfaces.

The seal path is first defined by gluing parallel strips of silicone foam to one of the two surfaces to be sealed. A continuous length of silicone rubber tubing ¼ in. (6 mm) in diameter is glued between the strips (see figure). One end of the tubing is plugged, and the other is attached to a pump or other source of pressure.

In operation, the other surface to be sealed is clamped against the tubing. The pressure in the tube is increased until the tube expands against both surfaces all around the perimeter. If not clamped, the tubing expands to 3/8 in. (9.5 mm) when inflated with air at 10 lb/in.^{2} (70 kPa) or contracts to a flat strip 1/8 in. (3.2 mm) thick with an internal vacuum. This thickness variability ensures an effective seal over a wide range of gap sizes.

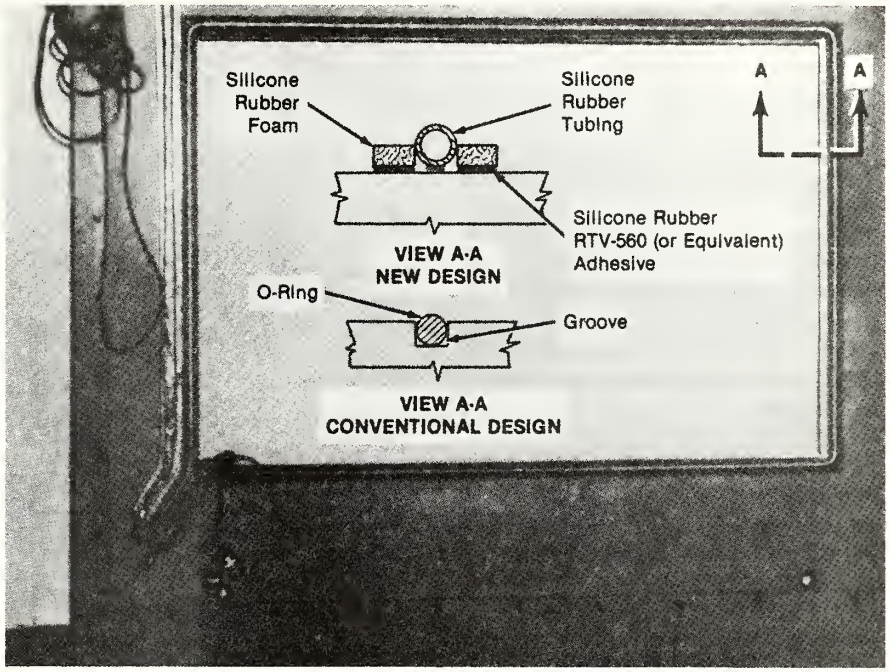

The **Inflatable Tubing Needs No Groove**, unlike an O-ring seal. The expense and time of machining a groove is therefore avoided. Since the tubing is continuous except at one point, leakage at splices and corners is nearly eliminated.

This work was done by Clayton C. Shepherd, Jr., of Rockwell International Corp. for **Johnson Space Center**. *No further documentation is available.*
MSC-20608 /TN

FOR ADDITIONAL INFORMATION: *Contact: Director, Technology Transfer Division, P.O. Box 8757, BWI Airport, MD. 21240; (301) 621-0100 Ext. 241*
REFER TO THE NUMBER LISTED AT THE END OF THE ARTICLE

NASA Tech Brief
National Aeronautics and Space Administration
Marshall Space Flight Center, Alabama

Protecting a Ball-Bearing-Deflection Monitor

A thin barrier isolates a probe from liquid oxygen.

A deflectometer probe monitors the deflection of a ball-bearing race in liquid oxygen with the aid of a small window or diaphragm. Until now, the practice has been to drill a port through the bearing housing so that an optical deflectometer probe can monitor the local, radially outward deformation of the race as each ball passes. In a turbopump or similar machine, the probe is in direct contact with the pumped fluid. However, this method cannot be used if the fluid is liquid oxygen or any other fluid with which the probe is incompatible.

When the outer race is press-fit into the housing, the problem can be avoided by not drilling the probe-access hole all the way into the bearing cavity; a thin wall of metal is left in the housing (see figure). The thin wall acts as a diaphragm in direct contact with the outer race. It therefore transmits the deformation of the race to the probe. At the same time, the diaphragm keeps the pumped fluid away from the probe. Of course, the diaphragm should not be so thin that it will rupture from fatigue or pressure. This can be determined from stress calculations.

When the outer race is not press fit, there will be a small gap between it and the housing. In that case, the diaphragm does not respond to race deformation. Instead, the access port is drilled through, and a window is inserted in it. The probe observes the race through the window, protected by it from the fluid.

This work was done by George A. Kuhr of Rockwell International Corp. for **Marshall Space Flight Center**. *No further documentation is available.*
MFS-19913 /TN

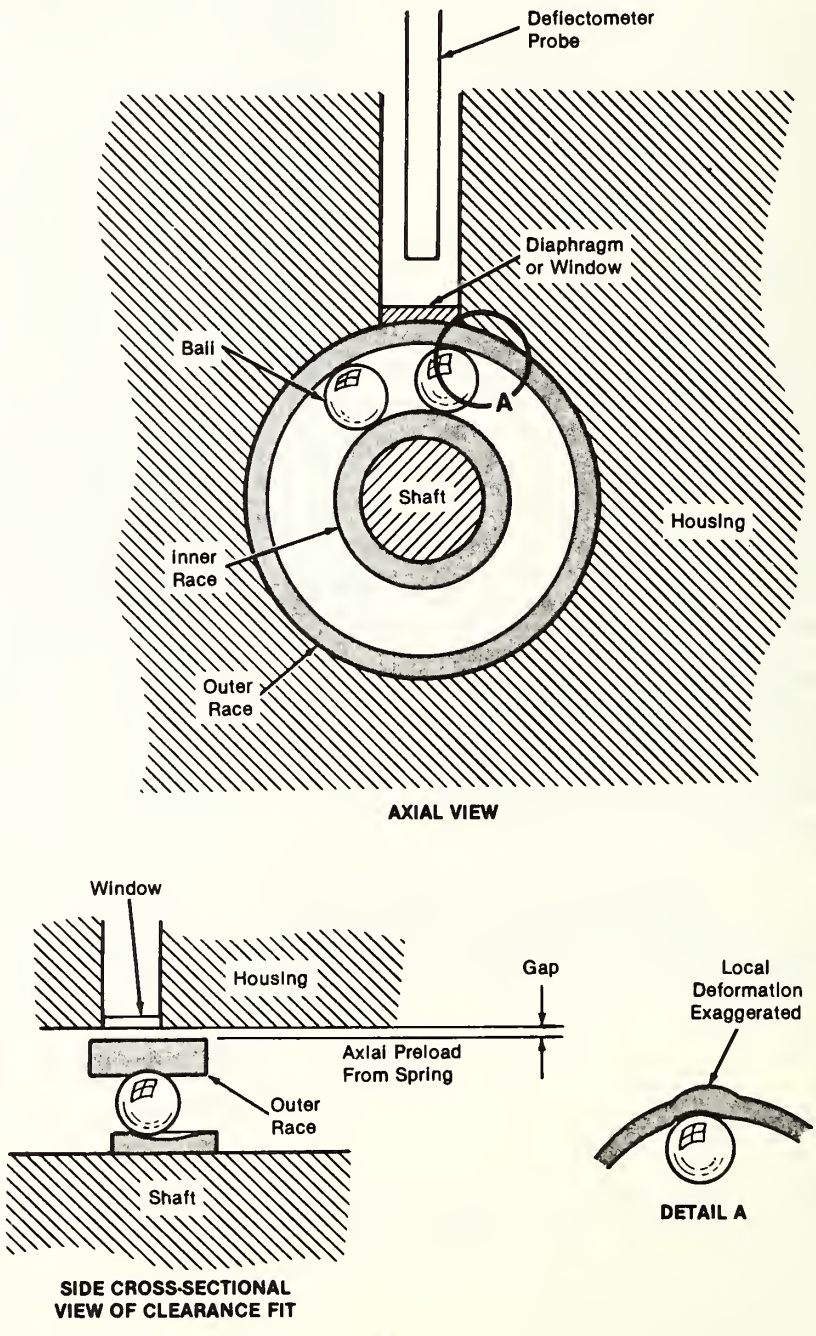

A **Diaphragm or Window Isolates** an optical deflectometer from liquid oxygen or other fluid in a ball bearing. At high pressures, the diaphragm—an integral part of the housing—is preferable to the window, since there would be no leakage.

FOR ADDITIONAL INFORMATION: *Contact: Director, Technology Transfer Division, P.O. Box 8757, BWI Airport, MD. 21240; (301) 621-0100 Ext. 241*
REFER TO THE NUMBER LISTED AT THE END OF THE ARTICLE

NASA Tech Brief
National Aeronautics and Space Administration
Marshall Space Flight Center, Alabama

Licensing Opportunity

Low-Turbulence Valve

A valve promotes diffusion mixing of liquids rather than turbulence mixing.

A valve opens and closes ports without introducing significant turbulence to the fluid passing through them. The valve was developed for an experiment involving mixing of solutions by diffusion. It allows the diffusion of contents between adjacent chambers with minimum turbulent mixing.

The valve mechanism forms a wall between the chambers, both of which are filled to capacity before the valve is operated. A central spindle through chamber 1 rotates one of the two valve plates (see figure).

External threads on the spindle mate with internal threads on the rotary plate in a light interference fit so that the spindle and rotary plate move as a unit except when the rotary plate is restrained from turning. A pin on the stationary plate catches a notch on the rotary plate to stop the rotation when the valve is fully open or fully closed.

The tip of the spindle rests in a blind hole in the hub of the stationary plate; the rotary plate is thus aligned axially with the stationary one. The alignment minimizes friction during opening and closing and helps to ensure a good seal in the closed position.

The stationary plate sits in facing grooves in the mating chamber housings. Gaskets seal the plate near its circumference. Similarly, a gasket or O-ring seals the spindle at its support point in the housing.

A spring washer applies a biasing force against the spindle. In the closed position, this force presses the rotary plate firmly against the stationary plate, preventing leakage between the chambers. In the open position, the force preloads the spindle to prevent looseness and chattering from vibration.

The first step in opening the valve is to rotate the spindle clockwise. This pulls the rotary plate away from the stationary plate. Next, the spindle is turned counterclockwise. Separated from the stationary plate, the rotary plate is now free to turn with the spindle, and so it, too, rotates counterclockwise and pulls one of its notches away from the stopping pin.

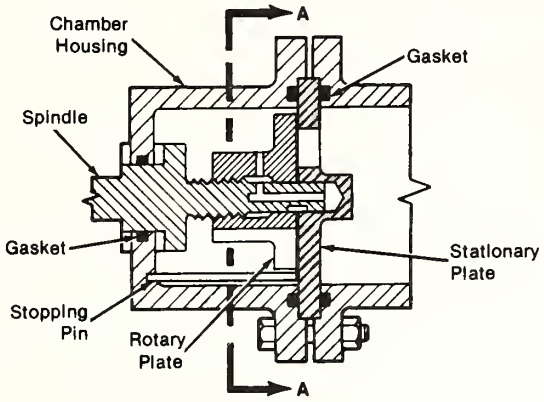

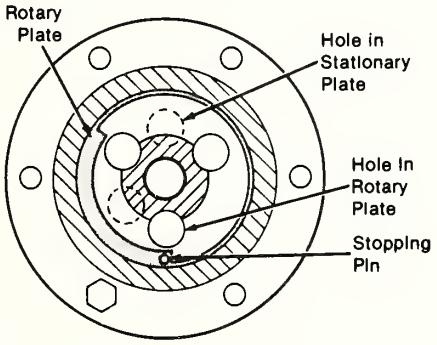

SECTION A-A, VALVE CLOSED

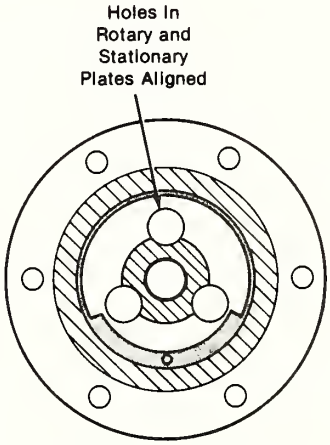

SECTION A-A, VALVE OPEN

Holes In Valve Plates Are Rotated clockwise into alignment to open the valve and counterclockwise out of alignment to close the valve. A stopping pin limits the overall rotation to 120° for opening and closing.

After about 60° of rotation, the three ports in the rotary plate are aligned with the three ports in the stationary plate. The solutions can now diffuse from one chamber to another.

The first step in closing the valve is to rotate the spindle counterclockwise about 60° until the notch on the rotary plate comes to rest on the stopping pin. The parts in the two plates no longer face each other. The rotary plate is now restrained against further rotation, and further counterclockwise rotation of the spindle forces the rotary plate axially against the stationary plate, thereby sealing the ports.

This work was done by Robert R. Below of **Marshall Space Flight Center.**

Inquiries concerning rights for the commercial use of this invention should be addressed to the Patent Counsel, Marshall Space Flight Center Refer to MFS-28058 /TN

George C. Marshall Space Flight Center
Technology Utilization Officer:
Ismail Akbay
Code AT01
Marshall Space Flight Center,
AL 35812
(205) 544-2223
Patent Counsel:
Leon D. Wofford, Jr.
Mail Code CC01
Marshall Space Flight Center,
AL 35812
(205) 544-0014

FOR ADDITIONAL INFORMATION: *Contact: Director, Technology Transfer Division, P.O. Box 8757, BWI Airport, MD. 21240; (301) 621-0100 Ext. 241*
REFER TO THE NUMBER LISTED AT THE END OF THE ARTICLE

Materials

890 Urethane Structural Adhesives

891 NDS Steel in High-Temperature Recuperators — The alloy is far stronger than ordinary Inconel* alloys at temperatures above 1,650 F (899 C).

892 Age Hardening in Binary Iron/Nickel Martensites — Increasing the nickel content and cooling the alloy to a low temperature improves its hardenability.

893 Strengthening Procedure for Magnesium-Base Sheet Alloys

894 Correlating Abrasive Wear to Alloy Additions in Low-Alloy Steel

895 New Foam Traps Moisture and Provides Structural Support

896 New Polymeric Precursors of Silicon Carbide — Silicon carbide is made by pyrolizing the polymers. (Licensing Opportunity)

897 Electrically Conductive, Heat-Resistant Paint — A graphite/silicate paint for titanium substrates withstands vibration and thermal shock.

898 Long-Term Tests of 38 Ball-Bearing Greases — Perfluoroalkylpolyether lubricants performed best.

899 Amorphous-Metal-Film Diffusion Barriers — Incorporation of N into Ni/W films reduces their reactivity with Si substrate.

900 Evaluation of Fiber-Reinforced Composites — The mechanical properties of a graphite/epoxy material are determined.

901 Polyenamines for Films, Coatings, and Adhesives — A relatively easy process makes polymers with good mechanical properties. (Licensing Opportunity)

902 Oxygen-Barrier Coating for Titanium — Submicron Al/SiO_2 coating significantly reduces titanium embrittlement. (Licensing Opportunity)

Testing & Instrumentation

903 Detection and Charactization of Damage in Thick Composities

904 Specimen and Holder for Sliding-Mode Fatigue Tests — A single-ended notch design facilitates accurate measurements of crack progression. (Licensing Opportunity)

905 Measuring Poisson Ratios at Low Temperatures — A simple extensometer ring measures the bulges of specimens in compression. (Licensing Opportunity)

Other items of Interest

871 Die-Target for Dynamic Consolidation of Powers

U.S. Army Belvoir R&D Center
Technology Application

Army Troup Support Command, Fort Belvoir, VA 22060

Urethane Structural Adhesives

As part of a project to perform a technology assessment of urethane structural adhesives and as a result of this assessment determine which adhesives to select and acquire, a technology assessment was made for the application of urethane adhesives to the situation described below. This was accomplished principally through discussions with suppliers of available commercial urethane adhesives, developmental urethane adhesives, and adhesive raw materials. In addition, an extensive study of the technical and commercial literature on urethane structural adhesives was conducted.

Initially a list of 40 domestic suppliers of urethane adhesives and/or urethane resin components was developed. The companies have all been contacted and wherever possible extensive discussions with their adhesive specialists carried out. Of these companies, approximately fourteen companies were found to manufacture urethane structural adhesives with properties potentially suitable for the applications of interest.

This effort is part of the U.S. Army requirements for bridging which have become more rigorous in the past decade. The bridges must remain transportable from site to site on tanks, trucks or trailers. The Army has gone to advanced materials for the construction of their bridges in order to meet these requirements. Epoxy-graphite fiber composites in combination with high strength aluminum are being developed as materials of construction for lightweight tactical bridging by the U.S. Army Belvoir Research, Development and Engineering Center. The construction and repair of these portable structures requires innovations in assembly technology since conventional riveting, bolting and welding are not as efficient as is required. The use of structural adhesives provides a bonding/fastening technology that can potentially meet the construction and repair requirements.

FOR ADDITIONAL INFORMATION: A list of the urethane adhesive suppliers and the specifications of the fourteen chosen adhesives are contained in a technical report available from NTIS. Order report number, AD-A175676/6NAC, price code A03.

To discuss this effort further, contact project manager Brian Hornbeck, Army Belvoir RD&E Center, STRBE-JBC, Ft. Belvoir, VA 22060; (703) 664-5176.

MANUFACTURING TECHNOLOGY NOTE

U.S. ARMY MATERIEL COMMAND

Deputy Chief of Staff for Manufacturing Technology, Alexandria, VA

Project Number: 1L162105AH84 Filing Code: 71J037

NDS Steel in High-Temperature Recuperators

The alloy is far stronger than ordinary Inconel* alloys at temperatures above 1,650 °F (899 °C).

A study has shown the feasibility of using nitride-dispersion-strengthened (NDS) stainless steel in fabricating a recuperator for advanced gas turbine engines. The study for the U.S. Army Materials and Mechanics Research Center found that one such alloy — NDS 300 — has tensile properties that are comparable to those of Inconel 625* at temperatures up to 1,650 °F (899 °C) and exceed those of that alloy at higher temperatures.

Historically, dispersion-strengthened alloys have been expensive to produce because of the complex procedures needed to ensure uniform particle distribution. However, a new process promises to lower the cost of production significantly (see figure). The process uses a gaseous-ammonia treatment to create a titanium nitride dispersoid within a stainless-steel base; nitriding a titanium-containing austenitic stainless steel at a high temperature creates a stable TiN dispersoid, leading to the pronounced strengthening inherent in dispersion-strengthened metals. The nitriding process is analogous to the older internal oxidation process but is several orders of magnitude faster.

In creep tests, NDS stainless steel was 3 times as strong as Inconel 625* above 1,650 °F (899 °C). The NDS material demonstrated adequate formability and joinability by brazing with a filler metal of nominal composition Ni-19Cr-10Si. The same filler metal was a good coating for oxidation resistance at high temperatures. Tests on specimens in a typical plate-fin recuperator configuration confirmed the strength of the brazing alloy and demonstrated the marked superiority of the NDS material over Inconel 625*.

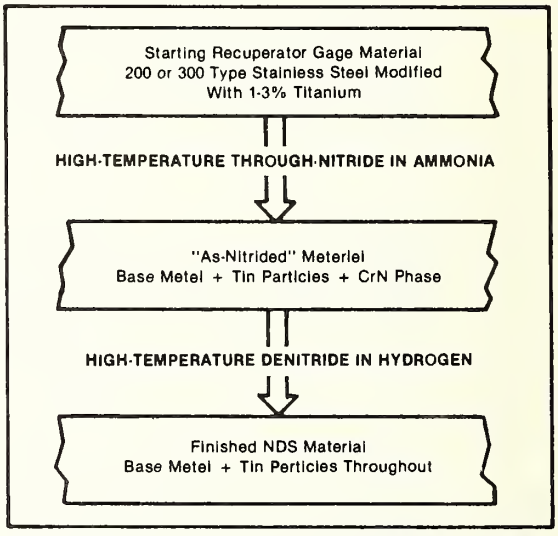

A relatively low-cost **Nitride Strengthening Process** uses ammonia to form titanium nitride particles in stainless steel. The uniformly spaced array of fine, inert particles gives the steel both strength and stability at high temperatures.

*Inconel is a registered trademark of the Inco family of companies.

Project officer Paul J. Fopiano
(617) 923-3327 or AV 955-3327.

FOR ADDITIONAL INFORMATION

You can learn more details about this technology by ordering the NTIS report(s):
Development of a Nitride Dispersion Strengthened (NDS) Metallic Alloy for High-Temperature Recuperators.
Order number: AD-A161958/NAA
Price code: A07

Order from:
National Technical Information Service
5285 Port Royal Road
Springfield, VA 22161

This document was prepared under the sponsorship of the U.S. Government. Neither the United States Government nor any person acting on behalf of the United States Government assumes any liability resulting from the use of the information contained in this document, or warrants that such use will be free from privately owned rights.

MANUFACTURING TECHNOLOGY NOTE

U.S. ARMY MATERIEL COMMAND

Deputy Chief of Staff for Manufacturing Technology, Alexandria, VA

Project Number: NONE

Filing Code: 71J038

Age Hardening in Binary Iron/Nickel Martensites

Increasing the nickel content and cooling the alloy to a low temperature improves its hardenability.

Age hardening of binary iron/nickel martensites was investigated to determine the nature and kinetics of the hardening reaction. In a study for the U.S. Army Research Office, six Fe/Ni alloys containing 24 to 34 weight percent Ni were austenitized, quenched, and cooled to 16 °C to retain austenite or to −196 °C to promote the transformation to martensite.

Specimens were aged at six temperatures between 270 and 450 °C for up to 14,000 h. Four other ferritic/martensitic alloys containing 5 to 30 weight percent Ni, previously cold-rolled and aged 8,000 h, were also aged. Specimens were studied by hardness and tensile testing (see table), x-ray diffraction, electron microscopy, and Fe-57 Mossbauer spectroscopy.

Age hardening occurred in all of the 24- to 34-weight-percent Ni martensites and at all of the aging temperatures. The maximum hardening occurred in an Fe-32Ni martensite after aging for 8,000 h at 300 °C; the hardness of this alloy increased by 270 Vickers hardness numbers (HV), from 210 HV to 480 HV.

Hardening was attributed to Ni-rich, disk-shaped austenite particules formed on (110) matrix planes during aging. The typical particle in a hardened specimen was 15 nm thick and 150 nm in diameter. The Ni contents of particles formed at 335 and 370 °C were found to be 59 ± 5 and 57 ± 5 percent, respectively. The 30- to 34-weight-percent Ni alloys cooled to 16 °C were largely austenitic, very soft, and not age-hardenable.

Specimen	Vickers Hardness Numbers	Yield Strength, MPa	Tensile Strength, MPa	Uniform Elongation, %	Reduction of Area, %
Fe-24Ni	229	512	645	1.0	2.2
Fe-26Ni	230	496	577	0.7	5.2
Fe-28Ni	231	497	720	2.9	78
Fe-30Ni	230	496	723	4.4	72
Fe-32Ni	211	484	640	4.4	73
Fe-34Ni	195	484	593	5.5	73
Fe-24Ni 500 h 300 °C	253	659	702	0.8	7.0
Fe-26Ni 1000 h 370 °C	289	726	778	0.8	4.8
Fe-28Ni 1000 h 370 °C	385	1095	1217	2.2	6.6
Fe-30Ni 1000 h 370 °C	403	1134	1294	1.8	4.9
Fe-32Ni 1000 h 335 °C	411	1024	1024	0.6	2.6
Fe-34Ni 1000 h 300 °C	305	644	1012	3.4	3.9

Mechanical Properties of the iron-nickel alloys were measured with and without aging. The maximum yield strength of the unaged specimens decreased with increasing nickel content. However, for the aged specimens, the mechanical properties generally improved with increasing nickel content until this content reached about 32 percent.

FOR ADDITIONAL INFORMATION

You can learn more details about this technology by ordering the NTIS report(s):

Age Hardening of Binary Iron-Nickel Martensites
Order Number: AD-A161407/NAA
Price code: A05

Order from:

National Technical Information Service
5285 Port Royal Road
Springfield, VA 22161

This document was prepared under the sponsorship of the U.S. Government. Neither the United States Government nor any person acting on behalf of the United States Government assumes any liability resulting from the use of the information contained in this document, or warrants that such use will be free from privately owned rights.

Technology News
From the Bureau of Mines, United States Department of the Interior

Strengthening Procedure for Magnesium-Base Sheet Alloys

As part of a long-range program directed toward reducing national dependence on critical metals, the U.S. Bureau of Mines, Rolla Research Center, has examined the feasibility of strengthening magnesium-base alloys by thermomechanical processing rather than by reliance on large amounts of alloying. Certain magnesium base alloys are known to exhibit an unusual response to cold working operations; as the amount of reduction is increased, strength is decreased and ductility is increased. This behavior is referred to as "strain softening". Subsequent heat treatment will result in strengthening that can, in some cases, provide a sheet alloy product that has attractive properties. Studies were undertaken at the Rolla Research Station to extend the information available on the thermomechanical strengthening process to determine whether it could provide an attractive alternative to more conventional strengthening processes for magnesium-base alloys.

Sixteen binary and ternary compositions were selected for examination. These alloys contained various amounts of manganese, misch-metal, zirconium, and calcium in total amounts of 1.5 weight percent or less. Small ingots were cast in the laboratory and hot rolled to 0.125-inch-thick plate at 750 F. The plates were then cold rolled at approximately 2 percent per pass to 0.025-inch-thick sheet (80 percent cold reduction). Some of the material was also processed to 0.025-inch-thick sheet entirely by hot rolling. Samples of both cold rolled and hot rolled sheet were then annealed for 24 hours at either 355 F (180 C) or 390 F (200 C). The tensile properties were determined and the four most attractive alloys were selected for more detailed study. The nominal compositions of these four alloys (in weight percent) were:

Alloy A	1.0 misch metal-0.5 zirconium
Alloy B	0.5 misch metal-0.5 manganese
Alloy C	0.5 misch metal-0.5 zirconium
Alloy D	1.5 misch metal

Two additional annealing treatments were applied to cold rolled samples from the four alloys, 24 hours at 285 F (140 C) and 24 hours at 320 F (160 C). The response of the four alloys to cold rolling reductions less than 80 percent total reduction was also determined.

The properties of the four alloys as hot rolled, as cold rolled, and after annealing at four different temperatures are shown in Figure 1. All four of the alloys, when suitably thermomechanically processed, appeared capable of meeting the minimum tensile properties for AZ31B-H24 (39.0 ksi tensile strength, 29.0 ksi yield strength, and 6 percent elongation). Data were also reported for the alloys processed using different cold rolling schedules. It was suggested that, in addition to reducing the amount of alloy addition required to achieve strength, the thermomechanical processing method might prove useful in two other areas, reducing anisotropy of properties and permitting the production of sheet from thin-gage cast slabs.

FOR ADDITIONAL INFORMATION:
A copy of the report, "Strengthening Low-Alloy Magnesium Sheet by Strain Softening and Annealing", is available from NTIS, Springfield, VA 22161; (703) 487-4600.
NTIS order number: PB85-240091/NAC
Price code: A02

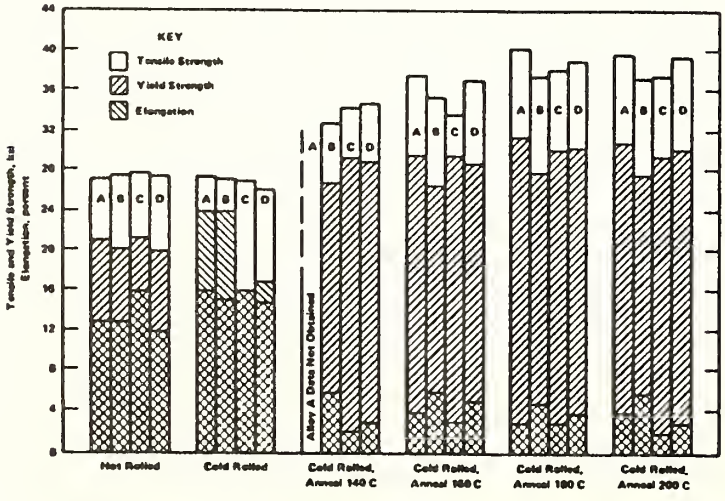

Figure 1. Tensile Properties of Experimental Magnesium Alloy Sheet in the As-Hot-Rolled, the As-Cold-Rolled, and the Cold-Rolled-Plus-Annealed Conditions. Cold Rolling Was at Nominal 2 Percent Reduction per Pass to 80 Percent Total Reduction.

Laboratory Technology
U.S. Department of the Interior

Correlating Abrasive Wear to Alloy Additions in Low-Alloy Steel

Low-alloy steels are inexpensive materials widely used in ore transport and mineral-processing equipment, such as ore chutes, truck beds, and bin walls. A simulation for the field condition of loose ore flowing over steel is the use of the well-known dry-sand, rubber-wheel abrasion test, in which loose sand abrades a test specimen. This test has become an ASTM standard (1) for abrasive wear and was used for this work.

Research was designed to determine the effect of different alloy additions on sliding abrasive wear of low-alloy steels, and to optimize the composition of two types of low-alloy steels: one type with low (0.3 pct C) carbon level to make it more easily weldable, and another type without a carbon limit. Other alloying additions investigates were Cr, Mn, Mo, Ni, Si, Al, S, and Cu. Whether or not chromium is useful in providing wear resistance in low-alloy steels was of particular interest because of U.S. dependence on imports for this strategic metal.

Abrasion tests were conducted on a dry-sand, rubber-wheel abrasion test apparatus in accordance with ASTM G65-81, procedure B. This test consists of a rubber-coated wheel, a test specimen mounted on a pivoting load arm, and a sand nozzle that produces a sand curtain between the specimen and the rubber wheel.

Steels with the least wear were found to be hardened high-carbon steels containing 0.55 to 1.0 wt pct C. These steels had enough alloying additions, 0.6 to 1.0 wt pct Mn, along with a sufficient carbon level, to provide full hardening in small specimens. Sulfur, in small amounts, also decreased the wear for the unhardened steels. Other alloy additions were not significant in reducing wear. The best steels tested were hardened experimental steels that fell within the specifications for AISI 1055 and 1078.

Carbon was found to reduce the wear of both hardened and nonhardened steels. Manganese decreased wear in all of the steels because it strengthens ferrite and increases the hardenability of the steels, thus reducing wear in hardened steels.

Other alloy additions may be useful for other purposes. A plain carbon steel has limited hardenability; therefore, additional alloying elements may be necessary to increase the depth of hardening. Chromium and molybdenum, despite being shown as generally detrimental to the wear resistance of steels, would probably be added in order to increase the hardenability.

Molybdenum and silicon were shown to increase wear. Molybdenum, being a carbide former, probably combines with carbon that might otherwise strengthen the steel. The reason that silicon increases abrasive wear of steel is still undetermined.

This work suggests that the best abrasive wear resistance in a low-alloy steel is obtained by--

1. Making the steel as hard as practical.
2. Having a high carbon level, at least up to 0.7 to 0.8 wt pct. It increases hardness in hardened steels, and improves work hardening in nonhardened steels.
3. Using a fairly large amount of manganese. It is useful in reducing wear in nonhardened steels, within the limits tested of 0 to 2 wt pct Mn.
4. Adding other alloying elements to adjust other properties. For example, add Ni for toughness and Cr and Mo for hardenability.

For Additional Information:

A copy of a report discussing these results is available from NTIS, Springfield, VA 22161; (703) 487-4650. Reference order number, PB87-139564/NAC, price code A02.

To discuss this effort further, contact J.H Tylczak, Metallurgist, Albany Resarch Center, U.S. Bureau of MInes, P.O. Box 70, Albany, OR 97321.

TABLE 2. - Dry-sand, rubber-wheel abrasive test data

Sample	Alloy	Condition	Hardness, HV	DSRWAT[1] wear mm^3	Coefficient variation, pct	Sample	Alloy	Condition	Hardness, HV	DSRWAT[1] wear mm^3	Coefficient variation, pct
1....	Ferro Vac. E.....	R	70	187.8	1.3	26....	AISI 1340.....	R	269	57.3	0.04
2....	Cor 99.....	R	93	166.0	1.5			WQ	640	38.5	5.3
3....	Experimental steel	R	112	170.9	1.4	27....	AISI 4142.....	A	172	95.0	5.0
4....	...do.....	R	116	155.6	2.6			R	192	86.7	1.3
5....	...do.....	R	118	148.7	4.3			OQ, T	556	44.3	1.8
6....	...do.....	R	159	120.3	2.3	28....	Experimental steel	R	214	64.4	1.5
7....	AISI 1018.....	R	139	129.6	.98			WQ	653	37.2	2.1
8....	AISI 4620.....	R	190	141.3	2.8	29....	AISI 6150.....	A	192	80.4	3.8
		A	135	134.6	2.1			R	346	83.0	2.4
		WQ	426	76.2	2.0			OQ	610	32.7	2.5
9....	USS "T1".....	RQ	243	104.4	1.3	30....	Experimental steel	R	216	52.6	3.7
		WQ	434	74.2	3.1			WQ	718	24.1	1.3
10....	USS "T1", Type B..	RQ	283	121.5	2.8	31....	AISI 1060.....	A	176	84.3	6.1
11....	Experimental steel	R	346	99.4	.66			R	227	60.4	4.6
		WQ, T	458	73.0	.5			WQ	708	32.1	3.4
12....	AISI 8620.....	A	133	137.7	3.6	32....	Experimental steel	R	170	75.3	7.8
		R	170	121.7	2.0			WQ	725	40.7	.82
		WQ	434	67.6	2.7	33....	AISI 5160.....	A	208	76.8	5.2
13....	Experimental steel	R	322	110.6	2.7			R	306	51.3	8.4
		WQ	424	70.0	1.6			WQ	709	39.6	3.0
14....	...do.....	R	145	128.3	5.2	34....	Omegalloy 61.....	RQ	801	29.8	5.3
15....	...do.....	R	187	113.7	4.3	35....	Experimental steel	R	312	40.5	1.9
16....	...do.....	R	170	95.3	4.5			WQ	842	24.1	.98
		WQ, T	423	74.4	2.6	36....	...do.....	R	346	36.2	.55
17....	...do.....	R	307	103.0	.06			OQ	817	25.2	1.4
		WQ	512	63.7	3.30	37....	...do.....	R	230	47.3	2.3
18....	...do.....	R	404	95.3	2.1			WQ	861	26.2	2.7
		WQ	513	60.5	4.2	38....	...do.....	R	384	37.3	1.3
19....	...do.....	R	212	119.5	1.7			OQ	820	32.1	3.0
		WQ	456	82.6	3.9	39....	...do.....	R	340	43.4	3.8
20....	...do.....	R	216	103.4	.93			OQ	766	33.8	.4
		WQ	453	60.8	6.4	40....	...do.....	R	333	38.8	4.7
21....	REM 500.....	A	176	136.6	3.0			OQ	766	33.9	2.0
		RQ	505	64.6	2.3	41....	AISI 52100.....	A	184	89.2	2.8
22....	Experimental steel	WQ	511	47.8	.11			R	346	39.3	1.35
		R	148	97.6	.23			OQ, T	720	35.2	4.7
23....	AISI 4340.....	WQ	595	46.6	6.2	42....	W1.....	R	158	99.9	3.3
		R	170	113.1	2.1			A	176	82.9	4.2
24....	AISI 4342.....	OQ	530	54.3	6.7			WQ	800	29.1	2.5
		R	184	102.4	2.1	43....	Experimental steel	R	298	47.5	.6
25....	AISI 8740.....	WQ	633	42.0	1.9			WQ	832	28.3	5.7
		A	165	97.0	1.2						
		R	254	97.6	.4						
		WQ	591	39.4	4.5						

[1]Dry-sand, rubber-wheel abrasion test.

NOTE.--A Annealed. R Hot rolled (assumed for purchased commercial steels). OQ Oil quenched.
RQ Received in hardened condition. WQ Water quenched. T Tempered.

New Foam Traps Moisture and Provides Structural Support

A new type of foam that can be molded into strong, solid shapes and that traps water vapor and other gases has been developed at Sandia National Laboratories in Livermore.

The foam's main purpose is to prolong the life of electronic equipment by maintaining dry conditions inside the equipment. Unlike other materials used for this purpose, it can be molded into complex shapes to fit odd-shaped spaces and, when cured, provides structural support.

Called molded desiccant foam, the new closed-cell material is made by combining polyurethane resins (the binder) and a zeolite powder (the filler). The foam works by adsorption, attracting vapor to the millions of tiny pores of the zeolite powder that is dispersed throughout the foam cells. Water vapor readily permeates the exterior of the foam and migrates to the inside where the zeolite traps it.

Zeolites, which occur naturally as aluminum silicate minerals, constitute one of several groups of chemical desiccants, agents that attract and hold moisture. (A commonly recognized desiccant is silica gel, a white powder often found in teabag-sized packets inside new camera and sound-equipment packages.)

May find several uses

Charles B. Frost of Sandia Livermore's Exploratory Chemistry Division developed molded desiccant foam to protect components inside a weapon system. However, he believes the new foam's features and advantages over some other types make it potentially useful for other defense and industrial applications. For example, the Sandia scientist says automotive and electronics industries may find the foam useful in spaces where both drying and reinforcing actions are needed.

The material is easy to form into precise shapes by injecting it into a mold right after it is mixed, while the foam is still fluid. It also has strong adhesive properties when molded directly into a part.

By varying the amount of zeolite from 10 to 60 weight percent of the mixture, the foam can be tailored to give different drying capabilities, up to about 18 percent of the weight of the dry foam. Frost's standard formula uses equal weights of resin and zeolite to make a foam that can trap moisture weighing up to 15 percent of dry foam weight.

The standard formula makes a foam that will adsorb water vapor and vapors from other low-molecular-weight liquids. By changing the type of zeolite used, the zeolite pore size can be varied to adsorb gases that have larger molecular weights—gas molecules up to about 10 Angstroms in diameter.

The physical properties of molded desiccant foam vary according to the exact formula used, but Frost says the zeolite powder apparently reinforces the foam at all densities and makes it more stable at higher temperatures.

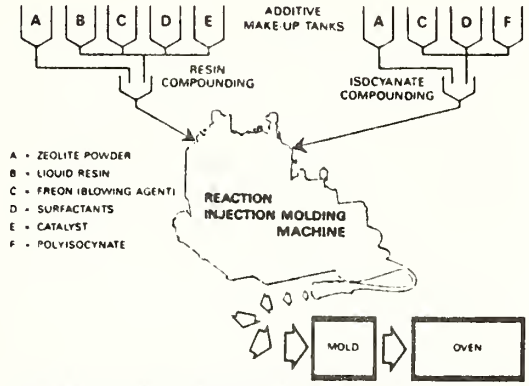

Schematic of the molded desiccant foam process. High-shear, high-viscosity mixers are required for zeolite dispersions.

Many applications require the maximum drying capability to be packaged into the smallest possible volume. As a result, most molded desiccant foam is of much higher density than the usual rigid foam used in thermal insulation or laminated core structures, which weighs about 2 lb/ft^3. A typical molded desiccant foam formula results in a foam that weighs 50 lb/ft^3 after it is cured (fully reacted) and is stable at elevated temperatures.

In comparison to a control polyurethane foam that does not contain zeolite filler, the 50-lb foam has a heat distortion temperature almost 100 degrees F higher and more than double the compressive strength—about 2,000 psi at 350°F and 6,550 psi at 68°F.

Frost says, "Even though we designed the new foam primarily for its drying capability, we were fortunate to formulate a desiccant foam that is even stronger than common polyurethane foams, especially at high temperatures. In my opinion, its real potential is as a dual-purpose material—a desiccant that also reinforces a weak structure."

Existing machinery used

Molded desiccant foam is made in the same basic way as conventional polyurethane rigid foams. However, certain formula changes and new mixing techniques were incorporated to make it possible to produce the new foam with existing foam-making machinery.

Two tanks are involved, one holding an isocyanate and the other a polyol (a type of alcohol). Special additives make the foam components flow more readily, and catalysts control the gelation and curing processes. The finely divided zeolite powders are dispersed in each of the two reactive components of the system.

The isocyanate and polyol are pumped at high pressure into a small chamber where they are mixed thoroughly. Normally, water would be added during the mixing process and would react to form carbon dioxide gas, which would act as a "blowing agent," causing the

mixture to expand. However, the large percentage of zeolite powder in the foam would simply soak up the water, so a freon gas is used as the blowing agent instead.

The mixture exits the chamber through a nozzle as a creamy fluid that is injected into a mold. There it expands, sweeps out the air, and sets up as a gel within a few minutes. After a standard cure in a conventional drying oven, the foam is removed from its mold and placed in a vacuum oven for about 3 hours at 350°F, which removes any residual moisture.

Comparable cost to other foams

Because Sandia makes and uses relatively small amounts of the specialized foam, Frost says it isn't possible to place a meaningful price tag on it. However, the Sandia scientist adds that the manufacturing process, required equipment, and ingredients are all commonly available and that the foam should be no more costly to produce in large quantities than are many other polyurethane foams.

The new material can be reused or recycled if necessary. If the foam ever became saturated, it could be removed from its place of use and "reactivated" in a vacuum oven.

FOR ADDITIONAL INFORMATION

Public Information Division,
Code 3161,
Dept. of Energy,
Sandia National Laboratories,
Albuquerque, NM 87185-5800
(505) 844-4207.
Refer to announcement 22, No. 3

NASA Tech Brief
National Aeronautics and Space Administration
Lewis Research Center, Cleveland, Ohio

Licensing Opportunity

New Polymeric Precursors of Silicon Carbide

Silicon carbide is made by pyrolizing the polymers.

A method has been conceived for the preparation of poly(decamethylcyclohexasilanes) as precursors for the preparation of silicon carbide at a high yield. The technical potential of polysilanes as precursors of SiC ceramics is being explored. However, this potential is limited by the intractability of some polysilanes; the formation of small, cyclic polycarbosilane fragments during pyrolysis; and the overall low char yield and large shrinkage in conversion to ceramics.

The general objective of this work is to provide a novel polymer that has a high theoretical char yield and that can be used efficiently to make silicon carbide. To this end, a polymeric mixture of poly(decamethylcyclohexasilanes) of the type shown in the figure was prepared. When cross-linked, the polymer charred efficiently to give a 50-percent yield of silicon carbide. Presumably, the method can be improved, because the maximum theoretical char yield is 75 percent.

As an example, the 1,4-diphenyldecamethylcyclohexasilane polymer has been isolated and is being evaluated as a precursor of strong silicon carbide fibers. The polymer is also under study as matrix material for a ceramic-matrix composite. Because of the high char yield, the number of impregnations required to form a SiC matrix is reduced, reducing the processing time and cost in comparison with state-of-the-art materials.

This work was done by M. H. Litt and Kanta Kumar of Case Western University for **Lewis Research Center**. *No further documentation is available.*

Inquiries concerning rights for the commercial use of this invention should be addressed to the Patent Counsel, Lewis Research Center Refer to LEW-14272/TN

Lyndon B. Johnson Space Center
Technology Utilization Officer:
Dean C. Glenn
Mail Code EA4
Houston, TX 77058
(713) 483-3809
Patent Counsel:
Edward K. Fein
Mail Code AL3
Houston, TX 77058
(713) 483-4871

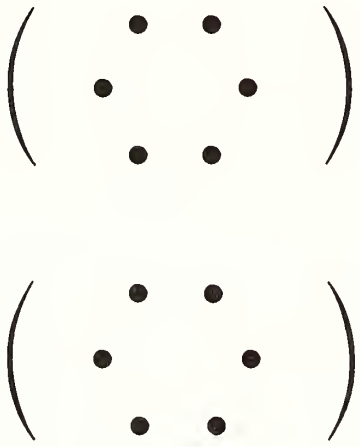

These **Poly(Decamethylcyclohexasilanes)** can serve as precursors of silicon carbide. (Each dot represents a silicon atom with sufficient methyl groups attached to bring the total valency of silicon to four.)

FOR ADDITIONAL INFORMATION: *Contact: Director, Technology Transfer Division, P.O. Box 8757, BWI Airport, MD. 21240; (301) 621-0100 Ext. 241*
REFER TO THE NUMBER LISTED AT THE END OF THE ARTICLE

NASA Tech Brief
National Aeronautics and Space Administration
NASA's Jet Propulsion Laboratory, Pasadena, California

Electrically Conductive, Heat-Resistant Paint

A graphite/silicate paint for titanium substrates withstands vibration and thermal shock.

An improved, sprayable, thermal- and electrostatic-discharge-control coating for titanium possesses excellent adhesion and high resistance to both vibration and thermal shock. The coating is an improved formulation of the one described in "High-Temperature Coatings for Titanium" (NPO-16222) page 498, *NASA Tech Briefs*, Vol. 8, No. 4, (Summer 1984).

As originally formulated, the coating consists of a graphite pigment with a potassium silicate binder. In the cured state, the pigment-to-binder ratio is 1:1. In the wet-mixture state, the original coating material consists of 19 percent of graphite pigment (20-μm average pigment-particle size), 53 percent of a 35-percent potassium silicate solution, and 28 percent distilled water. The pigment, binder, and water are processed in a jar mill for 3 hours. The contents of the mill are then applied to the titanium surface, using a state-of-the-art spray gun at an air pressure of appoximately 35 psi (241 kPa). A curing time of 24 hours is recommended.

The new coating liquid consists of 76.2 weight percent of the original formulation, 9.5 weight percent zinc oxide, and 14.3 weight percent WB-500 (or equivalent) carbon. After this mixture has been milled for about 1.5 hours, 10 to 20 grams of water are added to each 100 grams of mixture to reduce the viscosity to enable easy spraying.

The original coating failed certain tests at high temperatures, with possible evidence of vaporization of beaded water in the coating matrix and occasional blistering and loss of adhesion of the coating to the titanium substrate. In addition to meeting the thermo-optical and electrical-conductivity requirements of the spacecraft application for which the new coating was devised, cured test samples suffered no observable effects when subjected to oven thermal shock at 70 to 400 °F (21 to 204 °C), 70 to 800 °F (21 to 427 °C), and to hot-plate thermal shock at about 70 to 500 °F (21 to 268 °C). No effects were noted with conventional thermal and water-immersion testing. Compared to plasma-spray-coated iron titanate on titanium foil, the original and modified coatings show similar emissivity and absorptivity but slightly higher surface electrical resistivity.

This work was done by Victor F. Hribar and Richard J. Mell of Caltech for **NASA's Jet Propulsion Laboratory**. *NPO-16325 /TN*

FOR ADDITIONAL INFORMATION: *Contact: Director, Technology Transfer Division, P.O. Box 8757, BWI Airport, MD. 21240; (301) 621-0100 Ext. 241*
REFER TO THE NUMBER LISTED AT THE END OF THE ARTICLE

NASA Tech Brief
National Aeronautics and Space Administration

Long-Term Tests of 38 Ball-Bearing Greases

Perfluoroalkylpolyether lubricants performed best.

The final report in a series presents the results of a program of long-term testing of ball-bearing greases in vacuum, oxidizing, and otherwise hostile environments. The earlier reports in the same series were described in "Tests of 38 Ball-Bearing Greases," (MFS-25624), *NASA Tech Briefs*, Vol. 6, No. 3, page 330, and "Further Tests of 38 Ball-Bearing Greases," (MFS-27043), *NASA Tech Briefs*, Vol. 9, No. 1, page 111.

The greases were tested in ball bearings of electric motors that were subjected to a variety of operating conditions, including humid oxygen, vacuum at 38°C, vacuum at 93.3°C, vacuum at ambient temperature with start/stop operation, and low-temperature start (various temperatures). The lubricants were evaluated qualitatively in terms of the occurrence or nonoccurrence of bearing failure and quantitatively in terms of bearing weight loss.

The findings remain essentially unchanged from the earlier reports: The class of lubricants based on perfluoroalkylpolyether (PFPE) continued to give the best results in vacuum operation in both 1-year and 5-year tests. In 5-year start/stop tests, one of the PFPE lubricants showed the lowest weight loss. Some silicone, mineral, and synthetic-ester lubricants also showed promise in 1-year vacuum ambient-temperature tests.

This work was done by E. L. McMurtrey of **Marshall Space Flight Center.** *Further information may be found in NASA TM-86480 [N85-11239/NSP], "An Evaluation of Grease-Type Ball Bearing Lubricants Operating in Various Environments (Final Status Report No. 8)."*

Copies may be purchased from the National Technical Information Service, Springfield, Virginia 22161, [A02]
MFS-27089 /TN

FOR ADDITIONAL INFORMATION: *Contact: Director, Technology Transfer Division, P.O. Box 8757, BWI Airport, MD. 21240; (301) 621-0100 Ext. 241*
REFER TO THE NUMBER LISTED AT THE END OF THE ARTICLE

NASA Tech Brief
National Aeronautics and Space Administration

Amorphous-Metal-Film Diffusion Barriers

Incorporation of N into Ni/W films reduces their reactivity with Si substrate.

A paper describes the reactions between Si substrates and deposited amorphous Ni/W or Ni/N/W films. The thermal stability of amorphous Ni/W films as diffusion barriers in Si is markedly improved by the introduction of N into the Ni/W films during deposition.

Amorphous films on Ni/W and Ni/N/W were deposited on single-crystal silicon with discharge gases of Ar or Ar + N_2 by radio-frequency cosputtering of Ni and W. The reaction of these Ni/W and Ni/N/W films with the Si substrates were studied in the temperature range of 450 to 750 °C by a combination of backscattering spectrometry, X-ray diffraction, cross-sectional-transmission electron microscopy (XTEM), and measurements of electrical resistivity.

The results have shown films with composition $Ni_{36}W_{64}$ to be stable below 500 °C. Both NiSi and $NiSi_2$ form at 500 °C and WSi_2 forms rapidly in the temperature range of 625 to 650 °C. The nickel silicide forms adjacent to and within the Si, while the outer layer becomes a mixture of WSi_2 and $NiSi_2$. The crystallization temperature of amorphous $Ni_{36}W_{64}$ films on SiO_2 is also near 650 °C.

Adding nitrogen to form amorphous $Ni_{30}N_{21}W_{49}$ films lowers the crystallization temperature but raises the reaction temperature with Si to 750 °C. (Interestingly, X-ray diffraction shows that the amorphous $Ni_{30}N_{21}W_{49}$ film crystallizes before it reacts with the Si substrate.) The reduced reactivity of Ni in the nitrogen-containing film is unlikely to be the result of the binding of Ni by N, since Ni does not form stable nitrides at these elevated temperatures. Rather, the enhanced stability may be the result of a kinetic barrier formed by the stable W_2N. Detailed XTEM studies are needed to answer this question.

This research is important because it is desirable to reduce the diffusion of electrical-contact materials into silicon electronic devices. Thus, the reduced reactivity of amorphous films is noteworthy. Possible ways to suppress or circumvent the undesirable local reactions below the crystallization temperature include the following:

- Replacement of Ni by an element with a higher silicide formation temperature;
- Use of buffer layer (e.g., NiSi) between the amorphous film and the Si substrate;
- Use of ternary amorphous films (e.g., Ni/N/W); or
- Use of multilayered amorphous films. In view of the practical interest, these possibilities may soon be tested.

This work was done by Marc A. Nicolet of Caltech for **NASA's Jet Propulsion Laboratory**. *"Reaction of Amorphous Ni-W and Ni-N-W films with Substrate Silicon," NPO-16637 /TN*

FOR ADDITIONAL INFORMATION: *Contact: Director, Technology Transfer Division, P.O. Box 8757, BWI Airport, MD. 21240; (301) 621-0100 Ext. 241*
REFER TO THE NUMBER LISTED AT THE END OF THE ARTICLE

NASA Tech Brief
National Aeronautics and
Space Administration

Evaluation of Fiber-Reinforced Composites

The mechanical properties of a graphite/epoxy material are determined.

A report describes procedures for evaluating properties of advanced fiber-reinforced composite materials. The procedures include quality control, fabrication techniques, specimen machining, test methods, and data collection and interpretation. The procedures were applied to a specific material: Thornel P-100 carbon fiber combined with Fiberite 934 epoxy resin in the form of unidirectional tape.

Special emphasis is given to quality control during the preparation of samples. Tests on the prepreg material, including measurements of gel time, resin solids content, tack, volatile content, and flow, are detailed. The steps of the fabrication and machining processes are described.

Both destructive and nondestructive techniques were used to assess the properties of the cured laminates. Mechanical tests were performed to measure the tensile strength and modulus, compressive strength and modulus, interlaminar and inplane shear strength, and flexural strength and modulus.

The results are compared with data generated by the manufacturer. The agreement between the two sets of data is good for the fiber-dominated properties. But because two different resins were used, comparisons of matrix-dominated properties would not be meaningful. However, other evidence indicates that the results for the matric dominated properties are resonable.

This work was done by Raymond G. Clinton, Jr., of Georgia Institute of Technology for **Marshall Space Flight Center**.
"Mechanical Property Characterization of P-100/934 Graphite-Epoxy Composite Material," MFS-27149 /TN

FOR ADDITIONAL INFORMATION: *Contact: Director, Technology Transfer Division, P.O. Box 8757, BWI Airport, MD. 21240; (301) 621-0100 Ext. 241*
REFER TO THE NUMBER LISTED AT THE END OF THE ARTICLE

NASA Tech Brief
National Aeronautics and Space Administration
Langley Research Center, Hampton, Virginia

Licensing Opportunity

Polyenamines for Films, Coatings, and Adhesives

A relatively easy process makes polymers with good mechanical properties.

As part of an effort to develop high-performance/high-temperature polymers for functional and structural applications, the reaction of aromatic diacetylenic diketones with various monomers is under investigation. Polymers can be formed readily from the reaction of these diketones with a variety of such nucleophilic monomers as primary aromatic diamines to yield polyenamines. It was postulated that the six-membered ring formed by the hydrogen-bonded interaction in these enamines in a polymer could provide high thermal stability.

This synthesis involves the Michael-type addition polymerization (see figure) of two diacetylenic diketones: 1,1′-(1,3-phenylene)bis(3-phenyl-2-propyn-1-one) (1,3-PPPO) and 1,1′-(1,4-phenylene)bis (3-phenyl-2-propyn-1-one) (1,4-PPPO), with various aromatic diamines in *m*-cresol at 60 to 130 °C. Polyenamines with high molecular weights and inherent viscosities as high as 1.99 dl/g were prepared. Tough, clear, amber films with tensile strengths of 12,400 psi (86 MPa) and tensile moduli of 397,000 psi (2.74 GPa) were cast from solutions of the polymers in chloroform. Thermogravimetric analysis showed polymer decomposition temperatures of approximately 390 °C and 300 °C in nitrogen and air, respectively. The polymers exhibited glass-transition temperatures as high as 235 °C and weight losses of 14 percent after aging at 232 °C in circulating air for 60 hours.

This technique provides a synthetic route to high-molecular-weight polyenamines with moderate thermal stability and good mechanical properties. The polyenamines thus produced exhibit potential for use as films, coatings, adhesives, molding compounds, and composite matrices.

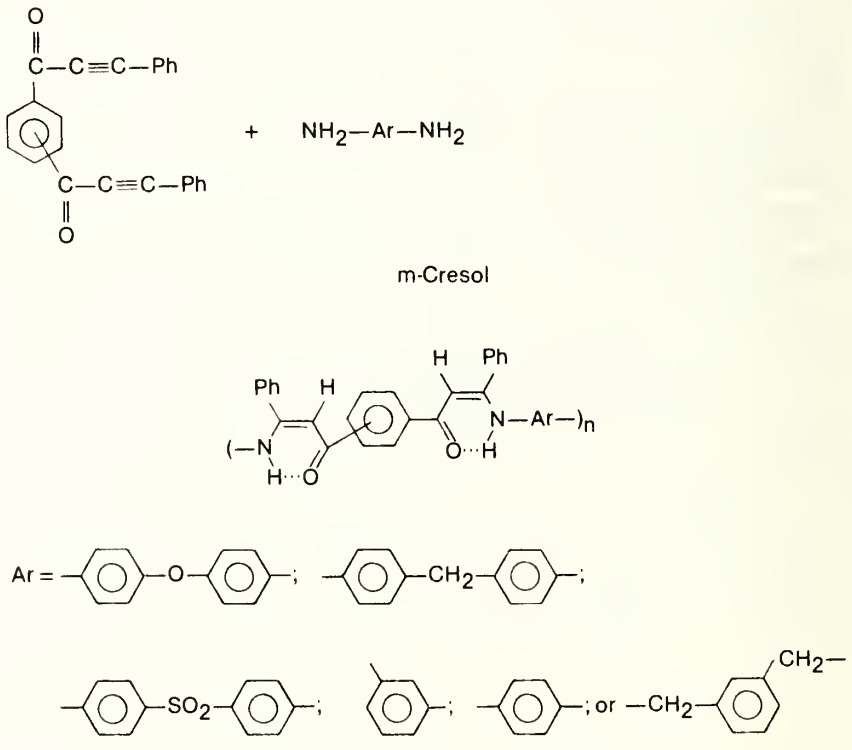

The **Polyenamines** are synthesized by addition polymerization.

This work was done by Paul M. Hergenrother of **Langley Research Center** *and Robert G. Bass, Mark S. Sinsky, and John W. Connell of Virginia Commonwealth University.*

This invention is owned by NASA, and a patent application has been filed. Inquiries concerning nonexclusive or exclusive license for its commercial development should be addressed to the Patent Counsel, Langley Research Center Refer to LAR-13444. /TN

Langley Research Center
Technology Utilization Officer:
John Samos
Mail Stop 139A
Hampton, VA 23665
(804) 865-3281
Patent Counsel:
Howard J. Osborn
Mail Code 279
Hampton, VA 23665
(804) 865-3725

FOR ADDITIONAL INFORMATION: *Contact: Director, Technology Transfer Division, P.O. Box 8757, BWI Airport, MD. 21240; (301) 621-0100 Ext. 241*
REFER TO THE NUMBER LISTED AT THE END OF THE ARTICLE

NASA Tech Brief
National Aeronautics and Space Administration
Langley Research Center, Hampton, Virginia

Licensing Opportunity

Oxygen-Barrier Coating for Titanium

Submicron Al/SiO_2 coating significantly reduces titanium embrittlement.

Titanium and titanium alloys are of prime interest for aerospace applications because of their favorable strength-to-density and high-temperature strength characteristics. However, titanium reacts with oxygen at elevated temperatures, leading to embrittlement and degradation of mechanical properties. Because of the loss of ductility of titanium alloys exposed to environments containing oxygen, long-term uses have been limited to temperatures below 800 °F (430 °C) and short-term uses have been generally limited to temperatures below 1,000 °F (540 °C). Because of these limitations, the oxygen-barrier coating for titanium was developed to provide an effective and low-cost means for protecting titanium alloys from oxygen in the environment when the alloys are used in high-temperature mechanical or structural applications.

The oxygen-barrier coating for titanium provides a protective surface layer, which reduces the extent of surface oxidation of the alloy and forms a barrier to the diffusion of oxygen, thereby limiting the contamination of the substrate alloy by oxygen. The coating consists of a submicron layer of aluminum deposited on the surface of the titanium by electron-beam evaporation, with a submicron layer of silicon dioxide sputtered onto the aluminum to form a top coat. On exposure to high temperatures, the titanium alloy interacts with the aluminum and silicon dioxide layers to form aluminide and silicide compounds that are nearly impervious to oxygen, even during exposure to temperatures as high as 1,300 °F (700 °C). This blocking of oxygen diffusion to the alloy substrate restricts oxygen contamination of the alloy in the region near the surface, thereby reducing the source of embrittlement of the alloy.

Test results indicate that the level of oxygen contamination in the coated material is only one quarter that in the uncoated material when exposed to air at 1,300 °F (700 °C) for 25 hours. The ductility (see figure) of coated titanium samples exposed at 1,150 °F (620 °C) for 24 hours is about 2.5 times that of uncoated samples.

This work was done by Ronald K. Clark of **Langley Research Center** *and Jalaiah Unnam of Analytical Services & Materials, Inc.*

This invention is owned by NASA, and a patent application has been filed. Inquiries concerning nonexclusive or exclusive license for its commercial development should be addressed to the Patent Counsel, Langley Research Center Refer to LAR-13474. /TN

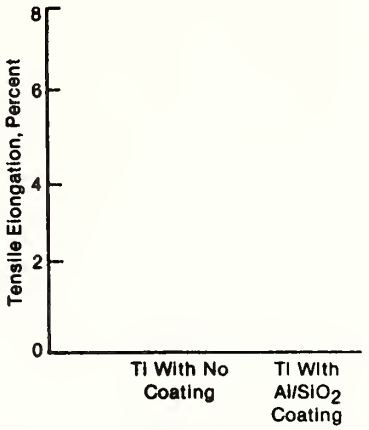

The Ductility of Titanium Foil Coated With Al/SiO_2 foil is more than double that of the uncoated titanium after 25 hours exposure at 1,150 °F.

Langley Research Center
Technology Utilization Officer:
John Samos
Mail Stop 139A
Hampton, VA 23665
(804) 865-3281
Patent Counsel:
Howard J. Osborn
Mail Code 279
Hampton, VA 23665
(804) 865-3725

FOR ADDITIONAL INFORMATION: *Contact: Director, Technology Transfer Division, P.O. Box 8757, BWI Airport, MD. 21240; (301) 621-0100 Ext. 241*
REFER TO THE NUMBER LISTED AT THE END OF THE ARTICLE

Detection and Characterization of Damage in Thick Composites

Thick graphite/epoxy composite materials are used for components in critical structural systems such as submarines. Because of their thickness these composites are more difficult to manufacture without defects, and hence require more nondestructive evaluation to ensure material integrity. But also because of their thickness, these materials are more difficult to evaluate nondestructively using conventional methods such as X-rays, thermography, or ultrasonic C-scans. With X-rays, there can be no assurance that penetrants can reach all the defects. With thermography, the depth of penetration or thickness is quite limited. Ultrasonic C-scans work well for defects with a relatively large area lying parallel to a surface, but they do not work well for defects oriented perpendicular to a surface. Among the latter are transverse matrix cracks in cross-ply laminates. The insert in Figure 1 shows a cross-ply laminate under tensile loading and the transverse matrix cracking which occurs under this type of load. Also shown in Figure 1 are plots of the crack density as a function of load and the stress-strain curve for the same specimen. The top curve, crack density vs. stress, shows that the crack spacing decreases as stress increases until a spacing that is close to the thickness of the cross-ply layer is obtained. This limiting condition is known as the characteristic damage state (CDS). Beyond CDS, further increase of stress results in other types of failure, such as delaminations and fiber fracture.

As stated above, transverse matrix cracks are difficult ot detect using ultrasonic C-scans. But an ultrasonic technique has been combined with an analytical approach to allow characterization of the average spacing of these matrix cracks. This should be a useful tool, when combined with methods of fracture mechanics, for determining the remaining life of cross-ply laminates if this type of damage has occurred.

FOR ADDITIONAL INFORMATION: This research was conducted by J. D. Achenbach, I. M. Daniel, G. Kechter and S. C. Wooh of the Department of Civil Engineering, Northwestern University, Evanston, IL 60201. A copy of the report is available from NTIS, Springfield, VA 22161; (703) 487-4600.

NTIS order number: AD-A175939/8/NAC
Price code: A02

NASA Tech Brief
National Aeronautics and Space Administration
Lewis Research Center, Cleveland, Ohio

Licensing Opportunity

Specimen and Holder for Sliding-Mode Fatigue Tests

A single-ended notch design facilitates accurate measurements of crack progression.

A novel test specimen and a novel loading fixture have been developed for the fatigue and fracture testing of materials under Mode II, or sliding-mode, loading. Such testing is required for the analysis of failures in structural materials, bearings, and the like. Under Mode II loading, fracture in this specimen proceeds in a direction that is in line with the starter notch (see Figure 1), as half of the specimen "slides" vertically past the other half, analogously to the sliding of half a deck of cards past the other half. Important features of this specimen are that a nearly-pure Mode II condition exists at the test zone and that the single-ended notch design permits the simple, accurate measurement of crack progression.

Examples of the type of fracture and fatigue cracking obtained with this specimen are shown in Figure 2. Analyses of the specimen have been performed using finite-element and boundary-collocation methods.

A method of introducing measured amounts of Mode I (opening-mode) loading has also been developed for this specimen for mixed-mode (I and II) testing. This method utilizes fixed/controlled separation of the pins at the free end of the test specimen.

This work was done by Robert J. Buzzard, George Succop, and Bernard Gross of **Lewis Research Center**. *Further information may be found in:*

NASA TM-83722 [N84-29248/NSP], [A02] "Mode II Fatigue Crack Growth Specimen Development," and

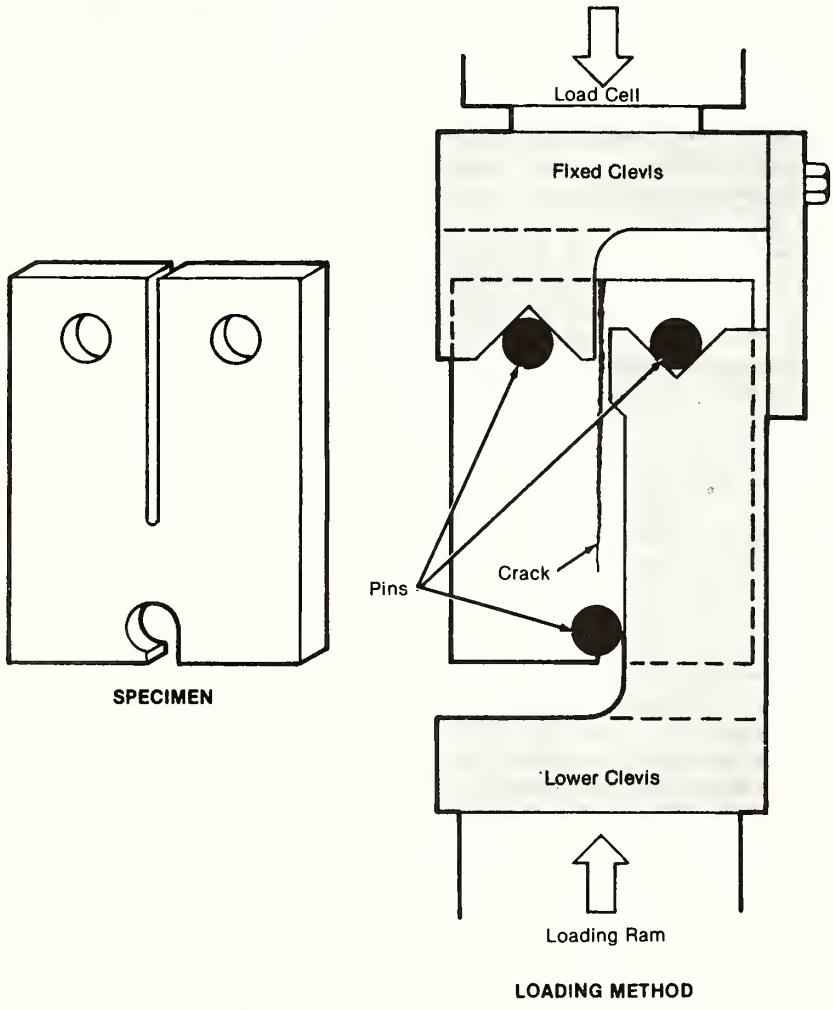

Figure 1. In **Mode II Testing**, the specimen is placed in a slotted testing fixture. A compressive load is applied through pins, causing the specimen to crack as shown.

NASA TM-86908 [N85-16205/NSP], [A02] "Experimental Compliance Calibration of the NASA Lewis Research Center Mode II Fatigue Specimen."

Copies may be purchased from the National Technical Information Service, Springfield, Virginia 22161,

This invention is owned by NASA, and a patent application has been filed. Inquiries concerning nonexclusive or exclusive license for its commercial development should be addressed to the Patent Counsel, Lewis Research Center Refer to LEW-14281 /TN

Lewis Research Center
Technology Utilization Officer:
Daniel G. Soltis
Mail Stop 7-3
21000 Brookpark Road
Cleveland, OH 44135
(216) 433-5567
Patent Counsel:
Gene E. Shook
Mail Code 60-2
21000 Brookpark Road
Cleveland, OH 44135
(216) 433-5753

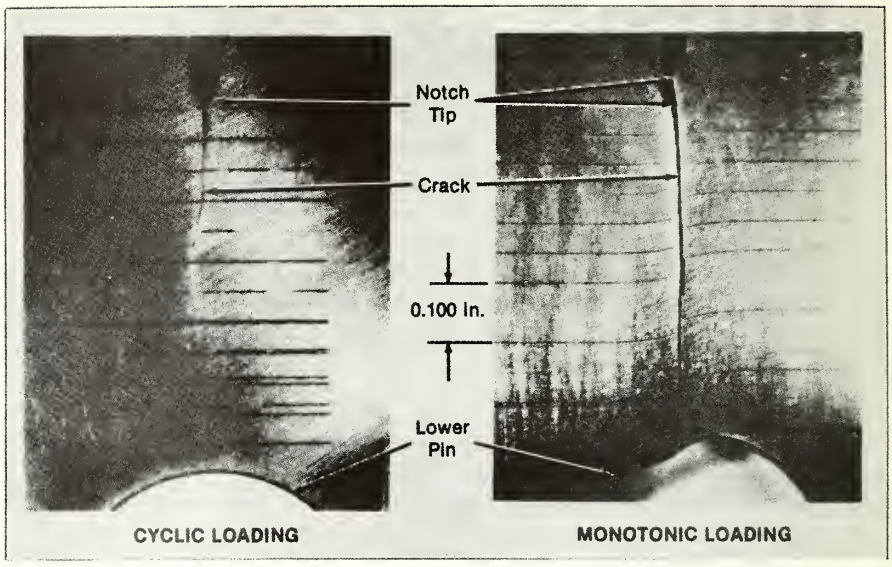

Figure 2. These **Mode II Test Specimens** were subjected to two different kinds of loading, resulting in two different cracking patterns.

FOR ADDITIONAL INFORMATION: *Contact: Director, Technology Transfer Division, P.O. Box 8757, BWI Airport, MD. 21240; (301) 621-0100 Ext. 241*

REFER TO THE NUMBER LISTED AT THE END OF THE ARTICLE

NASA Tech Brief
National Aeronautics and Space Administration
Marshall Space Flight Center, Alabama

Licensing Opportunity

Measuring Poisson Ratios at Low Temperatures

A simple extensometer ring measures the bulges of specimens in compression.

A new method of measuring Poisson's ratio can be used on brittle ceramic materials at cryogenic temperatures. Ordinarily, Poisson's ratio (the ratio of the change in relative thickness of a specimen under tensile or compressive stress to its change in relative length) is determined by placing a specimen in tension are separated by a gap (see figure). The inner segment is a thin aluminum band that makes contact with the circumference of the specimen. The outer band presses the inner band lightly against the specimen and holds strain gauges, which vary in resistance as the gap changes. The ring, therefore, produces an electrical output that varies with the specimen circumference. The output can be readily calibrated to give the change in diameter as a function of the output signal, and a plot can be made of the change in diameter as a function of the change in length.

The ring is designed for a specimen 2.5 in. (6.35 cm) in diameter. To allow for thermal contraction and specimen variability and to provide an adequate measurement range, the working range of the extensometer is from a diameter of 2.4 in. to just under 2.6 in. (6.1 to 6.6 cm). The specimen stack is 7.7 in. (19.6 cm) long and is made of 11 disks, each 0.7 in. (1.8 cm) thick, bonded together at the axis with epoxy adhesive.

This work was done by Robert S. Boozon and John A. Shepic of Martin Marietta Corp. for **Marshall Space Flight Center**.

Inquiries concerning rights for the commercial use of this invention should be addressed to the Patent Counsel, Marshall Space Flight Center
Refer to MFS-28107 /TN

George C. Marshall Space Flight Center
Technology Utilization Officer:
Ismail Akbay
Code AT01
Marshall Space Flight Center,
AL 35812
(205) 544-2223
Patent Counsel:
Leon D. Wofford, Jr.
Mail Code CC01
Marshall Space Flight Center,
AL 35812
(205) 544-0014

and measuring the decrease in thickness and the increase in length. However, ceramics tend to fracture at low temperatures when placed under tension, and the conventional method cannot be used.

In the new method, Poisson's ratio is measured in compression instead of in tension. A cylindrical column of stacked ceramic disks is compressed axially on a testing machine. The increase in diameter resulting from the compression load is measured by a specially designed extensometer ring, and the decrease in length is measured in the conventional way.

The extensometer ring consists of inner and outer segments, the tips of which

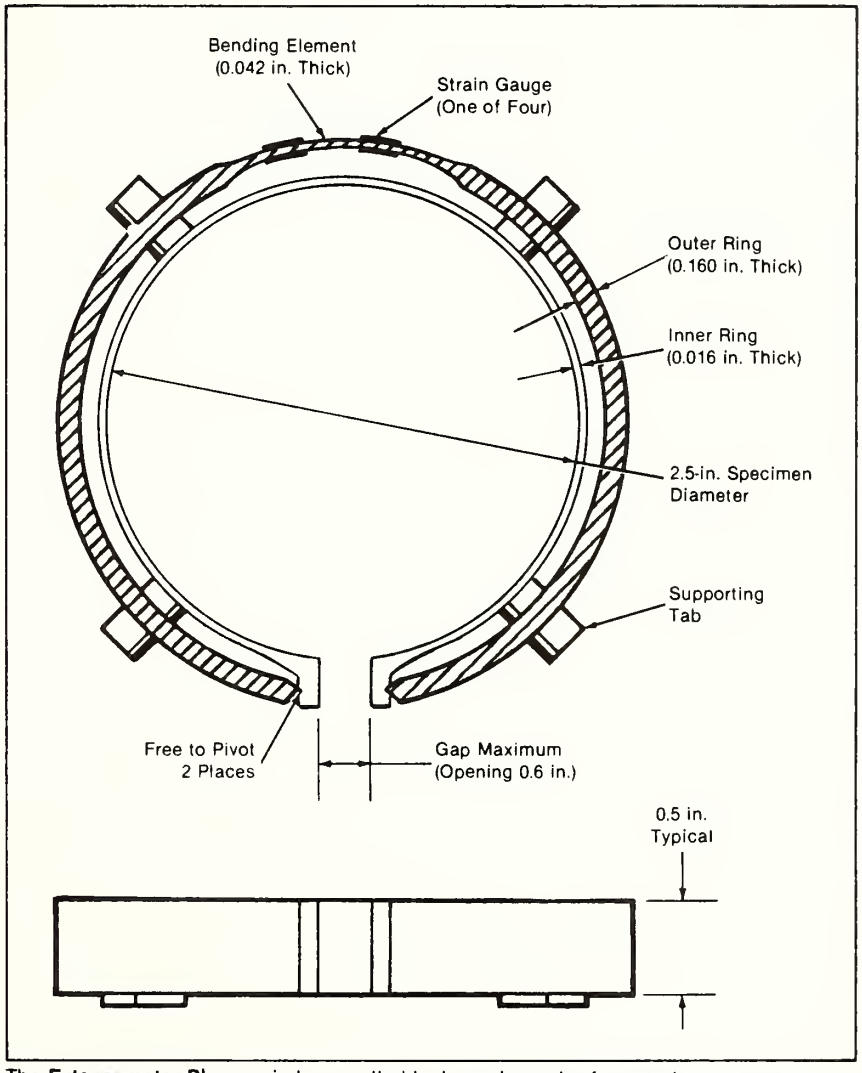

The **Extensometer Ring** encircles a cylindrical specimen. Its four strain gauges are connected in a fully active Wheatstone bridge that is self-temperature-compensating. It can be used at temperatures as low as that of liquid helium.

FOR ADDITIONAL INFORMATION: *Contact: Director, Technology Transfer Division, P.O. Box 8757, BWI Airport, MD. 21240; (301) 621-0100 Ext. 241*
REFER TO THE NUMBER LISTED AT THE END OF THE ARTICLE

Medicine & Biology

906 NIGMS Human Genetic Mutant Cell Repository

907 Promising New Immunological Adjuvant

Testing & Instrumentation

908 Boosting Cholesterol Test Accuracy is Aim of New Materials

909 New Transducer Could Detect Brain Aneurysms

910 Hand-Strength Meter — A grip meter measures hand strength accurately and reproducibly.

Other items of Interest

859 Large-Area Radiation Portal/Personnel Monitor — A faster, more sensitive personnel monitoring system

911 More Oil and Gas May Be Recovered by Using New Fracture Mapping Tool

NIH
Research & Technology

U.S. Department of Health and Human Services Public Health Service National Institutes of Health

NIGMS Human Genetic Mutant Cell Repository

Cell cultures from individuals with well-documented genetic diseases are available from the Human Genetic Mutant Cell Repository located at the Coriell Institute for Medical Research in Camden, New Jersey. The cell cultures, which are verified, well-characterized, and contamination-free, can be a crucial asset for studying genetic diseases, says Dr. Arthur E. Greene, director of the repository.

Analysis of the cell lines may lead to tests used for early diagnosis of genetic diseases and methods for preventing, understanding, and treating many inherited disorders. Researchers can use the cell lines to develop prenatal diagnostic tests which would identify those individuals who are carriers of genetic diseases. Researchers also may be able to develop techniques to replace defective genes

The repository, which was started in 1972 and is supported primarily by the National Institute of General Medical Sciences, is the largest facility in the world to store cell lines of this type.

More than 4,000 different cell cultures are available from the repository. Approximately 500 cell lines represent different biochemically characterized genetic diseases, including disorders of amino acid, carbohydrate, lipid, protein, and nucleic acid metabolism There are also approximately 500 cell lines from individuals with chromosomal aberrations. including inversions—in which a segment of the chromosome is turned 180 degrees from normal—and duplications. Other abnormal chromosomal cell lines available are from individuals with translocated chromosomes—a part of one chromosome is moved to another chromosome.

Many of the cell lines available consist of lymphocytes that are made "immortal" with a marmoset Epstein-Barr virus. These cell lines are particularly useful for gene-mapping studies. Other cell lines consist of skin fibroblasts, which have been the main tool for the study of many metabolic disorders and chromosomal abnormalities.

Some of the cultures that are available are from members of an extended Venezuelan family and from members of an American family, many of whom were victims of Huntington's disease, a rare hereditary disorder. The repository has cell lines from four generations of an Amish family whose members have a high incidence of depression or manic depression. Other cell lines in the NIGMS repository have been used to attempt to identify genetic markers for cystic fibrosis, various eye diseases, Tay-Sachs disease, and both adult and juvenile diabetes.

Another special area for which cell lines are available is thalassemia. The cell lines in the repository represent mutations accounting for most of the beta-thalassemia alleles that are found in inhabitants of the Mediterranean region and South China.

Cell lines from individuals who are free of known genetic disease are available as controls.

Using cell lines from the repository, researchers have obtained important information about genes responsible for causing several genetic diseases. For example, scientists have discovered that a gene that predisposes individuals to manic-depressive illness is on chromosome 11 and a gene that causes Huntington's disease is located on chromosome 4. Prenatal diagnostic tests have been developed to screen for this disease in affected families.

Researchers at the repository, along with colleagues at the University of Pennsylvania, have been studying cells from indi uals with hypophosphatasia, inherited metabolic disord Children with this disease h severe bone abnormalities their skeletons are unable to s port their body structure. Richard Mulivor, a repository entist, has developed an as that identifies affected fetuses the basis of the amount of a tain type of alkaline phosphat produced in fibroblasts cultu from amniotic fluid. The searchers are now trying to n the gene associated with this order.

Each of the 4,000 cell li available is described in the pository's catalog. It contains formation on the type of cult media researchers should us grow the cells, how the c should be handled, a descrip of where the cells came from, mode of inheritance of the ease, and references to any p lications involving that partic cell line. The catalog also c tains a chromosomal map t details what cultures are av able representing different ch mosomal aberrations. The ca log is available free to interes investigators.

Specimens of cell lines, wh are stored frozen in liquid ni gen at the repository, are av able to researchers at nonpr institutions for $60 each and commercial companies for $1 The cell lines are shipped in ture medium to the researche

Approximately 3,000 spe mens of cell lines are shipped investigators each year. Seve collections of cell lines that frequently requested are fr members of the Utah pedigr These cultures were obtain from large Mormon families a are very useful for gene mapp studies because individuals Mormon families have kept v accurate family histories. C lines obtained from Amish in

viduals are also frequently requested for gene mapping studies.

The repository staff are in the process of acquiring additional cell lines from people suffering from either form of diabetes, polycystic kidney disease, and retinitis pigmentosa, a progressive hereditary loss of retinal response.

—Barbara J. Proujan

For more information about the Human Genetic Mutant Cell Repository, contact:
Dr. Arthur E. Greene
Coriell Institute for Medical Research
Copewood and Davis Streets
Camden, New Jersey 08103
Telephone: (609) 966-7377

Childhood Development Meeting

A conference focusing on issues of child development and research will be held April 23 to 26, 1987, in Baltimore, Maryland.

The conference is sponsored by the Society for Research in Child Development (SRCD). Topics to be discussed include social policy for mothers and infants in poverty; what infants learn on the day of birth; adolescent depression and suicide; children and the legal system; environmental contaminants and developmental disorders; and the origins of moral development.

For more information, contact:
Society For Research In Child Development
Ms. Carol Weissbrod, Chair, Media Committee
Department of Psychology
The American University
Washington, D.C. 20016
Telephone: (202) 885-1711

For Additional Information:

To locate information or professional contacts on this effort, contact:

Research Resources Information Center, 1601 Research Blvd., Rockville, MD 20850 (301) 984-2870

Refer to item XI, No. 4/TN

Photo courtesy of the Coriell Institute for Medical Research

Karyotyping verifies the cell type, insuring that researchers obtain the specific cell lines requested.

Promising New Immunological Adjuvant

A few years ago an immunologist at the Scripps Clinic observed that minor chemical modifications of the 8 position of the purine guanosine could cause the molecule to greatly stimulate B lymphocytes, the cells responsible for antibody production. The most potent form of the molecule is 8-mercaptoguanosine, where a sulfur atom replaces a hydrogen normally found in guanosine.

This observation has been developed with Office of Naval Research (ONR) funding to look at both the mechanism of action and possible applications of 8-mercaptoguanosine (8-MG) as an immunological adjuvant for vaccines. Guanosine plays many significant roles in cells, including serving as a component of the nucleic acids.

Researchers demonstrated that 8-MG, following phosphorylation, was incorporated into RNA but not DNA, lessening the likelihood that it would be mutagenic for cells. Its association with a class of regulatory proteins that modulate membrane signals, called G-proteins because of their dependence on phosphorylated guanosine, is under investigation. With regard to immune function, 8-MG was shown to potentiate in mice the formation of protective antibody to a bacterial polysaccharide antigen, pneumococcal p-14, to which mice do not ordinarily respond. It also stimulated antibody formation in immature mice and genetically deficient mice, suggesting that it replaces certain T lymphocyte functions.

Finally, it was shown to enhance monoclonal antibody clone production 10-1000 fold as a consequence of enhancing the rate of formation of productive clones. The latter observation will be considered for patenting. While 8-MG may prove to be too potent (toxic) for human use, its applications in monoclonal technology and its use for investigation of the role of guanosine in immune regulation represent significant outcomes of this ONR task.

For Additional Information:

Backup material on this effort is available from:

Navy Domestic Technology Fact Sheet
Reader Reply Service
Code E211
Naval Surface Weapons Center
Dahlgren, VA 22448-5000
(703) 663-8921

Refer to 120304/TN

NBS technology update

National Bureau of Standards
U.S. Department of Commerce
Gaithersburg, MD 20899

Boosting Cholesterol Test Accuracy is Aim of New Materials

Materials for improving the reliability of blood serum cholesterol tests, recently developed as part of a decade-long joint research agreement between NBS and the College of American Pathologists (CAP), are expected to be available by mid-summer from CAP. These "certified reference materials" are being introduced at a time when there is much concern over the accuracy of the roughly 100 million cholesterol tests performed yearly. Reference materials with known values are needed to ensure that the analytical instruments used to measure cholesterol give reliable results. The new materials are intended to fill this need at an affordable price. Bottled in the form of freeze-dried human blood serum, the materials are sold in high, average, and low cholesterol concentrations. Cost per kit is $42.50. The freeze-dried serum can be reconstituted into a liquid and run through the same cholesterol tests as a patient sample to check instrument accuracy.

FOR ADDITIONAL INFORMATION: Contact:
College of American Pathologists
5202 Old Orchard Rd.
Skokie, IL 60077-1034
(312) 966-5700

New Transducer Could Detect Brain Aneurysms

Scientists at the Naval Research Laboratory (NRL) have sponsored development of a device that may help save thousands of lives.

NRL's Underwater Sound Reference Detachment (USRD) reports the development of a water-coupled acoustic sensor capable of reliably detecting acoustics emanations that would indicate brain aneurysms.

Two prototype models of the unique sensor have been laboratory tested with excellent results.

The new transducers have maximized sensitivity with very low self-noise in the frequencies of interest (between 50 hertz and 1 kilohertz) and have a high degree of discrimination between the measured acoustic signal and the extraneous outside noise, making it an ideal device for the detection of brain aneurysms.

Intercranial aneurysms are operative with greater than 90-percent probability of complete recovery of the patient if detected early in development; but, if not detected early, an aneurysm can rupture, resulting in either crippling or death. Existing technology makes it difficult for early detection of intercranial aneurysms because the symptoms are not clearly distinguishable, and the bone mass of the skull reduces the effectiveness of X-ray or ultrasound readings.

Neurological researchers in France and the United States have shown a high degree of correlation between certain acoustics emanations detected near the eye and the onset of intercranial aneurysms. Although researchers have used air microphones placed very close to the eye to detect aneurysms, the technique has been marginally effective due to the low signal level and the masking due to air-coupled background noise

Research on this new technique is continuing with a view to develop specialized models that could be used to improve the diagnostic technique in the detection of intercranial aneurysms.

For Additional Information:

Backup material on this effort is available from:

Navy Domestic Technology Fact Sheet
Reader Reply Service
Code E211
Naval Surface Weapons Center
Dahlgren, VA 22448-5000
(703) 663-8921

Refer to 120303/TN

NASA Tech Brief
National Aeronautics and Space Administration
Langley Research Center, Hampton, Virginia

Hand-Strength Meter

A grip meter measures hand strength accurately and reproducibly.

In rehabilitation efforts, it is necessary to evaluate the therapeutic methods by monitoring the patient's progress in response to these methods. In hand rehabilitation, hand strength is an important parameter to monitor, as are dexterity and flexibility. A special grip-strength meter has been designed for accurate, reproducible measurement of hand rehabilitation.

The hand-strength meter, shown in the figure, is machined from a one-piece aluminum block. The upper and lower parts of the block are contoured for the proper grip. These two parts are connected by two parallel measuring beams to which four strain gauges are cemented. The four strain gauges are wired to form a Wheatstone bridge. Two power leads to the bridge and two signal leads from the bridge are tunneled through a small access hole in the back of the meter to an external display unit that consists of a dc power supply, a three-digit light-emitting diode (LED), and signal-conditioning circuitry. Both the meter and the display unit are compact and lightweight [0.5 lb (0.2 kg) and 3 lb (1.4 kg), respectively].

When the meter is gripped, the compressive force exerted by the hand is transmitted to the measuring beams. The beams are therefore deflected or strained, and this mechanical strain is sensed by the strain gauges and converted into an electrical signal. After amplification and conditioning, the signal is displayed on the LED as a measure of the gripping strength of the hand.

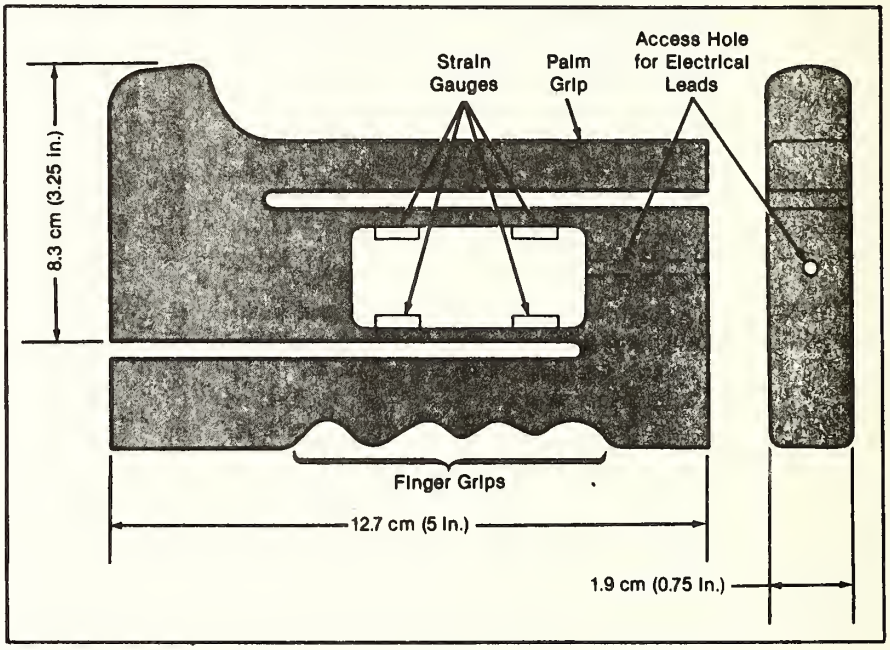

The Hand-Strength Meter includes four strain gauges connected in a Wheatstone bridge to measure the deflection caused by a gripping hand.

Laboratory calibration indicates that the meter is extremely linear for a gripping force ranging from 0 to 1,001 N (225 lbf), with a precision of ±0.67 N (±0.15 lbf). The display unit can be adjusted easily to show direct digital readings in pounds of force.

This work was done by Ping Tcheng of **Langley Research Center** *and Joe Elliot of the U.S. Army Aerostructures Directorate. LAR-13507 /TN*

FOR ADDITIONAL INFORMATION: *Contact: Director, Technology Transfer Division, P.O. Box 8757, BWI Airport, MD. 21240; (301) 621-0100 Ext. 241*
REFER TO THE NUMBER LISTED AT THE END OF THE ARTICLE

Natural Resources Technology & Engineering

911 More Oil and Gas May Be Recovered by Using New Fracture Mapping Tool

912 Microwave Properties of Quiet Seas — Measurements from a satellite provide information for comparisons and analyses.

Software

913 Ionospheric Communications Analysis and Prediction Program (IONCAP) — Predicts high-frequency skywave system performance

More Oil and Gas May Be Recovered by Using New Fracture Mapping Tool

Researchers at Sandia National Laboratories have designed and successfully tested a high-power, high-resolution tool that can help exploration engineers recover more energy from geothermal, oil, and gas reservoirs by precisely locating deeply buried fractures in rocks.

Key to the tool's performance is its ability to tell the direction that fractures are located from a borehole. No other mapping tool has a directional capability of this type.

A prototype, built by Southwest Research Institute, of San Antonio, Tex., has been successfully demonstrated at a special granite quarry test facility south of Albuquerque. During field tests, the tool has detected simulated fractures that were more than 30 ft away from a test borehole.

Emits very short pulses

The tool, which fits in a typical uncased borehole, emits pulses, each of which lasts just 8 nanoseconds [1 nanosecond (ns) is a billionth of a second.] The frequency spectrum of the pulses ranges up to the VHF band. FM radio and most TV broadcasts use the VHF band, which is between 30 and 300 MHz.

The tool determines fracture direction by transmitting highly directional and powerful radar pulses in a known direction from a borehole. Discontinuities in the rock interrupt and reflect radar signals; therefore, signals that return to the tool's receiving antenna indicate fractures. The return signal's time delay translates into distance from the borehole. The transmitter and receiver rotate in place, permitting the tool to scan for fractures in all directions from the borehole.

The tool has a diameter of 7 1/2 in. and is 20 ft long. The prototype model uses an aluminum housing; however, advanced development models would have a steel housing and a smaller diameter.

Tip holds power supply

The tip of the tool holds a 1700-volt power supply that drives the transmitting antenna, which is housed in a 15-in.-long fiberglass-covered section about a fourth of the way up the tool. A 3-ft-long isolator section separates the transmitting antenna from the receiving antenna.

The upper third, past the receiving antenna, contains additional electronic and mechanical components, including equipment that identifies the earth's magnetic north (necessary for reference), and a motor that turns the antenna sections 360 degrees.

During operation, the tool generates an 8-ns pulse that has a 2-ns rise time. Peak transmitting power is 50 kW.

Major technical accomplishments required for the design of Sandia's tool included:

— shrinking the radar's transmitting and receiving antennas to sizes that fit into typical uncased boreholes;

— designing the electronics to produce extremely powerful, but short pulses of electromagnetic energy; and

— developing a technique to transmit the radar's complete return signal through wires to data analysis equipment on the surface.

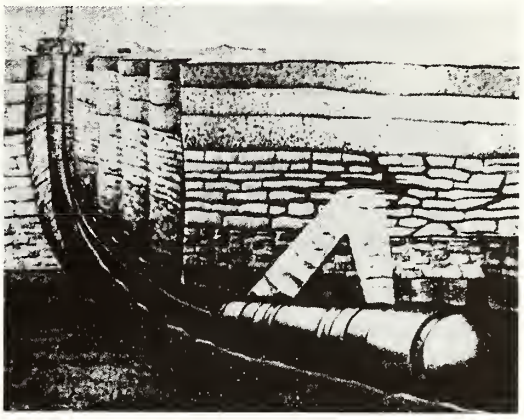

Artist's rendering illustrates the directional fracture mapping tool concept. Radio frequency signals travel from the tool to a fractured zone and then reflect back to the tool's receiver.

Although a critical need for better pictures of complex geothermal reservoir fracture systems motivated its design, the new tool could be used in a variety of ways after advanced development is complete.

"It could help pinpoint the location of an elusive oil- or gas-bearing reservoir, such as those tucked behind salt domes," says Hsi-Tien Chang, project leader. "Engineers and scientists may want to use it to show that significant fracturing does not exist near proposed underground radioactive waste repository sites or near Strategic Petroleum Reserve storage caverns in Texas and Louisiana.

"The tool could be used to find the lower portions of blow-out wells," says Chang, a member of Sandia's Geothermal Technology Development Division.

In a blow-out well, the upper portions of the well have failed by collapsing. It vents gases in an uncontrolled manner, and it cannot be re-entered. Therefore, a new intersecting well must be drilled into the lower, unharmed sections of the original well. The radar tool could locate that position so that the intersecting well can be properly located.

Chang believes the tool also could be adapted to conduct non-destructive inspection of subway or mine systems.

"In geothermal and petroleum exploration, a nonproductive dry hole constitutes the main frustration in drilling and field development," Chang says. "Worst of all, it is common to find dry holes close to producing wells."

Well-siting now inexact

Since extensive surface geophysical surveys usually are conducted beforehand, drilling operators have reason to believe that a reservoir exists in the general area before they drill. However, these techniques are unable to de-

fine the precise point to drill into an existing reservoir system.

Sandia's new tool seeks to eliminate those disadvantages, as well as those of other developmental downhole electromagnetic surveying techniques, which are unable to determine the direction of fractures from a borehole.

Early in the design stages, Chang determined that the tool's transmitter would have to operate up to the VHF band, because such a pulse can propagate to a reasonable distance, while providing excellent resolution. Higher frequency signals do not propagate far enough through rock to be useful; frequencies lower than VHF travel far enough, but don't offer the necessary resolution.

The major challenge was to design a directional antenna that fits inside a narrow borehole. For an antenna to provide any directionality, its dimension should be about a quarter wavelength. The free space wavelengths of the VHF band range from 33 to 3.3 ft.

Process reduces wavelength

Chang's solution involved immersing the antenna in a high dielectric constant material that essentially reduced the wavelength enough for the antenna to be one-tenth its theoretical optimum size.

The resulting 15-in.-long transmitting antenna section holds a 6-in.-diameter plastic pipe that has a taut copper wire (the transmitter's radiating element) running through it lengthwise. Barium titanate powder, whose high dielectric constant equals that of water, fills the pipe and surrounds the radiating element. Two 4-in.-wide, 15-in.-long copper plates are positioned at a 60-degree angle behind the plastic pipe. They form a corner reflector and give the antenna its directionality.

The receiving antenna is identical.

The use of electromagnetic pulses instead of continuous wave transmission gives the tool its powerful signal. The pulse's quick rise time and short duration are accomplished by using the special characteristics of avalanche transistors.

Chang considers the tool's ability to completely recover the electromagnetic signal for analysis to be another major achievement.

The result is significantly more data that helps provide a sense of a fracture's shape and orientation, Chang says.

FOR ADDITIONAL INFORMATION

Public Information Division,
Code 3161,
Dept. of Energy,
Sandia National Laboratories,
Albuquerque, NM 87185-5800
(505) 844-4207.
Refer to announcement 22, No.2

NASA Tech Brief
National Aeronautics and Space Administration

Microwave Properties of Quiet Seas

Measurements from a satellite provide information for comparisons and analyses.

The microwave fluxes from three quiet seas have been documented for five microwave frequencies. The measurements were taken by a satellite in Earth orbit with a mechanically scanned antenna. A 10-channel receiver was used to record simultaneously the signal intensities in both horizontal and vertical polarizations at each frequency.

A quiet sea is one in which the products of air/sea interaction — foam, bubbles, and spray — are minimal. The quiet sea serves as a reference-level sea that can be used for comparisons with other sea states as observed from Earth orbit.

The three quiet seas are an area on the Equator in the Pacific near South America, one at a middle latitude in the Sargasso Sea, and one at a high latitude in the Indian Ocean between Madagascar and Antarctica. Comparisons of the flux measurements of the three quiet seas are drawn, and the results are discussed and analyzed.

Microwave measurements can be used to deduce the thermal properties of the sea surface. They are not seriously degraded by tenuous and moderately dense clouds. However, raining clouds and clouds that contain water droplet do attenuate microwaves significantly.

A further advantage of microwave sensing is that the polarities of sea reflections may be discerned. Differences and ratios of polarized signal may be formed to provide information on important sea properties. For example the difference between horizontally and vertically polarized fluxes can be used to infer sea roughness and the presence of such pollutants as oil films.

The plots taken from the measurements show the following:

• The effects of the relative, on-axis gain

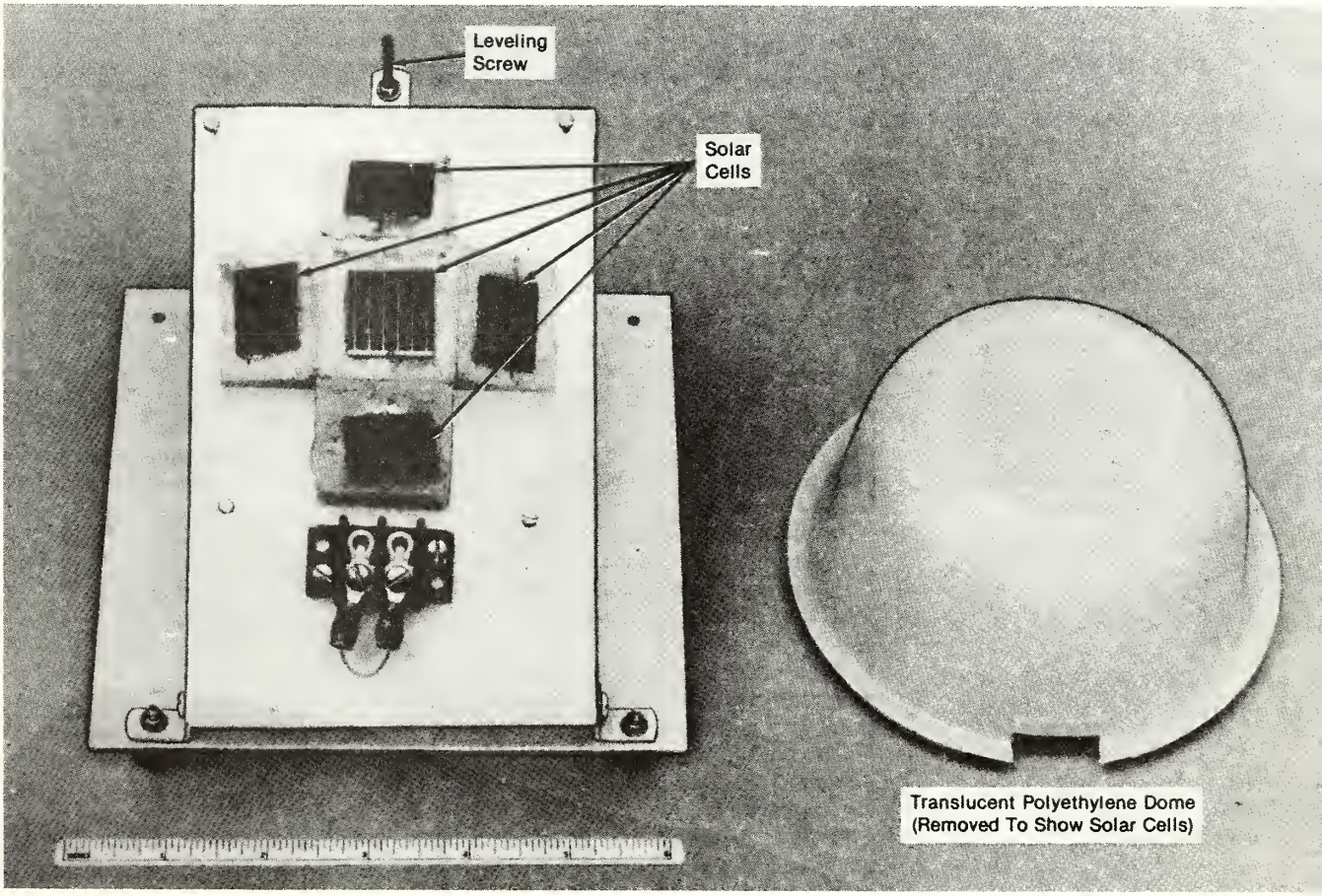

A **Translucent Dome** is placed over an array of silicon solar cells. By suppressing the effect of the Sun angle, the dome makes extra circuitry for angular corrections unnecessary.

of the collecting aperture for each frequency (6.6, 10.69, 18, 21, and 37 GHz);

- The effects of polarization rotation in the outputs of the receiver when the collecting aperture mechanically rotates about a fixed feed;
- The difference between the flux magnitudes for the horizontal and vertical channels, at each of the five frequencies, and for each pointing position, over a 44° scan angle; and
- The root-mean-square value of the clutter, as reckoned over the interval of a full swath and derived from the standard error of estimate of the plotted swath response for each channel.

The expected value of the background temperature is computed for each of the three quiet seas that were observed. The background temperature includes contributions from the cosmic background, the downwelling path, the sea surface, and the upwelling path.

This work was done by Joseph M. Stacey of Caltech for **NASA's Jet Propulsion Laboratory**. *Further information may be found in NASA CR-176199 [N85-35322/NSP], "Microwave Properties of a Quiet Sea."*

Copies may be purchased from the National Technical Information Service, Springfield, Virginia 22161, [A04]

NPO-16691 /TN

FOR ADDITIONAL INFORMATION: *Contact: Director, Technology Transfer Division, P.O. Box 8757, BWI Airport, MD. 21240; (301) 621-0100 Ext. 241*

REFER TO THE NUMBER LISTED AT THE END OF THE ARTICLE

Institute for Telecommunications Sciences
U.S. Department of the Interior

Ionospheric Communications Analysis and Prediction Program (IONCAP)
Predicts high-frequency skywave system performance

The computer program is an integrated system of subroutines designed to predict high-frequency (HF) skywave system performance and analyze Ionospheric parameters. It was developed by the National Telecommunications and Information Administration's Institute for Telecommunication Sciences located at Boulder, Colorado. These computer-aided predictions may be used in the planning and operation of high-frequency communication systems using skywaves. The product consists of 4 5 1/4 inch diskettes containing 26 files: 12 Binary data files (1 for each month of the year); 8 Binary link modules (containing IONCAP compile modules); 3 Binary link modules (containing link execute module and the associated library files); 1 batch command file (for linking IONCAP program); 1 ASCII file (controls the execution of IONCAP); 1 ASCII file (for IONCAP output computations and may be routed to the printer).

Software Description: The program is written in the FORTRAN programming language for implementation on an IBM PC-XT microcomputer using the DOS operating system. Memory requirement is 512K.The software is contained on 5 1/4-inch diskette, double sided, double density compatible with the IBM PC XT microcomputer. Diskettes are in the ASCII format. Price includes documentation, PB84-111210NAC.

For Additional Information:

For information about ordering this software, contact the
NTIS Computer Products Center, NTIS, 5285 Port Royal Road, Springfield, VA 22161; (703) 487-4763.

Refer to PB87-130993//NAC

Physical Sciences

914 Electrodeposition and Characterization of Niobium from Fused Salt Electrolytes

915 X-Ray Source is an Important Resource for X-Ray Spectroscopy

916 Tiny Device Allows Explosives to Be Ignited Much Faster

917 Reciprocal Taylor Series

918 Field-Reversal Source for Negative Halogen Ions — Large zero-energy electron-attachment cross sections would result in intense ion beams. (Licensing Opportunity)

919 High-Temperature Thermoelectric Energy Conversion — Semiconductor materials are the best choice.

Software

920 Thermal-Analysis Program — Temperature changes with time are modeled with the traditional electrical analog.

921 Designing Echelle Spectrographs — Performance numbers and output maps are computed from inputs supplied by the user.

Testing & Instrumentation

922 Pulse Injection Rate Synchronizer (PIRS) for Gamma Spectrometry

923 Pressure Regulation in a Reduced Pressure Chamber Using a Cryogenic Temperature Controller — An inexpensive, percise, and small regulator developed

924 Automated Laboratory System for Data Acquisition and Control — Programs and techniques detailed for a PDP-11 Computer

925 Sampling and Analysis for High-Molecular-Weight Polar Organic Compounds

926 Calibration of Germanium Resistance Thermometers — Six thermometers can be calibrated at once in the range below 2.17 K.

927 Measuring Shapes of Acoustically Levitated Drops — An instrument records shadows of drops in an acoustic field.

928 Containerless Atomic-Fluorescence Property Measurements — Laser-induced fluorescence can be used to measure high-temperature processes.

US Army Fact Sheet

Electrodeposition and Characterization of Niobium from Fused Salt Electrolytes

The electrodeposition of refractory metals such as tantalum, niobium, molybdenum, tungsten, and zirconium, appears to be a promising surface-coating method for protecting other metals against corrosion and high-temperature oxidation. Of these refractory metals, niobium is one of the more widely investigated, and appears to have potential to be developed for ordnance applications. For ordnance use, strength, low stress, and high hardness are additional properties needed to withstand both corrosive and erosive environments. Accordingly, Capsimalis, et al (U.S. Armament Research and Development Center, Benet Weapons Laboratory, Watervliet, N.Y.) carried out an investigation on the effects of temperature, current density, and bath additives on the electrodeposition of niobium from KF-NaF and LiF-NaF-KF (FLINAK) fused salt systems.(4)

The procedure used for preparing the fused salt niobium electrolytes involved the addition of 3.2 weight percent K_2NbF_7 to the binary eutectic mixture of NaF-KF, 2.5 weight percent to the ternary eutectic mixture of LiF-NaF-KF, and outgassing under vacuum at 400 C for one week to remove adsorbed moisture. The electrochemical cell reactor was made of 316 stainless steel and was heated with a single-zone Mellor furnace. Metallurgical grade niobium and OFHC copper plates served as the anode and cathode electrode plates respectively. The plating of niobium alloys containing chromium or boron was carried out by adding K_3CrF_6, up to 5.0 weight percent, and $NaBF_4$ at 10 weight percent to KF-NaF electrolyte. Niobium-tantalum alloy plating was also investigated by adding up to 12.5 weight percent K_2TaF_7 to the FLINAK electrolyte. The bulk of the electrodeposition experiments were carried out at current densities between 5 and 40 mA/sq cm and electrolyte temperatures between 1335 and 1475 F (725 and 800 C). Coating morphology was evaluated using optical and scanning electron microscopy, while coating structure and properties were characterized by X-ray diffraction analysis.

Although differential thermal analysis (DTA) measurement had indicated the melting points to be 842 F (450 C) and 1310 F (710 C) for the ternary and binary electrolytes, respectively, with added K_2NbF_7, it was necessary to operate both electrolytes at or above 1335 F (725 C) to obtain dense coherent deposits. With the FLINAK-K_2NbF_7 system, current efficiencies generally increased linearly with current density. For example, in the current density range of 15 to 40 mA/sq cm, current efficiencies (CE) at 1335 F (725 C) went from about 80 to 100 percent; at 1385 F (750 C) the CEs ranged from about 80 to 87 percent; at 777 CEs were from about 75 to 80 percent. At 1475 F (800 C), the CEs dropped from about 73 percent at 15 mA/sq cm to 65 percent at 40 mA/sq cm. With the KF-NaF + K_2NbF_7 system, maxima were generally found in the plots of current efficiency versus current density at all temperatures. For example, at 1385 F (750 C) the CE was about 60 percent at 10 mA/sq m, 73 percent at 27 mA/sq cm, and 68 percent at 35 mA/sq cm. The grain size of niobium deposits prepared from both types of electrolytes was influenced by current density. Some grain refinement generally was obtained by increasing the current density from 10 to 40 mA/sq cm in the electrodeposition of niobium from both electrolytes. In general, hardness values for niobium deposits from the FLINAK electrolyte varied between 102 and 124 KNH while deposits produced from the KF-NaF electrolyte varied between 119 and 144 KNH.

The addition of tantalum, boron or chromium to the baths resulted in improved surface finish, grain size, and hardness of the deposits. Detailed tabulated data on bath compositions, operating conditions, current efficiencies, and deposit properties, along with photomicrographs, are presented in the report.

FOR ADDITIONAL INFORMATION:
A copy of the report, Electrodeposition and Characterization of Niobium from Fused Salt Electrolytes, is available from NTIS, Springfield, VA 22161; (703) 487-4600.
NTIS order number: AD-A166668/NAC
Price code: A02
To discuss this effort further, contact:
G. Capsimalis
U.S. Army Armament Research and Development Center, Close Combat Armaments Center,
Benet Weapons Laboratory
Watervliet, NY 12189-4050

NBS technology update

National Bureau of Standards
U.S. Department of Commerce
Gaithersburg, MD 20899

Federal Technology Resource

X-Ray Source is an Important Resource for X-Ray Spectroscopy

The first year of experiments using the NBS X-24A beamline at the Brookhaven National Synchrotron Light Source (NSLS) confirms that this facility will be an important national resource for x-ray spectroscopy. X-rays can be tuned through the energy range from 500 to 5000 eV to a bandwidth of 0.2 to 0.5 eV, two to five times better than competing sources, and focused to a 1- by 2-mm spot at the sample chamber. Flux at the sample chamber is 10^{9} to 10^{13} x-rays/second. Current studies of argon, methyl chloride, various freons, and sulfur hexafluoride demonstrate that the instrumentation is sufficiently precise to separate x-ray spectrol features due to multiple electron effects from those due to specific bond orbitals, long a stumbling block in such research.

FOR ADDITIONAL INFORMATION:

To discuss this effort further, contact:
Dr. Paul Cowan
Physics Bldg., Room A-147
National Bureau of Standards
Gaithersburg, MD 20899
(301) 975-4846

Tiny Device Allows Explosives to Be Ignited Much Faster

A miniature device that can ignite explosives about a thousand times faster than conventional "hot wires" has been developed at Sandia National Laboratories. Called a semiconductor bridge (SCB), it results from about 5 years of development and testing by a Sandia technical team working closely with University of New Mexico (UNM) engineers.

The SCB is a semiconductor comprised of a heavily doped silicon or polysilicon area on a sapphire or silicon substrate. The semiconductor bridge is designed to replace and/or extend the capability of small metal bridgewires—commonly called hot wires—used to electrically ignite small explosive charges for various military, space, and civilian applications. For example, small charges are used to ignite rockets that power and control the course of missiles, to actuate certain functions in weapons, and to ignite explosives used in mining and construction industries.

Needs very little energy

In addition to igniting charges much faster than a hot wire, the SCB needs only about one-tenth the amount of energy for ignition (3 millijoules) and is much smaller, measuring about 100 microns long by 380 microns wide by 2 microns thick. The bridge fits on a chip about 1.5 mm square by a few tenths of a millimeter thick, and it is extremely rugged. Pressures of more than 30,000 psi have been applied with no apparent damage to the connecting welds or wires.

Robert W. Bickes, Jr., a physical chemist in Sandia's Explosive Components Department, leads the semiconductor bridge development and testing project. He says that the high-technology nature of the SCB means that it can be manufactured with automated techniques that incorporate great precision and control, resulting in improved reliability and consistency of performance. Bickes believes that automated manufacturing also will reduce production costs.

A semiconductor bridge operates about a thousand times faster than a typical hot wire. This large difference is explained by the fundamentally different way in which the two devices operate.

A hot wire heats up as electrical current runs through it (typically 3-5 amperes), similar to an element in an electric heater. After the wire reaches about 1,200°C, it ignites an explosive powder pressed against the wire, triggering an explosion. Although the entire process takes only a few thousandths of a second, it is much slower than a semiconductor bridge.

The SCB incorporates a heavily doped silicon or polysilicon area on a sapphire or silicon substrate. Doped with diffused phosphorus, the area forms the crossbar of an H-shaped pattern that allows good contact with an overlaid aluminum land.

As with the hot wire, an explosive powder is pressed against the SCB, and an electrical potential is applied across the SCB to ignite the powder. However, because the bridge is about 100 times smaller in volume than a conventional hot wire, it can be heated much faster. After a 3-millijoule electrical pulse is applied, the doped area turns into a plasma—superhot, highly ionized gas—that causes an instantaneous explosion. The explosion is triggered within a few tens of microseconds after the pulse is generated (a microsecond is one-millionth of a second).

Bickes acknowledges that the SCB's speed characteristics have yet to be fully exploited. "To some extent," he says, "we have a solution in search of a problem, but one area of application is for actuating rockets and other devices that make extremely fast course corrections for spacecraft and missiles. In some cases, rapid course corrections can mean the difference between success and failure of their missions."

Makes precise timing possible

The extremely fast ignition translates into another advantage—precise timing— that makes the SCB potentially useful for certain mining-industry applications. For example, precise timing is necessary to ensure that physically separated groups of explosives ignite simultaneously or that a series of explosions takes place in the proper sequence with the correct amount of time between them.

Paul D. Wilcox, Initiating and Pyrotechnic Components Division Supervisor, says these timing considerations can affect such things as the structural soundness of the arches in mining drifts (tunnels) and the relative efficiency of rubblizing operations.

Although mining, construction, and other civilian applications are envisioned, Bickes and Wilcox believe the SCB probably will be used first to replace hot wires in selected defense and space hardware.

Bickes says, "The facts that SCBs take less energy to

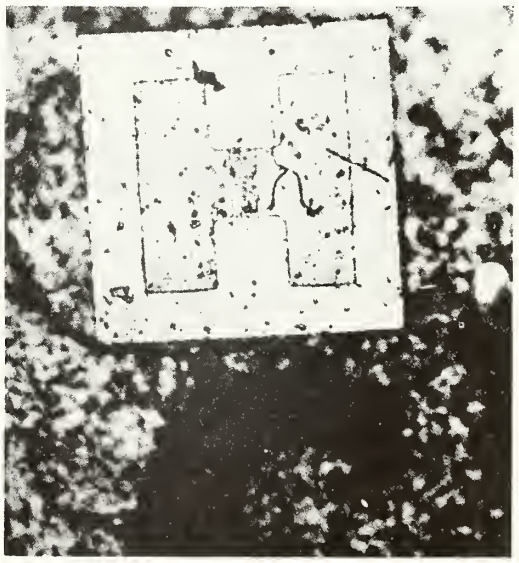

The semiconductor bridge is shown mounted on a chip about 1.5 mm square, lying next to the capital C on the "tails" side of a one-cent piece.

ignite and are considerably smaller than hot wires combine to make them especially attractive to designers of small 'smart' components."

Smart components incorporate logic to make sure incoming signals are coded correctly before ignition will take place. They are used in sophisticated missiles and nuclear weapons and could also be used to ensure that an explosive device could not be detonated by terrorists, extortionists, and other unauthorized groups who do not know the code.

A prototype of a smart component incorporating a semiconductor bridge has been built at Sandia and is now being tested. The device is about 1.5 inches in diameter, but another that is less than an inch in diameter is being designed. Kevin D. Marbach of Sandia's Fire Sets Department designed the smart electronic circuits.

Wilcox says Sandia tests show that SCBs are at least as safe as hot wires—maybe safer. The bridge requires a specific type of electrical signal—a fast, very short pulse of current—to ignite a charge.

Also, even though it takes much less energy to purposely ignite charges with semiconductor bridges, they are designed to withstand nearly double the amount of current (2 watts for 5 minutes) as hot wires without firing accidentally.

All SCB chips have been fabricated at the University of New Mexico's Center for High Technology Materials under the direction of Prof. Kenneth Jungling, the Center's Associate Director. SCBs may be manufactured commercially after patent licensing considerations are settled.

FOR ADDITIONAL INFORMATION

Public Information Division,
Code 3161,
Dept. of Energy,
Sandia National Laboratories,
Albuquerque, NM 87185-5800
(505) 844-4207.
Refer to announcement 22, No. 3

RECIPROCAL TAYLOR SERIES

The addition of a truncation error estimate term based on the reciprocal (Taylor) approximant (RA) to the partial sum of an infinite series has been shown to greatly improve the accuracy of the partial sum. This technique is less complex and, in many cases, more accurate than the often-used Padé approximant. For y = a function of x, the simplest form of the RA (the [1/1] approximant) can be expressed as

$$\Delta y \simeq yo'/(1/\Delta x - yo''/2\,yo') \quad .$$

The [1/1] RA has been used to obtain improved accuracy in the numerical integration of rate data for linear NOLOR functions (such that the ratio of the first derivative to the second derivative is linear in the independent variable). This application has been coded into a BASIC computer program.

Efforts are currently under way to use the [3/3] RA for the numerical differentiation of integrated rate data for complex functions that can be approximated with two or more data segments of linear NOLOR functions.

Additional information:

Office of Technology Applications
Information Service
Martin Marietta Energy Systems, Inc.
P.O. Box X
Oak Ridge, TN 37831
Telephone: (615) 574-4192; FTS 624-4192

R. W. Johnson, *Slab Diffusion Approximations from Time-Constant-Like Calculations,* Y-2068, Oak Ridge Y-12 Plant (December 1976).

R. W. Johnson and P. I. Tinnel, "Reciprocal Taylor Series," (abstract) in *Proceedings of the 149th National Meeting of the American Association for the Advancement of Science,* Detroit (1983).

R. W. Johnson and P. I. Tinnel, *Padé and Reciprocal Approximants and Linear NOLOR Functions,* Y-2350, Oak Ridge Y-12 Plant (June 1985).

R. W. Johnson and P. I. Tinnel, "Smoothing Rate Data by Repetitive Integration and Differentiation using Padé Approximants of Linear NOLOR Functions," (abstract) in *Proceedings of the 152nd National Meeting of the American Association for the Advancement of Science,* Philadelphia (1986).

NASA Tech Brief
National Aeronautics and Space Administration
NASA's Jet Propulsion Laboratory, Pasadena, California

Licensing Opportunity

Field-Reversal Source for Negative Halogen Ions

Large zero-energy electron-attachment cross sections would result in intense ion beams.

A concept for producing negative halogen ions takes advantage of the large cross sections at zero kinetic energy for the dissociative attachment of electrons to such halogen-containing gases as SF_6, $CFCl_3$, and CCl_4. Recent measurements of such cross sections show them to be much larger than previously expected. For example, the cross section for Cl^- production from $CFCl_3$ at zero electron kinetic energy is 7.57×10^{-14} cm^2, which is many orders of magnitude higher than that for H^- production from H_2 at higher electron energies. The large cross sections are due to the divergent nature of the s-wave electron attachment cross section.

In the ion source (see figure), a beam of electrons is injected into a chamber containing a beam of the target gas. As the beam passes through the gas, a negative voltage pulse is applied to a grid to produce a momentary electric field that reverses the direction of motion of the electrons before they reach the grid.

At the turning point, the electrons have essentially zero kinetic energy with respect to the gas molecules and tend to be captured by them, forming negative halogen ions as the molecules dissociate. Transverse electrostatic fields are used to extract and focus the resulting ions (but not the electrons) into a beam.

The incident electron beam may be confined electrostatically or magnetically. Standard electron guns and ion-extraction systems can be used. Such parameters as the electron-beam energy and divergence, gas pressure, size of the reversal region, pulse voltage, pulse duration, and ion-drawout voltages should be optimized experimentally. If necessary, a small permanent magnet may be placed outside the extraction aperture to serve as a momentum filter to remove electrons from the ion beam.

It should also be possible to extend the use of this source to the generation of negative ions through attachment resonances located at nonzero energies, since a continuous distribution of electron energies exists as the electrons are slowed down. A description of this work appears in the *Review of Scientific Instruments*, Volume 56, page 69 (1985).

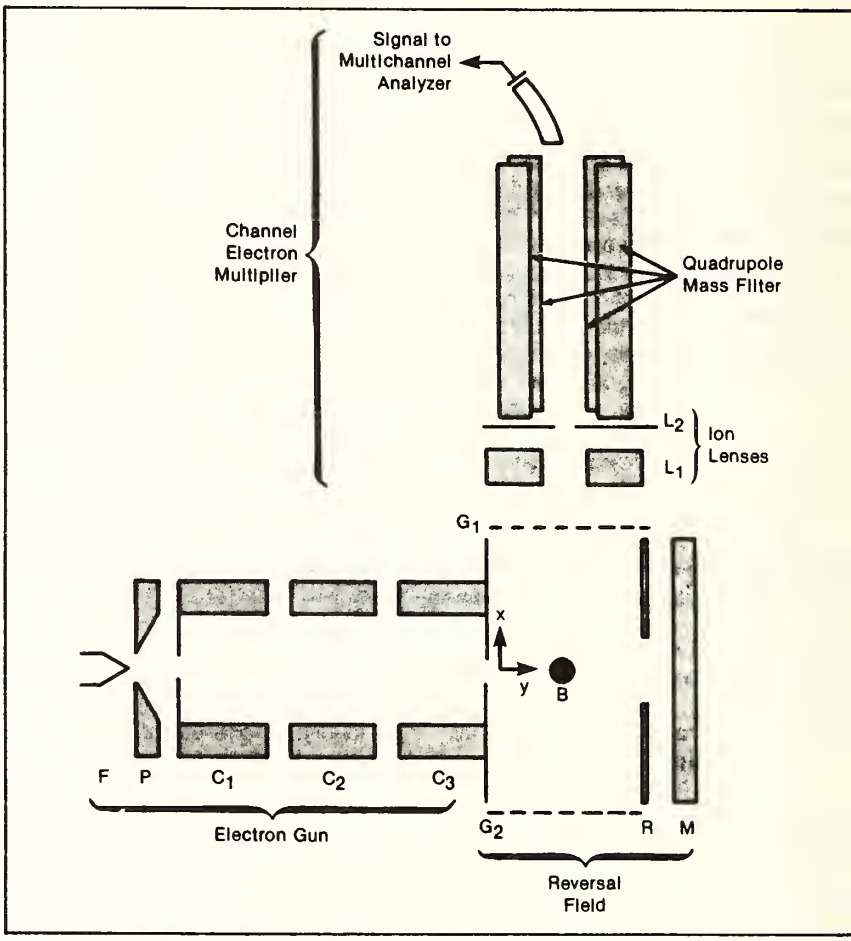

Schematic Diagram of the Apparatus shows the electron gun (F, P, C_1, C_2, C_3), the reversal electrodes (C_3, R, M) and extraction grids (G_1, G_2). The target molecular beam (B) is directed normal to the diagram. Ions are accelerated by lenses formed by L_1 and L_2 to a quadrupole mass spectrometer, counted, and the signal stored in a multichannel analyzer as a function of incident electron energy E_0 or potentials V_R, V_M.

This work was done by Ara Chutjian, Otto J. Orient, and Samuel H. Aladzhadzhyan of Caltech for **NASA's Jet Propulsion Laboratory**.

Inquiries concerning rights for the commercial use of this invention should be addressed to the Patent Counsel NASA Resident Office-JPL. Refer to NPO 16247. /TN

Jet Propulsion Laboratory
Technology Utilization Manager:
Norman L. Chalfin
Mail Stop 201-110
4800 Oak Grove Drive
Pasadena, CA 91109
(818) 354-2240

FOR ADDITIONAL INFORMATION: *Contact: Director, Technology Transfer Division, P.O. Box 8757, BWI Airport, MD. 21240; (301) 621-0100 Ext. 241*
REFER TO THE NUMBER LISTED AT THE END OF THE ARTICLE

NASA Tech Brief
National Aeronautics and Space Administration

High-Temperature Thermoelectric Energy Conversion

Semiconductor materials are the best choice.

The theory of thermoelectric energy conversion at high temperatures and the status of research on conversion materials are reviewed in a report. The report shows that the highest values of the thermoelectric figure of merit, Z, are found in semiconductor materials. Besides offering high Z, semiconductors have the advantage of being available in a wide choice of elements and compounds. Moreover, their electrical properties can be tailored to a particular application by impurity doping and control of stoichiometry.

The report develops a definition of Z that is useful for comparing materials and uses it to evaluate the potentials of different classes of materials—metals, semiconductors, and insulators. It explores the conditions for optimizing both broadband and narrowband semiconductors. For broadband materials, the highest Z values are in materials with high charge-carrier mobilities and large charge-carrier effective masses. For narrowband semiconductors, the requirements are for high lattice vibrational frequencies, large hopping distances, and hopping sites that are distributed in energy so as to allow the significant transport of vibrational energy.

The report notes that there is no theoretical basis for the widely held belief that a value of about 1 is the upper limit for ZT, the product of the figure of merit and the absolute temperature. In fact, the report suggests that ZT values considerably greater than 1 can be achieved at high temperatures. Z is not likely to be reduced significantly by radiation transfer at temperatures lower than 2,000 K.

Two groups of materials are especially promising for high Z: the rare-earth chalcogenides and the boron-rich borides. The report explains the electronic-transport properties of the rare-earth chalcogenides by regarding them as degenerate or partially degenerate n-type semiconductors. It proposes detailed explanations of the p-type hopping conductivity of boron-rich borides according to the particular compound.

This work was done by Charles Wood of Caltech for **NASA's Jet Propulsion Laboratory**.

"High Temperature Thermoelectric Energy Conversion Theory and Materials," NPO-16548 /TN

FOR ADDITIONAL INFORMATION: *Contact: Director, Technology Transfer Division, P.O. Box 8757, BWI Airport, MD. 21240; (301) 621-0100 Ext. 241*

REFER TO THE NUMBER LISTED AT THE END OF THE ARTICLE

Thermal-Analysis Program

Temperature changes with time are modeled with the traditional electrical analog.

The General Thermal Analyzer program solves transient and steady-state thermal problems using desk-top computers. The user models the thermal problem in terms of a resistance and capacitance network. The user defines the network, writes his own variable block, and has available most of the options associated with thermal-analyzer programs written for mainframe computers. Relax-network provisions for zero-capacitance nodes, one-way conductors for the simulation of fluid flow, and bivariate-data interpolation are some of the features included. The program currently handles up to 400 nodes. More nodes can be added if the program arrays are redimensioned, and the maximum number is limited only by the available memory.

This program is written in BASIC for interactive execution and has been implemented on two microcomputers. The General Thermal Analyzer was developed on an HP 9845 computer in 1982. In 1985, the program was adapted to an IBM PC operating under DOS.

This program was written by Don I. Levine of Rockwell International Corp. for **Johnson Space Center**. *MSC-21140 /TN*

FOR ADDITIONAL INFORMATION

CONTACT:
COSMIC®
112 Barrow Hall
University of Georgia
Athens, GA 30602
(404) 542-3265

NASA Tech Brief
National Aeronautics and Space Administration

Designing Echelle Spectrographs

Performance numbers and output maps are computed from inputs supplied by the user.

Echelle Spectrograph Design Aid program (EGRAM) aids in the design of spectrographic systems that utilize echelle/first-order cross-disperser combinations. This optical combination causes a two-dimensional echellogram to fall on a detector. EGRAM describes the echellogram with enough detail to enable the user to judge effectively the feasibility of the spectrograph design. By iteratively altering system parameters, the desired echellogram can be achieved without making a physical model. EGRAM calculates system parameters that are accurate to the first order and compare favorably to results from ray-tracing techniques.

The spectrographic system modeled by EGRAM consists of an entrance aperture, collimator, echelle, cross-dispersion grating, focusing optics, and a detector. The system is assumed to be free of aberrations, and the echelle, cross disperser, and detector should be planar. The EGRAM program is menu driven and has a HELP facility.

The user is prompted for such information as minimum and maximum wavelengths, slit dimensions, ruling frequencies, detector geometry, and angle of incidence. EGRAM calculates the resolving power and range of order numbers covered by the echellogram. A numerical map is also produced. This tabulates the order number, slit bandpass, and high/middle/low wavelengths. EGRAM can also compute the centroid coordinates of a specific wavelength and order (or vice versa).

EGRAM is written for interactive execution and is available in two versions. The first version is written in FORTRAN 77 and has been implemented on a DEC VAX-series computer operating under VMS. The second version is written in Microsoft BASIC A and has been implemented on an IBM PC-series computer operating under DOS. EGRAM was developed in 1985.

This program was written by Andrew Dantzler of **Goddard Space Flight Center**. *GSC-13009 /TN*

FOR ADDITIONAL INFORMATION

CONTACT:

COSMIC®
112 Barrow Hall
University of Georgia
Athens, GA 30602
(404) 542-3265

Pulse Injection Rate Synchronizer (PIRS) for Gamma Spectrometry

The Pulse Injection Rate Synchronizer for Gamma Spectrometry is designed to inject reference pulses into gamma ray spectra to improve the accuracy of quantitative gamma spectroscopy by simplifying dead-time and pileup corrections. The method utilizes an injection rate that is proportional to the gross gamma count rate. PIRS automatically adjusts the pulse injection rate as the gross count rate changes.

This instrument is better than existing technology because Pulse Injection Systems require specialized spectral processing equipment or operator intervention. PIRS is suitable for automated scanning spectrometers and as ap-aplications where count rate varies dramatically.

FOR ADDITIONAL INFORMATION: Contact:

Dr. Jane M. Welch
Idaho National Engineering Laboratory
Manager ORTA
P.O. Box 1625
Idaho Falls, ID 83415
(208) 526-8318.

US Army Fact Sheet

Pressure Regulation in a Reduced Pressure Chamber Using a Cryogenic Temperature Controller

An inexpensive, percise, and small regulator developed

In cryogenic studies, temperatures below 4.2°K are routinely required and are attained by reducing the pressure over a liquid helium bath. For temperature control, this pressure must be kept constant within a few mm Hg, at flow rates which vary with heat flow to the liquid helium bath. The laboratory's requirements for pressure regulation in a reduced pressure chamber containing a flat flame burner were similar, and with modifications, the regulator has been used to provide the required degree of precision.

In Figure 1, the major components of the regulator are shown. Gas from the system to be regulated enters the regulator at the connection on the left, passes through the regulator intake tip (1) into the tubular diaphragm (2) through the regulator outlet tip (3) and on to the vacuum pump (not shown) which must be able to maintain the desired pressure at the desired flow. The main flow of gas is not permitted to enter the regulator chamber (4), which is sealed with 0-rings to the aluminum backplate (5) and the plexiglass faceplate (6). The flow of gas through the regulator is permitted only so long as the pressure inside the tubular diaphragm (2) exceeds the pressure in the regulator chamber (4) so that the diaphragm does not cover the holes in the exhaust regulator tip (3). When the pressure inside the diaphragm (2) is less than that in the regulator chamber, the diaphragm collapses and closes off the holes in the exhaust regulator tip (3). The regulator chamber pressure is reduced by briefly opening valve (7), and increased by opening valve (8).

The strict on-off action described above is not desirable for most applications, so the regulator tips (1) and (3) are tapered. When the diaphragm begins to collapse, it closes off more and more of the holes in the tip (3) providing a variable-area orifice to pump through, and thus, proportional control.

DESIGN STANDARDS

For flame gases, the spacing and the diameters of the regulator tip holes is different than that for helium gas, which has much lower viscosity and requires less aperture for proper operation. If the diameter of the holes are made too large, the diaphragm will be sucked into them and will rupture, or will be too tightly held for the gas to push away from the holes. The angle of the taper also helps to determine the opening and closing pressures of the regulator. It is possible to calculate what the pressure on the diaphragm is at a given pressure difference, angle of taper and elastic constant of the diaphragm material, but such calculations serve only to give a starting point. For a given gas mixture, several sets of tips may have to be made in order to reach desired performance, each with different hole spacing and taper angle. Ideally, the sum of the areas of the holes in a regulator tip should at least equal the area of the pipes bringing gas to and from the regulator.

Although this design is certainly not the only or best one for pressure regulation in the fraction-of-an-atmosphere domain, it certainly has advantages over cartesian-diver types of devices, both in cost and in absence of the hazardous mercury metal required by most. For the volumes of gas that this regulator will pass, most other devices of this sort are large and cumbersome, or lack the degree of precision that is available.

FOR ADDITIONAL INFORMATION: A copy of the report is available from NTIS, Springfield, VA 22161; (703) 487-4600.

NTIS order number: AD-A091245/NAC

Price code: A02

To discuss this effort further, contact:

Mark Dewilde
U. S. Army Ballistic Research Laboratory
ATTN: SLCBR-IB
Aberdeen Proving Ground, MD 21005-5066
(301) 278-6518.

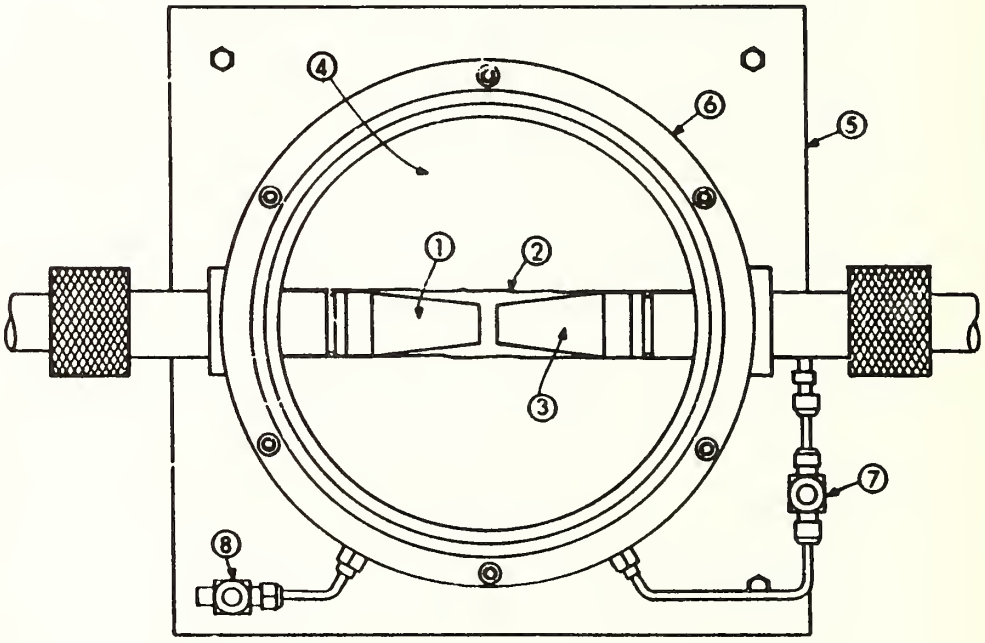

Figure 1. Regulator in TGTU

US Army Fact Sheet

Automated Laboratory System for Data Acquisition and Control

Programs and techniques detailed for a PDP-11 Computer

The use of a PDP-11 computer to fully automate laboratory experiments was demonstrated by the U. S. Army's Ballistic Research Laboratory. Since the PDP-11 is in common use, the results of this work should have wide interest.

In the case of this laboratory's work, an automated combustion diagnostics effort was developed. It was aimed at the application of laser-based probes to the study of flame chemistry. These probes include Raman spectroscopy, laser induced fluorescence, multiphoton laser induced fluorescence/ionization spectroscopy, and others. These techniques require numerous types of control signals and adjustments, and produce large quantities of data requiring further numerical processing for interpretation. As a typical example, a spontaneous Raman spectroscopy setup requires a laser beam shutter to be opened and closed, a spectrometer to be scanned, a burner that provides the flame under study to be moved so that different parts of the flame may be probed, and an optical multichannel analyzer that senses the signal light be read into digital form. In a simple profiling of a flame, it is possible that well over 1000 individual settings and operations be accomplished by an operator in order to take such data. If an automatic system were not utilized, such measurements would require a massive quantity of human intervention and would be prohibitively expensive. In such a situation, the purpose of automation is that of cost savings and release from tedium. In other cases, however, bringing the power of computer automation to bear on a problem makes possible measurements that are beyond the capabilities of non-computerized instruments and humans to accomplish. In addition, many modern state-of-the-art instruments are not designed to perform their full range of capabilities without the aid of a computer. In both of the latter cases, the decision to fully automate is unavoidable.

Much of the hardware is commercially available, and that which is not is described in the backup reports. The study did not document all of the instrumentation that has been connected to these systems, but rather lays the foundations of the general purpose portions of the systems that are built upon for special purposes. As part of this effort, an automated system for data acquisition and control via IEEE-488 interface to a general purpose laboratory computer was developed. Samples of data taken with the system on a multiphoton ionization spectroscopy experiment are shown, and all necessary additional control systems described in the technical report listed below. The IEEE-488 control system developed for this work represents a superior interface for the Dec PDP-11 computer than that available from the manufacturer. The software packages presented can be easily altered to support a wide range of IEEE-488 bus controllable devices.

FOR ADDITIONAL INFORMATION: The following reports detail this research effort.

Virtual Terminal Program for Inter-Computer System Communications under the RT-11 Operating System.
NTIS order number: AD-A174920/9
Price code: A02

Automated System for the Control of and Data Acquisition from Multiphoton Ionization and Fluorescence Lifetime Measurements
NTIS order number: AD-A173903/6
Price code: A07

Combustion Diagnostics Laboratory Data Acquisition and Control System
NTIS order number: AD-A173957/2
Price code: A04

For technical questions not covered by these reports, contact:
Dr. Mark DeWilde,
U. S. Army Ballistic Research Laboratory,
ATTN: SLCBR-IB,
Aberdeen Proving Ground, MD 21005-5066
(301) 278-6518.

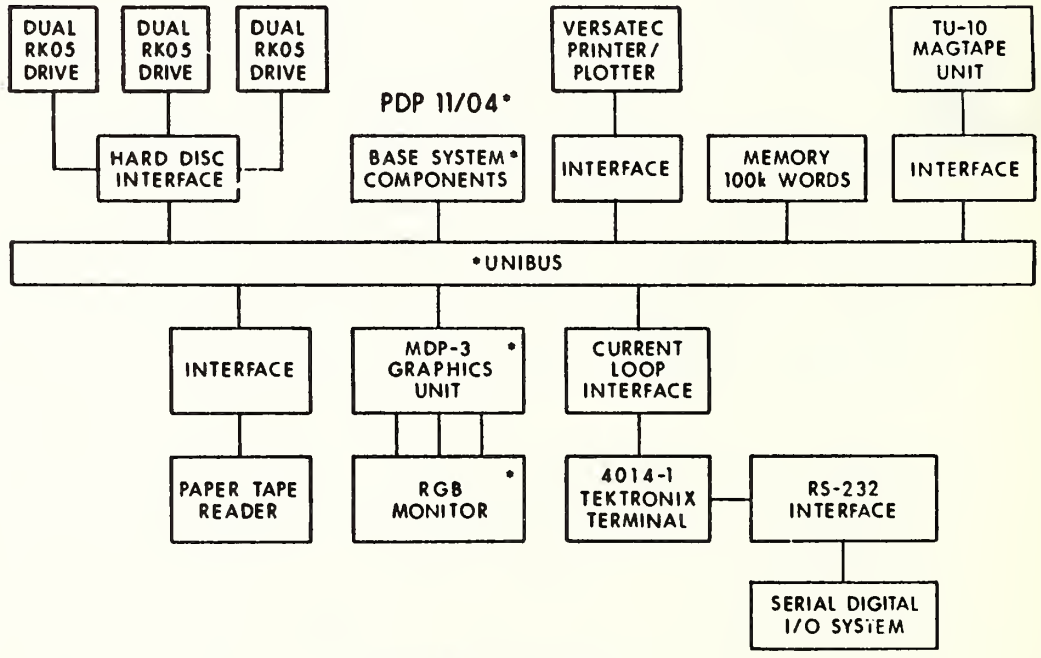

Actual System Configuration

United States
Environmental Protection
Agency

Air and Energy Engineering
Research Laboratory
Research Triangle Park NC 27711

Research and Development

EPA

Project Summary

Sampling and Analysis for High-Molecular-Weight Polar Organic Compounds

This report gives results of preliminary investigations into the determination of high-molecular-weight polar organic compounds from wood combustion residues. It is intended as a reference to be used by laboratories that are developing methods for the identification and quantification of high-molecular-weight compounds.

Introduction

No universal analytical method currently exists in the field of trace organic analysis that covers the more polar, less volatile components of environmental samples. While capillary gas-chromatographic methods may be sufficient for substances that are relatively volatile, there remain many large and polar molecules that have increasing environmental significance. With increasing molecular weight, the number of isomeric compounds to be resolved also increases proportionally. The methods for their determination have not yet been fully developed. Although high-performance liquid chromatography (HPLC) is capable of handling such large and polar molecules, improvements in the applications of this technique will be required for the characterization of high-molecular-weight fractions.

The proposed HPLC method is capable of giving functional-group class separation for semipreparative sample fractionation, and it may prove to be a useful analytical technique for the more polar constituents (pyrrolic, $-OH$, $-COOH$, and $-NH_2$ substituted). But these compounds constitute only about 40% (w/w) of the sample analyzed in this study. About 36% of the sample was judged to contain less polar compounds (carbonyl, nitro, and aza compounds). The remaining 24% were nonpolar compounds (hexane extractables). Unfortunately, the method did not distinguish between the alkyl- and benzyl-substituted proton-donating compounds and the nonionizable compounds. It appears that the higher the molecular weight, the greater the alkyl substitution; or the more ring conjugation present, the more inadequate the method becomes as an analytical technique.

The objective of this task was to develop methods for determining high-molecular-weight polar organic compounds derived from coal, synfuel, and wood combustion. The existing methodology was reviewed, and the analytical methodology was developed leading to the separation of as many of the high-molecular-weight species as possible in residues from wood combustion.

The proposed method was expected to be based on initial separation by liquid chromatography, which included such methods as liquid-solid chromatography, gel-permeation chromatography, or reversed-phase liquid chromatography. The use of the proposed method resulted in major subfractions and, ultimately, fractions containing fewer compounds. Qualitative analysis was expected to be based on a combination of techniques.

Fast atom bombardment/mass spectrometry (FAB/MS) and direct-insertion-probe/mass spectrometry (DIP/MS) were used to characterize fractions. The samples were also screened by Fourier-transform infrared spectroscopy (FTIR).

Conclusions

Separation by open-column liquid chromatography is not entirely satisfactory. Low-molecular-weight compounds need to be removed before separation of the woodburn sample into functional groups.

FAB/MS studies show that the spectra contain ions at almost every m/z to 1500, but the interpretation of the spectra is complicated by the relatively high abundance of low-molecular-weight compounds.

DIP/MS analyses indicate the presence of polar PAHs, but give little information above m/z 500.

The proposed HPLC (Method 8) is capable of giving sufficient class separation for semipreparative sample fractionation. It may prove to be a useful analytical technique for the more polar constituents (pyrrolic, –OH, –COOH, and $-NH_2$ substituted). But these compounds constitute only about 40% (w/w) of the woodburn Sample 233C. About 36% of the sample was judged to contain less polar compounds (carbonyl, nitro, and aza compounds).

HPLC Chromatographic Methods

1. Column: Waters μ-Styragel, 100 Å, 300 × 7.8-mm ID
   Solvent: Tetrahydrofuran
   Flow: 1 mL/min, isocratic

2. Column: ASI Ultragel, 100 Å, 250 × 7.8-mm ID
   Solvent: Tetrahydrofuran
   Flow: 1 mL/min, isocratic

3. Column 1: Waters μ-Styragel, 100 Å, 300 × 7.8-mm ID
   Column 2: AS1 Ultragel, 100 Å, 250 × 7.8-mm ID
   Solvent: Tetrahydrofuran
   Flow: 1 mL/min, isocratic

4. Column: Whatman Partisil, ODS-3, 10 μm, 250 × 4.6-mm ID
   Solvent A: Methanol
   Solvent B: Methylene Chloride
   Flow: 1 mL/min, gradient
   Program: 0% B to 100% B in 40 min.

5. Column: Waters μ-Bondapak-NH_2, 10 μm, 300 × 3.9-mm ID
   Solvent: n-Heptane
   Flow: 0.5 mL/min, isocratic

6. Column: Waters μ-Porasil-Si, 10 μm, 300 × 3.9-mm ID
   Solvent A: Carbon Tetrachloride
   Solvent B: Dimethyl Sulfoxide
   Flow: 1 mL/min, isocratic at 0.1%, 1.0%, 10%, or 25% B

7. Column: Waters μ-Porasil-Si, 10 μm, 300 × 3.9-mm ID
   Solvent A: Carbon Tetrachloride
   Solvent B: Dimethyl Sulfoxide
   Flow: 1 mL/min gradient
   Program: 0% B to 1% B in 10 min, then to 10% B in 10 min

8. Column: Chromanetics Spherisorb-Si, 5 μm, 250 × 4.6-mm ID
   Solvent A: Carbon Tetrachloride
   Solvent B: Dimethyl Sulfoxide
   Flow: 1 mL/min, isocratic

   Method option: A = 25% B
   B = 10% B
   C = 1.0% B
   D = 0.1% B

R. James, R. Adams, and H. Miller are with Southern Research Institute, Birmingham, AL 35255-5305.
***Merrill D. Jackson** is the EPA Project Officer (see below).*
The complete report, entitled "Sampling and Analysis for High-Molecular-Weight Polar Organic Compounds," (Order No. PB 87-119 434/AS; Cost: $13.95, subject to change) will be available only from:
National Technical Information Service
5285 Port Royal Road
Springfield, VA 22161
Telephone: 703-487-4650
The EPA Project Officer can be contacted at:
Air and Energy Engineering Research Laboratory
U.S. Environmental Protection Agency
Research Triangle Park, NC 27711

NASA Tech Brief
National Aeronautics and Space Administration
Marshall Space Flight Center, Alabama

Calibration of Germanium Resistance Thermometers

Six thermometers can be calibrated at once in the range below 2.17 K.

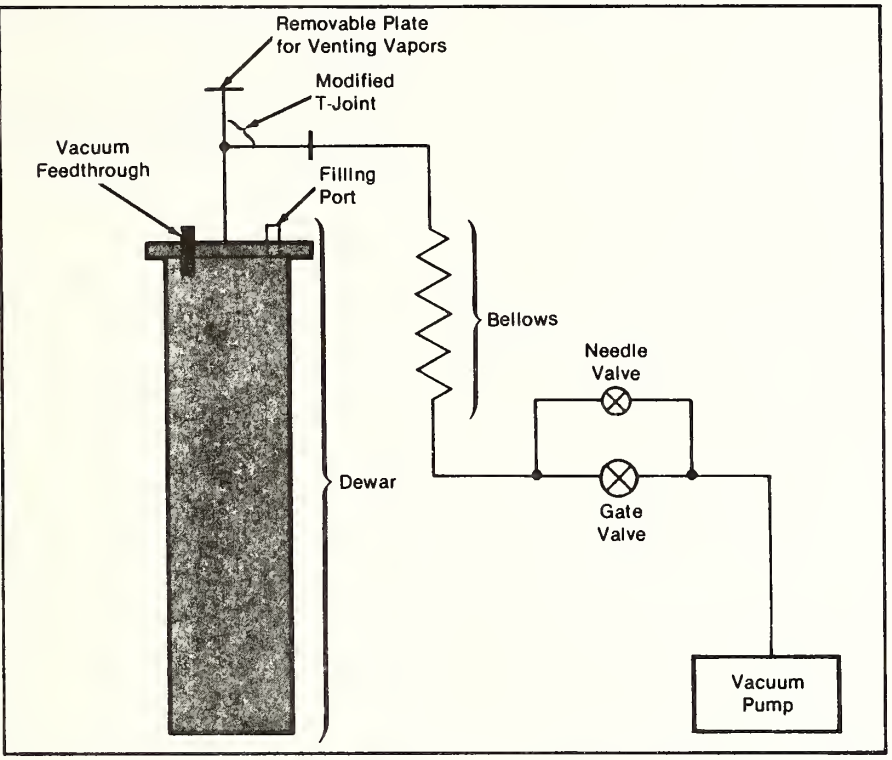

Figure 1. The **Cryostat** maintains a temperature less than 2.17 K through the controlled evaporation and removal of liquid helium from the Dewar.

A largely completed thermometer-calibration cryostat and probe will allow six germanium resistance thermometers to be calibrated at one time at superfluid-helium temperatures. In experiments involving several such thermometers, the use of this calibration apparatus could result in substantial cost savings: An uncalibrated germanium thermometer costs approximately $100 (1984 prices), whereas a calibrated thermometer, approximately $600.

Germanium thermometers are well suited for temperatures below 4.2 K because in this range their electrical resistances increase rapidly with decreasing temperature and because of the high reproducibility of the temperature dependence of resistance when the thermometers are cycled between liquid-helium temperatures and room temperature. In contrast, ordinary metallic resistance thermometers have low sensitivities in this range, while the temperature dependences of the resistances of carbon resistors are not reproducible under temperature cycling.

The cryostat (see Figure 1) includes a helium Dewar in which the helium space is enclosed by a cylindrical, 25-l aluminum-alloy can. The pumping line contains valves to regulate the pumping

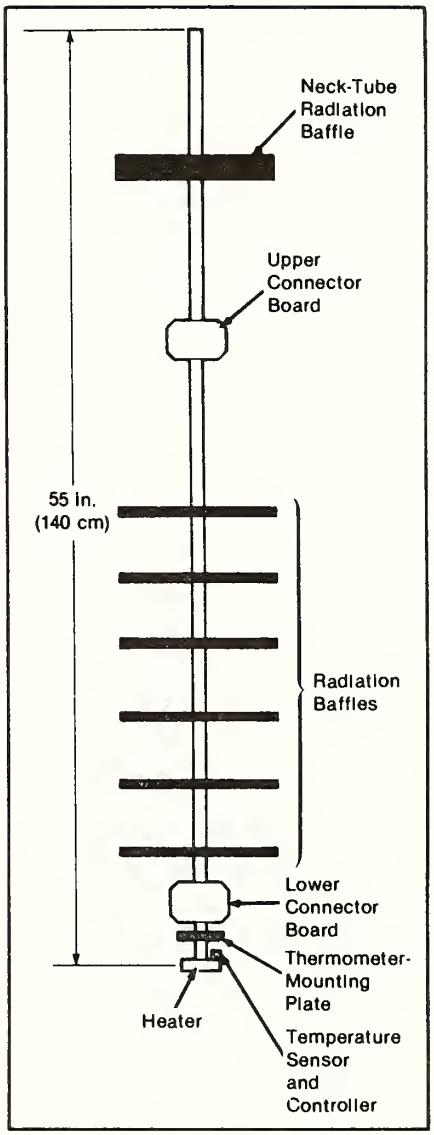

Figure 2. The **Probe** holds the thermometers to be calibrated and applies a small amount of heat as needed to maintain a precise temperature below 2.17 K.

speed and a section of vacuum bellows tube to suppress the effect of pump vibrations on the calibration process.

The Dewar is connected to the pumping line by a modified "T" joint in a flange at the top. The joint has an inside adapter that supports the probe. Also on top of the flange is a plate that is removed to allow the escape of vapors when helium is being added to the Dewar through the filling port. A 37-pin connector serves as the vacuum feedthrough for connecting the various probe components to the electronics.

The probe (see Figure 2) is a 55-in. (140-cm) long stainless-steel tube fitted with radiation baffles and supporting both the thermometer-mounting plate and a temperature sensor and controller with its associated temperature-regulating resistance heater. The heater wires are wound in a bifilar coil to minimize the production of magnetic fields, which could affect the resistances of the thermometers to be calibrated. The four wires from each of seven resistance thermometers (one calibrated, six to be calibrated), the three wires from the sensor of the temperature controller, and the two from the regulator heater are consolidated at the lower connector board and pass through rubber-grommeted holes in the radiation baffles to the upper connector board.

To determine the resistances of the uncalibrated thermometers as a function of temperature, their conductances are measured under a constant voltage, using a potentiometric conductance bridge. A rotary wafer switch permits each of the six uncalibrated resistors to be switched into the bridge, with the calibrated resistor being switched into the bridge after resistors 1, 4, and 6 in a cyclic manner. This allows for a quick, multiple measurement of the calibrated resistor at each temperature during a calibration run.

Since the calibrating temperature range lies between 2.17 and 1.5 K or lower, approximately one-third of the starting 25 liters of helium in the Dewar is pumped away to accomplish the λ transition at 2.17 K. After this temperature has been attained, the pumping speed is set by adjusting the valves in the pumping line until the approximate temperature of a calibration point is reached. The temperature is then maintained at the desired value by the regulator. A variety of temperatures can be maintained in this manner, allowing a resistance-versus-temperature calibration curve to be established for each of the uncalibrated thermometers.

This work was done by Dan Ladner and Eugene Urban of **Marshall Space Flight Center** *and Franklin Curtis Mason of Middle Tennessee University.*

MFS-27107 /TN

FOR ADDITIONAL INFORMATION: *Contact: Director, Technology Transfer Division, P.O. Box 8757, BWI Airport, MD. 21240; (301) 621-0100 Ext. 241*

REFER TO THE NUMBER LISTED AT THE END OF THE ARTICLE

NASA Tech Brief

National Aeronautics and Space Administration

NASA's Jet Propulsion Laboratory, Pasadena, California

Measuring Shapes of Acoustically Levitated Drops

An instrument records shadows of drops in an acoustic field.

The shapes of acoustically levitated liquid drops and gas bubbles can be examined by a shadow projector. Although acoustic radiation pressure counterbalances the gravitational force acting on levitated drops and bubbles, the pressure usually is not uniform over their surfaces and causes them to assume nonspherical shapes. The shape of the drop or bubble gives useful information about the acoustic field and the levitated material. For example, if the acoustic field is well known, the surface tension of a drop can be determined from its size and shape.

A vibrating lower plate (see figure) driven by a transducer at 20 kHz generates a standing acoustic wave in the space between the lower plate and an upper plate that serves as an acoustic reflector. A collimated laser beam illuminates a sample drop levitated in this acoustic field. After passing the drop, the beam is enlarged, and the shadow of the drop, enlarged 20 times, is photographed. A microphone probe is moved to various points to measure the acoustic pressure.

Drops of such liquids as decane, octane, and water evaporate substantially during experiments. These liquids are levitated at constant acoustic pressure. As a drop shrinks, the surface tension becomes more dominant than the acoustic radiation stress, and the aspect ratio of the projected shadow (the ratio of its width to height) approaches 1 as the drop becomes more nearly spherical.

On the other hand, drops of liquids like hexadecane and glycerine do not evaporate appreciably during the experiments. For these the acoustic pressure is gradually reduced. The drop becomes more spherical until the acoustic pressure is too weak to support it.

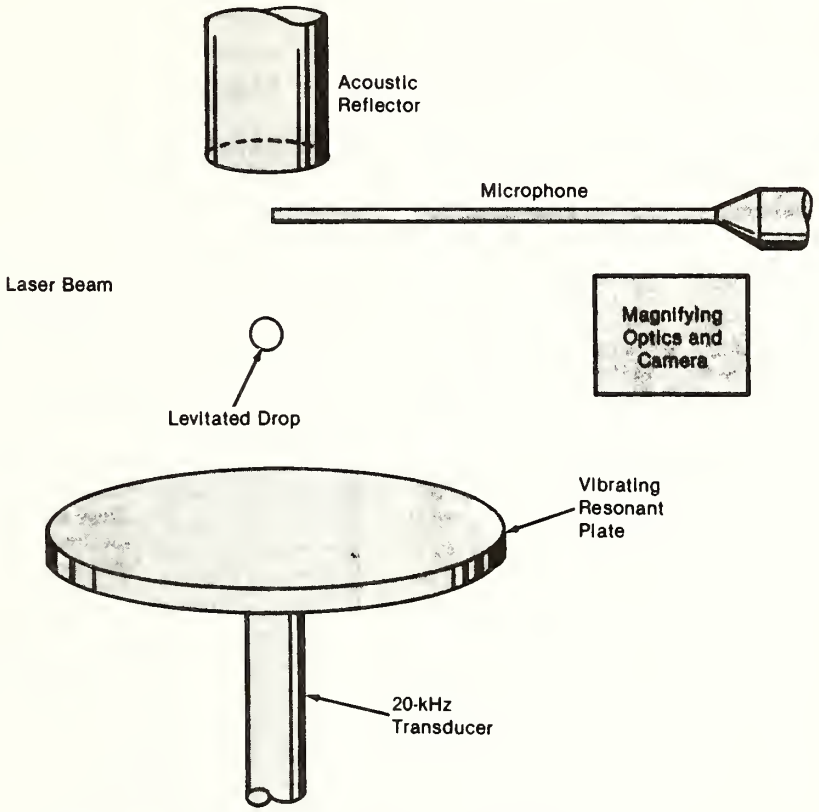

Held Aloft In a Laser Beam by an acoustic field, a liquid drop casts its shadow on photographic film. The changing shape of the drop is recorded in a sequence of exposures.

Regardless of the volatility of the liquid, the film records of the aspect ratios can be compared with the values predicted by theory. In one set of experiments, drops were 1 mm or less in diameter. The surface tensions ranged from 20 to 70 dyn/cm, the acoustic pressure varied from 160 to 165 dB, and the aspect ratios were between 1 and 2. There was close agreement between the theory and the measurements at aspect ratios less than 1.5 and drop sizes less than about 0.06 of the sound wavelength.

This work was done by Eugene H. Trinh and Chaur-Jian Hsu of Caltech for **NASA's Jet Propulsion Laboratory**. *NPO-16746 /TN*

FOR ADDITIONAL INFORMATION: *Contact: Director, Technology Transfer Division, P.O. Box 8757, BWI Airport, MD. 21240; (301) 621-0100 Ext. 241*

REFER TO THE NUMBER LISTED AT THE END OF THE ARTICLE

NASA Tech Brief
National Aeronautics and Space Administration

Containerless Atomic-Fluorescence Property Measurements

Laser-induced fluorescence can be used to measure high-temperature processes.

A report describes studies conducted to establish and verify the use of laser-induced fluorescence in monitoring and controlling high-temperature containerless processes. Specimens were levitated by gas jets or electromagnetic fields and heated by laser beams or electromagnetic induction while being irradiated and detected by the fluorescence technique. The reported work includes the development of an apparatus and its use in studies of the following phenomena:

- Chemical reactions on Al_2O_3, Mo, W, and LaB_6 specimens;
- Methods for noncontact measurements of specimen temperature;
- Properties of levitating gas jets; and
- Radiative lifetimes and collisional energy-transfer rates for electronically excited atoms.

A pulsed dye laser was used to induce fluorescence in atomic Hg, Al, Mo, W, La, and B. The Hg atoms were added to a jet of Ar. Al atoms were produced by the continuous-wave laser heating of aerodynamically levitated sapphire and polycrystalline alumina spheres or of self-supported sapphire filaments. Mo atoms were evaporated from solid spheres that were inductively levitated in a vacuum and heated by a laser. W atoms were evaporated from electrically heated filaments. La and B atoms were evaporated from an aerodynamically-levitated and laser-heated LaB_6 sphere.

The report makes quantitative and qualitative comparisons among three new methods of temperature measurement, all of which rely on laser-induced fluorescence. One method is gas-density thermometry with a seed gas (usually Hg). This method requires an inert ambient atmosphere. The other two methods involve measurements of the velocities of evaporating atoms or of the population ratios of different electronic states. These methods require the assumption that the gas is in thermal equilibrium with the hot surface of interest and provide a check on the assumption in that when the assumption is not correct, they yield equal temperatures only by coincidence.

The enthalpies of evaporation of W and Mo measured in these experiments agree, within experimental uncertainty, with the values in the literature. The evaluation of the LaB_6-evaporation results is complicated by theoretical difficulties in calculating radiative transitions of B atoms and the relationship between concentration and self-absorption of radiation. A further complication arises from the disagreement between earlier reported results and the results of these experiments. The discrepancies may be due in part to reactions with effusion cells.

The authors conclude that if accurate temperature measurements are taken, then containerless measurements of laser-induced fluorescence, coupled with calculations based on the third law of thermodynamics, can lead to the accurate determinations of reaction enthalpies. For binary compounds, the required data are the activities of the elemental components, which can be determined directly from the ratios of the intensities of laser-induced fluorescence over the material of interest to those over the pure elements at the same temperature. Gas-phase/condensed-phase equilibrium is required for such determinations, and approximate equilibrium would be achieved over high-temperature liquids. Equilibrium can be further assured by the use of an inert-gas atmosphere to retard evaporation.

This work was done by P. C. Nordine, R. A. Schiffman, and C. A. Walker of Midwest Research Institute for **Marshall Space Flight Center**. *Further information may be found in NASA CR-171038 [N84-25481/NSP], "Containerless High Temperature Property Measurements by Atomic Fluorescence."*

Copies may be purchased from the National Technical Information Service, Springfield, Virginia 22161, [A04]
MFS-27070 /TN

FOR ADDITIONAL INFORMATION: *Contact: Director, Technology Transfer Division, P.O. Box 8757, BWI Airport, MD. 21240; (301) 621-0100 Ext. 241*
REFER TO THE NUMBER LISTED AT THE END OF THE ARTICLE

Transportation

929 Helicopter Icing Spray System — A spray boom assembly is deployed 19 feet (5.7m) beneath the aircraft from a torque tube through the cargo compartment.

930 Service-Life Extension of Explosive Escape Devices — Chemical and functional tests yield conservative service-life estimates.

931 Translating Canard — Longitudinal trim control is augmented when landing flaps are deployed. (Licensing Opportunity)

MANUFACTURING TECHNOLOGY NOTE

U.S. ARMY MATERIEL COMMAND

Deputy Chief of Staff for Manufacturing Technology, Alexandria, VA

Project Number: 1K-2-DT-168-01-1K-1K

Filing Code: 51A063

Helicopter Icing Spray System

A spray boom assembly is deployed 19 feet (5.7 m) beneath the aircraft from a torque tube through the cargo compartment.

A test program has evaluated the operational performance and spray cloud characteristics of the helicopter icing spray system. A modified CH-47C helicopter (see figure) was operated as an airborne spray tanker for helicopter qualification tests in artificial icing conditions. Configuration changes made during the first two phases of the program, which was conducted for the U.S. Army Aviation Systems Command, reduced previous spray system problems of water leakage, freezing, and nonuniform flow patterns from the boom assembly.

In-flight spray cloud data taken from an aircraft by particle-measuring spectrometers found peak mass concentrations in the desired 15- to 25-μm drop diameter range. Larger drops (bigger than 50 μm), not normally found in natural stratiform clouds, were also observed.

An aft-facing radar altimeter at the rear of the helicopter allows positioning of test aircraft at a known standoff distance. A calibrated outside air temperature probe and a dewpoint hygrometer provide ambient temperature and humidity measurement. Thermocouples and pressure transducers installed on the boom assembly allow in-flight measurement of pressure and temperature for both boom air and water during spraying.

Many aspects of ice formation produced on various test aircraft compared favorably to natural accretions. Ability of the artificial cloud to produce nonstreamlined "double-horn" ice shapes on main rotor blades at −5 °C was substantiated for the first time.

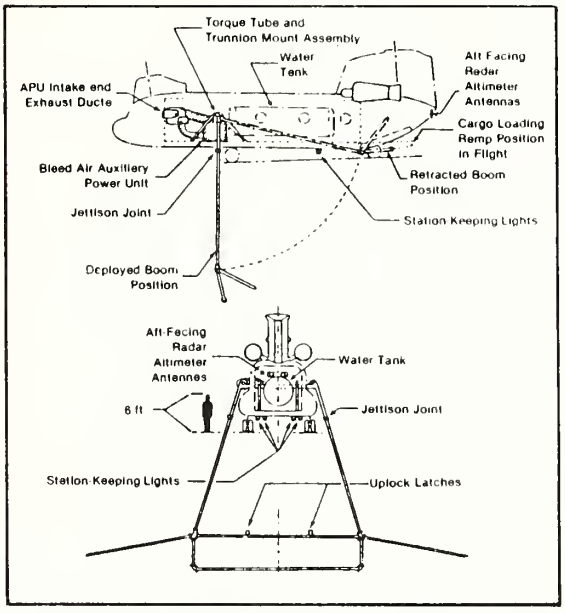

A **Helicopter Icing Spray System** is shown in sideview and rearview schematics. The boom assembly consists of two parallel 27-ft (8.1-m) trapeze section with 5-ft (1.5-m) vertical separators and tow 17.6-ft (5.3-m) outriggers attached by four-way junctions to the upper trapeze.

FOR ADDITIONAL INFORMATION:

You can learn more details about this technology by ordering the NTIS report(s):

Helicopter Icing Spray System (HISS) Evaluation and Improvements
Order number: AD-A170732/NAA
Price code: A08

Order from:
National Technical Information Service
5285 Port Royal Road
Springfield, VA 22161

This document wes prepered under the sponsorship of the U.S. Government. Neither the United Stetes Government nor eny person ecting on behelf of the United Stetes Government essumes any liebility resulting from the use of the information contained in this document, or werrents thet such use will be free from privetely owned rights.

NASA Tech Brief
National Aeronautics and Space Administration
Langley Research Center, Hampton, Virginia

Service-Life Extension of Explosive Escape Devices

Chemical and functional tests yield conservative service-life estimates.

An approach to the extension of the service lives of explosive devices in aircraft escape systems has been developed, supported by testing of representative candidate devices to evaluate quantitatively the effects of service, age, and degradation, and to enable responsible, conservative service-life determinations. Five types of explosive components were evaluated: rigid and flexible explosive transfer lines; one-way transfers; flexible, linear-shaped charges; and initiation-handles.

A wide variety of explosive devices has been successfully applied to military and NASA aircraft to provide emergency escape for the flight crews. The establishment of the rated service life was previously approached on a very conservative basis because the function involved is critical to human life. Generally, a relatively short service life was arbitrarily established.

The extension of service in a realistic manner provides both cost savings and increased system reliability. Removal and replacement costs that can be reduced include those associated with the removal of the aircraft from service, transfer of the aircraft to and from refurbishment sites, procurement of replacement components, and use of a specially trained labor force. System reliability can be increased by avoiding too frequent teardown and replacement of the devices, with the accompanying potential for damage and improper assembly.

The devices were evaluated functionally and chemically. Velocity measurements were made of detonation fronts and of explosively driven fragments, and output energies were measured on several devices. The status of the explosive materials in the devices was determined using color photographs, scanning electron microscopy, and high-pressure liquid chromatography, which provides the quantity of each explosive by weight in a sample. Samples of each test group were dissected at several points for analysis. A series of nondestructive tests was also conducted, and "performance-standard" groups were used to establish functional and chemical composition standards against which all subsequent test groups were compared. Repeat thermal-qualification tests and degradation investigations were also conducted on some of the devices.

The results of the program indicate that this test methodology (inspection, chemical, and functional) should be incorporated into the original specifications for explosive devices and then used for subsequent evaluation testing. "Accelerated aging" techniques should not be applied, because there is no verified relationship to age or service.

Rigid explosive transfer lines and one-way transfers should be considered for service extension for all applications. Flexible explosive transfer lines should allow only thermal-annealing cycles that do not exceed 350 °F (177 °C), and service extension should be cautious when these devices are used. Flexible linear-shaped-charge applications should provide mechanical support of end tips to maintain seals and performance, and service extension should be cautious. For initiation handles, service extension should be approached with extreme caution because of the difficulty of fully evaluating all explosive components, particularly the percussion primers, which are the weakest components in these devices.

This work was done by Laurence J. Bement of **Langley Research Center** *and Morry L. Schimmel of McDonnell Aircraft Co. Further information may be found in NASA TM-86323 [N85-22381/NSP], "Approach for Service Life Extension of Explosive Devices for Aircraft Escape Systems."*

Copies may be purchased from the National Technical Information Service, Springfield, Virginia 22161, [A02]
LAR-13462 /TN

FOR ADDITIONAL INFORMATION: *Contact: Director, Technology Transfer Division, P.O. Box 8757, BWI Airport, MD. 21240; (301) 621-0100 Ext. 241*
REFER TO THE NUMBER LISTED AT THE END OF THE ARTICLE

NASA Tech Brief
National Aeronautics and Space Administration
Langley Research Center, Hampton, Virginia

Licensing Opportunity

Translating Canard

Longitudinal trim control is augmented when landing flaps are deployed.

A translating canard provides automatic pitch trim when the wing flaps of an airplane are deployed. Heretofore, a general disadvantage of nontranslating canard configurations has been the inability to use wing flaps to achieve high lift (and therefore slower stalling speeds) for landing approaches. To achieve a longitudinally stable canard configuration, it is necessary to locate the center of gravity between the canard and the wing. This placement causes a significant moment to be associated with the lift centers of the canard and the wing. Therefore, large nosedown pitching moments associated with lift increments due to the use of wing flaps would require equivalent noseup pitching-moment contributions from the canard to provide pitch trim. In a stable canard arrangement, the canard must have a lift coefficient higher than that of the wing to provide pitch trim. Because of this requirement, the canard cannot provide pitch trim when the wing trailing-edge flaps are deflected.

The translating-canard concept is shown in the figure. The translating canard would be mechanized by a worm-screw system with a set of tracks to guide the movement of the canard. In addition, the movement of the canard would be geared to the movement of the wing flap since canard translation would be needed only when the wing flap is deployed.

Besides providing the automatic pitch adjustment required for trim when landing flaps on the main wing are deployed, this system maintains the stable pitch break inherent in the canard design. Test data indicate that a significant improvement in pitch-trim capability can be achieved with the translating canard concept. Additionally, the lift effectiveness of the translating canard does not change with the distance translated.

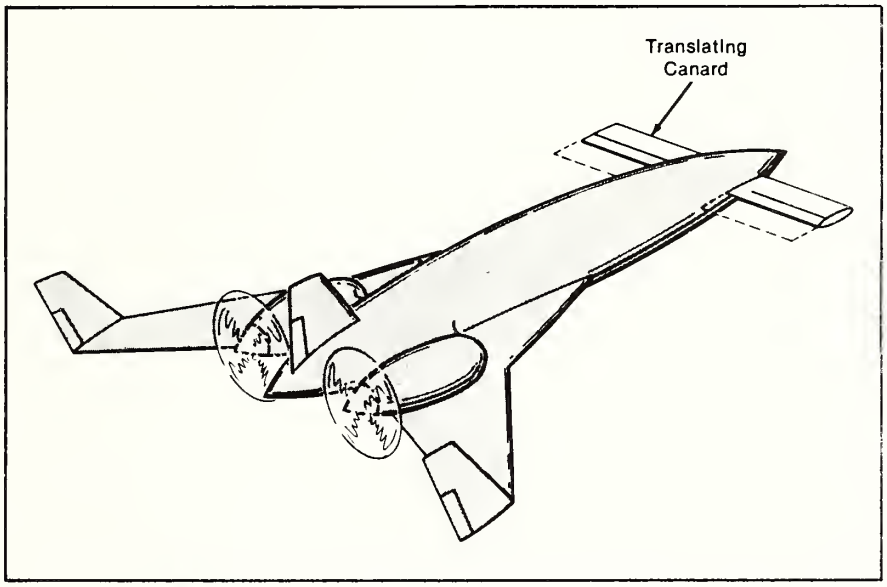

The **Translating Canard** provides automatic pitch trim for the wing-flap system while maintaining a stable pitch break.

This work was done by Long P. Yip, Richard D. Robinson, and Joseph L. Johnson of **Langley Research Center**. *No further documentation is available.*

Inquiries concerning rights for the commercial use of this invention should be addressed to the Patent Counsel, Langley Research Center. Refer to LAR-13498/TN

Langley Research Center
Technology Utilization Officer
John Samos
Mail Stop 139A
Hampton, VA 23665
(804) 865-3281
Patent Counsel
Howard J. Osborn
Mail Code 279
Hampton, VA 23665
(804) 865-3725

FOR ADDITIONAL INFORMATION: *Contact: Director, Technology Transfer Division, P.O. Box 8757, BWI Airport, MD. 21240; (301) 621-0100 Ext. 241*
REFER TO THE NUMBER LISTED AT THE END OF THE ARTICLE

NTIS Order Form

NTIS Telephone Numbers

To Order Reports
(703) 487-4650

For Subscription Questions
(703) 487-4630

Other Information
(703) 487-4600

Editorial Questions
(703) 487-4838

Postage:
NTIS uses First Class Delivery, or equivalent service, on all shipping. For information about one day RUSH ordering, call (703) 487-4600.

NTIS PRICE CODE SCHEDULE *

This schedule gives the current values to the price codes cited in those Tech Notes having a backup report available from NTIS.

Microfiche	
A01	$6.50
Paper copy	
A02	9.95
A03	11.95
A04 through A05	13.95
A06 through A09	18.95
A10 through A13	24.95
A14 through A17	30.95
A18 through A21	36.95
A22 through A25	42.95
A99	Call for price

Customers in Canada, United States, and Mexico use this schedule. Other addresses should write for the price listing, number PR-360-4.

Prices effective January 1, 1987

Use this form ONLY to order reports designated as available from NTIS

MAIL ORDER TO: National Technical Information Service
U.S. DEPARTMENT OF COMMERCE
5265 Port Royal Road
Springfield, VA 22161
(703) 487-4650

Send me the reports I have selected on this form. I have placed order numbers in appropriate blanks and have indicated the quantity. IF ADDRESS LABEL IS NOT CORRECT, CALL OUR SUBSCRIPTIONS DEPARTMENT.

Last Name: .....

Title: .....

Company/Organization: .....

Address: .....

.....

City/State/Zip: .....

Telephone Number: .....

METHOD OF PAYMENT

☐ Check enclosed payable to NTIS for $ .....

☐ Charge to my NTIS Deposit Account, No: ....-.....

☐ Purchase order number: .....

Charge to: ☐ American Express ☐ VISA ☐ MasterCard

Card Number: .....

Expation date: .....

Signature: .....
(Required to validate order)

NTIS ORDER NUMBER (Use only for backup reports stated as available from NTIS)

NTIS Order Number	*Price**	*Quantity*	*Total Price*
.....	.....	.....	.....
.....	.....	.....	.....
.....	.....	.....	.....
.....	.....	.....	.....
.....	.....	.....	.....
		Shipping and handling fee	$3.00
		Total	.....

- Agriculture & Food
- Computers
- Electrotechnology
- Energy
- Engineering
- Environmental Science & Technology
- Manufacturing, Machinery, & Tools
- Materials
- Medicine & Biology
- Natural Resources Technology & Engineering
- Physical Sciences
- Transportation

Route To:

PENN STATE UNIVERSITY LIBRARIES
A000072009888

:PARTMENT OF COMMERCE
al Technical Information Service
ld, Va. 22161

- BUSINESS
or Private Use, $300

AN EQUAL OPPORTUNITY EMPLOYER

BULK RATE
POSTAGE & FEES PAID
NTIS
Permit No. G-292